
Distinction of vasculitis-associated ANCA subsets
and their pathogenic role in a new mouse model
with the humanized target antigen



Distinction of vasculitis-associated ANCA subsets and their pathogenic role in a new mouse model with the humanized target antigen

Dissertation zur Erlangung
des Doktorgrades der Naturwissenschaften
an der Fakultät für Biologie
der Ludwig-Maximilians-Universität München

angefertigt am
Max-Planck-Institut für Neurobiologie,
Abteilung Neuroimmunologie
und
Helmholtz Zentrum München,
Comprehensive Pneumology Center

vorgelegt von
Lisa Christina Hinkofer
aus Altötting

München, November 2014

Erstgutachterin:	Prof. Dr. Elisabeth Weiß
Zweitgutachterin:	PD Dr. Barbara Lösch
Mitgutachter:	Prof. Dr. Heinrich Jung
	Prof. Dr. Marc Bramkamp
Sondervotum:	PD Dr. Dieter Jenne
Einreichung der Dissertation:	03.11.2014
Datum der mündlichen Prüfung:	18.02.2015

Der Beginn aller Wissenschaften ist das Erstaunen,

daß die Dinge sind, wie sie sind.

Aristoteles

Acknowledgments

First of all I would like to thank my supervisor PD Dr. Dieter Jenne for his continual guidance, support and his time for long scientific discussions. He taught me to critically approach scientific topics and that every result is a good result in research.

I am very thankful to Prof. Dr. Elisabeth Weiß, my doctoral thesis supervisor at the faculty of biology at the Ludwig-Maximilians-Universität München, for her time, her interest in my research and her valuable suggestions. I also want to thank the members of my thesis examination committee, namely PD Dr. Barbara Lösch, Prof. Dr. Heinrich Jung, Prof. Dr. Marc Bramkamp, Prof. Dr. Ute Vothknecht and Prof. Dr. Angelika Böttger for their time and contribution to this work.

Prof. Dr. Hartmut Wekerle is acknowledged for the opportunity to start my thesis at the Max-Planck-Institute of Neurobiology, his interest in the project and his valuable feedback. I want to thank Prof. Dr. Oliver Eickelberg for hosting our group at the Comprehensive Pneumology Center of the Helmholtz Zentrum München and for the warm welcome and support.

Further, I am very grateful to the members of my thesis committee Dr. Ulf Schönermarck and Dr. Gurumoorthy Krishnamoorthy for their time, their continuous interest in my project and their helpful feedback.

I acknowledge the financial support by the European Union Seventh Framework Programme (FP7/2007-2013) under Grant Agreement 261382 (INTRICATE).

Further I want to thank Heike Kittel, Lisa Stegmann, Natascha Perera, Therese Dau and Jessica Götzfried for the great atmosphere in the Jenne Lab. Thanks for the good cooperation, the support and a lot of fun.

I also benefited greatly from my fellow PhD students and my research school class. Especially I want to thank Conny and Franzi for their moral support and the great time together.

I dearly thank my fiancé Thomas for always believing in me. Even in discouraging times he never got unnerved and was always able to make me laugh.

Last but not least, I want to thank my family, especially my parents for their continual input in my education, their encouragement, but also for their critical advice. Thank you all for your continuous love and support.

Summary

Granulomatosis with Polyangiitis (GPA) is an ANCA (anti-neutrophil cytoplasmic antibody) associated vasculitis. It typically starts in the respiratory tract and the lungs and progresses to a generalized life-threatening, relapsing-remitting disease of small blood vessels in multiple essential organs such as the lungs and kidneys. GPA is strongly associated with the presence of autoantibodies, so-called ANCA, which are mainly directed against the neutrophil serine protease proteinase 3 (PR3). Despite numerous attempts to determine the role of ANCA at the onset and during progression of GPA, the pathogenicity of ANCA remains still unclear. The aim of this thesis was to explore the mechanisms by which ANCA contribute to the development of GPA and influence disease progression and severity.

The induction of small-vessel vasculitis by the action of ANCA was investigated using a newly developed humanized mouse model. Transfer of monoclonal antibodies (mAbs) against human PR3 (hPR3) into a hPR3 knock-in mouse was planned to provide new insights into the pathogenicity of ANCA. Expression and functionality of hPR3 in the neutrophils of the newly generated mouse line was observed. Active hPR3 was transported to the surface of the neutrophils and was thus accessible to antibodies. Based on the literature, antibodies, which are able to inhibit the proteolytic activity of PR3, were thought to have the highest pathogenic potential and to influence the development of relapses. Characterization of mAbs indeed revealed one mAb, MCPR3-7, as inhibiting for PR3 and this mAb even impaired the interaction of PR3 with its natural inhibitor, α 1-proteinase inhibitor. This antibody, however, could not be used for transfer experiments, due to its inability to bind to membrane-bound PR3. Analysis of a large GPA patient cohort confirmed the existence of ANCA with inhibitory capacity towards PR3. Inhibitory ANCA, however, were not restricted to samples from relapsing patients, but occurred also during remission phases. No correlation of inhibitory ANCA with disease outbreak, relapses or severity could be detected. Therefore, instead of transferring inhibitory PR3 antibodies, non-inhibitory antibodies of different IgG subclasses were evaluated in hPR3 knock-in mice. One mAb was indeed able to induce a strong inflammatory response in the mice, proofing their pathogenic potential. After recruitment of immune cells, activation and degranulation of neutrophils led to vasculitis-like and pulmonary lesions. IgG2a antibodies were able to elicit a stronger inflammatory response than IgG2b, suggesting that the development of a GPA-like phenotype seems to be dependent on the IgG subclass.

Zusammenfassung

Granulomatose mit Polyangiitis (GPA) ist eine ANCA (Anti-Neutrophile Cytoplasmische Antikörper) assoziierte Vaskulitis. Nach anfänglichen Problemen in den Atemwegen und der Lunge, entsteht im fortgeschrittenen Stadium eine generalisierte, lebensbedrohliche, schubförmig wiederkehrende Vaskulitis kleiner Blutgefäße in essentiellen Organen wie der Lunge oder den Nieren. GPA ist eng mit dem Vorkommen von Autoantikörpern, den sogenannten ANCAs, assoziiert. Diese richten sich gegen die Neutrophilen-Serinprotease Proteinase 3 (PR3). Trotz vieler Versuche, den Einfluss der ANCAs auf den Ausbruch und den Verlauf der Krankheit zu bestimmen, konnte die Pathogenität der ANCAs noch nicht bewiesen werden. Das Ziel dieser Arbeit war es, den Einfluss der ANCAs auf die Entstehung, den Verlauf und den Schweregrad von GPA zu erforschen.

Die Fähigkeit von ANCAs eine Vaskulitis kleiner Gefäße auszulösen wurde mit einem neuen humanisierten Mausmodell untersucht. Transfer monoklonaler Antikörper (mAk) gegen humane PR3 (hPR3) in hPR3 Knock-in-Mäuse sollte neue Einsicht in deren Pathogenität gewähren. Humane PR3 wurde in der neuen Mauslinie exprimiert und war funktionell. Durch Transport der aktiven PR3 auf die Oberfläche der Neutrophilen war diese zugänglich für Antikörper. Nach bisher publizierten Daten sollten Antikörper, die die proteolytische Aktivität von PR3 inhibieren, die höchste Pathogenität aufweisen und Rückfälle auslösen. Durch Charakterisierung verschiedener mAk konnte ein Antikörper identifiziert werden, der PR3 inhibiert und die Interaktion von PR3 mit ihrem natürlichen Inhibitor (α 1-Proteinase Inhibitor) vermindert. Verwendung dieses Antikörpers für Transferexperimente war allerdings nicht möglich, da er membrangebundene PR3 nicht erkennt. Die Analyse einer großen GPA-Patienten-Kohorte bestätigte die Existenz von inhibitorischen ANCA. Diese ANCAs kamen jedoch auch während Remissionsphasen vor. Eine Korrelation von inhibitorischen ANCAs mit Krankheitsausbruch, Rückfällen oder Schweregrad der Krankheit konnte nicht detektiert werden. Statt inhibitorischer Antikörper wurden deshalb nicht-inhibitorische Antikörper unterschiedlicher IgG Subklassen transferiert. Einer der mAk löste eine starke Entzündungsreaktion in den humanisierten Mäusen aus. Immunzellen wurden rekrutiert und durch die Aktivierung und Degranulierung von Neutrophilen entstanden Vaskulitis-artige und pulmonale Läsionen. Da der Transfer von IgG2a Antikörpern eine stärkere Entzündungsreaktion auslöste als IgG2b Antikörper, scheint die Entwicklung des GPA-ähnlichen Phänotyps von der IgG Subklasse abzuhängen.

Table of Contents

1.	Introduction	1
1.1	Anti-neutrophil cytoplasmic autoantibody associated vasculitis (AAV)	1
1.2	Granulomatosis with Polyangiitis (GPA)	1
1.3	Proteinase 3 – the target autoantigen in GPA	3
1.3.1	Neutrophil granulocytes	3
1.3.2	The neutrophil immune response	3
1.3.3	Neutrophil serine proteases (NSPs).....	4
1.3.4	Protease specificity – The Schechter and Berger nomenclature	5
1.3.5	Proteinase 3 (PR3).....	6
1.4	Anti-neutrophil cytoplasmic antibodies (ANCA).....	7
1.5	The role of PR3, ANCA and the neutrophil immune response in GPA	7
1.5.1	ANCA with inhibitory capacity towards PR3	8
1.6	The role of protease inhibitors in GPA.....	9
1.6.1	Alpha-1-proteinase inhibitor (α 1PI)	9
1.6.2	The role of α 1PI in GPA	10
1.7	Animal models for GPA	11
1.8	Objective.....	12
2.	Material and Methods.....	13
2.1	Material.....	13
2.1.1	Chemicals and consumables.....	13
2.1.2	Plasmids	13
2.1.3	Cell lines.....	13
2.1.4	Recombinant and purified proteins	14
2.1.5	Antibodies	14
2.1.6	Synthetic substrates	15
2.1.7	Oligonucleotides.....	15
2.1.8	Mouse strains.....	16

2.1.9	Laboratory equipment	16
2.2	Molecular biological methods	17
2.2.1	Plasmid DNA purification from <i>E.coli</i>	17
2.2.2	Polymerase chain reaction (PCR)	17
2.2.3	Agarose gel electrophoresis	18
2.2.4	Restriction digest.....	19
2.3	Recombinant protein expression	19
2.3.1	Transfection of HEK 293E.....	20
2.4	Protein analysis.....	20
2.4.1	Purification of recombinant proteins.....	20
2.4.2	Determination of protein concentration	21
2.4.3	Sodium dodecyl sulfate polyacrylamide gel electrophoresis (SDS PAGE).....	21
2.4.4	Protein detection.....	22
2.4.5	Processing of proPR3 by enterokinase.....	23
2.4.6	Measurement of enzymatic activity	24
2.5	Mouse model analysis	25
2.5.1	Isolation of genomic DNA from mouse tails	25
2.5.2	Mouse-genotyping.....	25
2.5.3	Isolation of bone marrow leukocytes	25
2.5.4	Isolation of neutrophils.....	26
2.5.5	Reverse transcriptase (RT) PCR.....	26
2.5.6	Transfer of mAb into hPR3 ^{+/+} mice	27
2.5.7	Immune cell analysis after mAb transfer	28
2.5.8	Periodic acid-Schiff (PAS) staining of lung slices.....	29
2.6	Cell biological methods	30
2.6.1	Determination of cell count and viability.....	30
2.6.2	Isolation of PMNs from human blood.....	30
2.6.3	Preparation of total cell lysates	30
2.7	Immunological methods	31
2.7.1	Western blot	31
2.7.2	Enzyme-linked immunosorbent assay (ELISA).....	32
2.8	Flow cytometry.....	33

2.8.1	Cell surface staining of PR3	33
2.8.2	Measurement of PR3 activity on the cell surface.....	34
2.9	Thermophoresis	34
2.9.1	Fluorescent labeling of proteins	34
2.9.2	Thermophoretic quantification	34
2.10	Patient material analysis	35
2.10.1	Precipitation of total IgG from plasmapheresis material	35
2.10.2	Affinity purification of PR3-specific ANCA	35
2.10.3	Protein G purification of antibodies from patient plasma	36
2.10.4	Measurement of inhibitory capacity of ANCA from patient plasma	37
2.11	Statistical analysis	37
3.	Results	38
3.1	Generation of hPR3 knock-in mice	38
3.1.1	Removal of the neomycin and backcrossing to 129S6/SvEv background.....	39
3.2	Characterization of hPR3 expression in hPR3 ^{+/+} mice	40
3.2.1	Human PR3 ^{+/+} mice express hPR3	40
3.2.2	Human PR3 expressed in hPR3 ^{+/+} mice is catalytically active	41
3.2.3	Human PR3 in hPR3 ^{+/+} mice is transported to the neutrophil surface	42
3.2.4	PR3 on the surface of hPR3 ^{+/+} neutrophils is active	43
3.3	Characterization of monoclonal antibodies for transfer experiments.....	45
3.3.1	Interference of mAbs with catalytic activity of PR3.....	45
3.3.2	Interaction of mAbs with PR3 inhibitor complexes.....	46
3.3.3	MCPR3-7 impairs α 1PI-PR3 complexation	48
3.3.4	Influence of mAbs on non-covalent α 1PI-PR3 complexation	49
3.3.5	Characterization of the MCPR3-7 epitope	51
3.3.6	MCPR3-7 is unable to bind to PR3 in its active conformation	52
3.3.7	Binding of MCPR3-7 alters the peptide binding pocket	53
3.3.8	MCPR3-7 cannot bind to membrane-bound PR3	55
3.3.9	Generation of new mAbs against PR3	56
3.4	Transfer of mAbs into hPR3 ^{+/+} mice	58
3.4.1	Infiltration of immune cells in the lungs after antibody injection.....	58
3.4.2	Lung vasculitis and pulmonary lesions after antibody injection.....	61

3.5	Characterization of different types of ANCA in patients	63
3.6	Detection of activity modulating ANCA in serum from patients with GPA.....	64
3.7	Correlation of activity modulating ANCA with disease progression in GPA.....	66
3.7.1	Inhibitory ANCA in baseline samples do not correlate with disease severity ...	67
3.7.2	Presence of inhibitory ANCA is not related to organ involvement	69
3.7.3	Disease activity does not correlate with activity modulating ANCA	70
3.7.4	Epitopes of inhibitory ANCA are located on the active site surface of PR3	71
3.7.5	Inhibitory ANCA bind not directly into the active site cleft.....	73
3.7.6	Inhibition mechanism of some ANCA resembles MCPR3-7 inhibition.....	74
4.	Discussion	78
4.1	Expression and functionality of PR3 in the humanized mouse	78
4.2	MCPR3-7, a unique antibody with PR3-inhibiting potential	80
4.2.1	MCPR3-7 in comparison to other antibodies	80
4.2.2	MCPR3-7 and its mechanism of inhibition.....	81
4.2.3	Limitations of MCPR3-7.....	83
4.3	The GPA mouse model.....	84
4.3.1	Induction of inflammation by transfer of hPR3 antibodies.....	84
4.3.2	The immune response is triggered by properties of immunoglobulins.....	86
4.4	Contribution of ANCA to GPA development and disease progression	88
4.4.1	Influence of activity modulating ANCA on disease progression.....	88
4.4.2	Interference of activity modulating ANCA with α 1PI inhibition of PR3.....	92
4.4.3	Activity modulating ANCA inhibit PR3 by different allosteric mechanisms....	93
4.5	Conclusions	94
5.	Bibliography.....	96
6.	Abbreviations	106
7.	Appendix	108
7.1	Vector maps	108
7.1.1	pcDNA5/FRT/V5-His-TOPO [®]	108
7.1.2	pTT5	109
7.2	Sequences	110
7.2.1	SigIg κ -proPR3-H ₆	110
7.2.2	Δ hPR3-S195A	111

8.	Curriculum vitae.....	112
9.	Publications and meetings	113
9.1	Publications	113
9.2	Conference Abstracts.....	113
9.3	Presentations at international conferences.....	114
9.3.1	Oral presentations.....	114
9.3.2	Poster presentations	114
	Eidesstattliche Erklärung.....	115

1. Introduction

1.1 Anti-neutrophil cytoplasmic autoantibody associated vasculitis (AAV)

Anti-neutrophil cytoplasmic autoantibody (ANCA) associated vasculitis (AAV) is a systemic autoimmune disease, which is characterized by necrotizing inflammation of blood vessel walls. In adults it is the most frequent form of primary small-vessel vasculitis. Predominantly small vessels like arterioles, capillaries and venules are affected. Furthermore, AAV is strongly associated with the development of autoantibodies, so-called ANCA. These ANCA are mainly directed against proteinase 3 (PR3) and myeloperoxidase (MPO). PR3-specific ANCA occur mainly in patients suffering from Granulomatosis with Polyangiitis (GPA, previously called Wegener's granulomatosis), whereas MPO-ANCA are a hallmark for microscopic polyangiitis (MPA). Besides GPA and MPA the group of AAV further comprises idiopathic necrotizing crescentic glomerulonephritis and the Churg-Strauss syndrome (CSS) (Kallenberg et al., 2006).

1.2 Granulomatosis with Polyangiitis (GPA)

GPA, formerly also known as Wegener's granulomatosis, was first described by Heinz Klinger in 1931. In 1936 Friedrich Wegener observed a similar clinical presentation of necrotizing granulomas in the respiratory tract in three additional patients. The hallmarks of GPA, necrotizing granulomatous lesions in the upper and lower respiratory tract, necrotizing glomerulonephritis and systemic vasculitis of small blood vessels, were established and accepted a few years later (Olivencia-Simmons, 2007).

GPA is a rare disease with a worldwide prevalence of 23.7 – 156.5 per million (Mahr, 2009). The annual incidence was estimated to 3.0 – 14.4 per million (Reinhold-Keller et al., 2005). It affects both genders equally and occurs typically in adults between 40 and 55 years of age

(Langford and Hoffman, 1999). As GPA is a multi-system disorder, symptoms manifest individually in the patients and diagnosis proves to be difficult. Mostly patients present with upper and lower airway symptoms. Only in its generalized form GPA leads to an involvement of the kidneys and the vessels. The most common clinical symptoms of patients with GPA unfold in the following order. In about 95% of patients involvement of the upper respiratory tract occurs in the early stage of disease. Characteristic symptoms therefor are for instance cough, rhinitis and sinusitis (Almouhawis et al., 2013). Pulmonary manifestations occur in about 85% of patients throughout the course of disease. This also leads to nonspecific symptoms like for example cough or dyspnea. The most common lesions in the lungs are nodules, which can be observed in about 70% of patients with lung involvement (Delèveaux et al., 2005). Further complications in the lungs can be formation of granulomas, vasculitis or alveolar hemorrhage. About 77% of patients are affected by renal disease (Olivencia-Simmons, 2007). The most serious renal manifestation is the glomerulonephritis. If left untreated, glomerulonephritis can lead to complete renal failure. Renal involvement is indicated by hematuria, azotemia and proteinuria. Other important clinical manifestations of GPA are furthermore inflammation of the vessel walls, mainly affecting small and medium-sized vessels, and cardiac manifestations. According to disease severity two different forms of GPA are discriminated; severe and limited disease. Limited disease is defined as a disease, which is not ultimately threatening the life of the patient or the function of vital organs and is normally confined to the upper respiratory tract and lungs (Stone and The Wegener's Granulomatosis Etanercept Trial Research Group, 2003). Severe disease is mostly characterized by rapidly progressing glomerulonephritis and alveolar hemorrhage and represents an imminent threat on the life of the patient. The differentiation between those two disease forms is as well important for the choice of therapeutic agents (Wung and Stone, 2006). Therapy of GPA consists of two phases, the remission induction therapy and the maintenance of remission. In general the therapy is performed by using a combination of corticosteroids and immunosuppressants. Combination of those two agents enables prolongation of remission. The choice of therapeutic agent depends on disease severity. For treatment of severe disease therapeutics with higher toxicity are applied (cyclophosphamide and glucocorticoids), whereas less toxic agents are used for patients with limited disease (methotrexate and glucocorticoids) (Wung and Stone, 2006).

GPA is strongly associated with the presence of autoantibodies, so called anti-neutrophil cytoplasmic antibodies (ANCA). Thus GPA is assigned to the group of autoimmune diseases

(Hewins et al., 2000). The target antigen of ANCA in GPA is proteinase 3 (PR3). Strong association of GPA with ANCA, which are directed against PR3 (PR3-ANCA), leads to the assumption that ANCA play an important role in the pathogenesis of GPA. In the following chapters PR3, ANCA and their role in GPA are introduced in detail.

1.3 Proteinase 3 – the target autoantigen in GPA

1.3.1 Neutrophil granulocytes

Granulocytes (polymorphonuclear leukocytes) are myeloid cells, which are characterized and named according to their high content of densely packaged granules in their cytoplasm. There are three different types of granulocytes, the neutrophil granulocytes, in the following called neutrophils, the eosinophil and the basophil granulocytes. The different types are classified according to the staining properties of their granules. Neutrophils represent about 50% to 70% of all circulating leukocytes. They are relatively short-lived cells, which only survive a few days. One of the characteristic features of neutrophils is the segmented nucleus, which is why they are also called polymorphonuclear cells (PMNs). Neutrophils are the first line of host defense against a wide range of pathogens. Thus they are produced in increasing numbers during the immune response and are the first cells to arrive at a site of inflammation. In contrast to the high number of neutrophils, eosinophil and basophil granulocytes are only present in the blood in low numbers. Only about 1 to 5% of leukocytes represent the eosinophil granulocytes and 0.5 to 1% the basophil granulocytes.

1.3.2 The neutrophil immune response

After production of neutrophils in the bone marrow, the cells circulate in the blood for a few hours before they are recruited to injured or infected tissue. At these peripheral extravascular sites they form the first line of cellular immune defense. The neutrophils reach the site of inflammation via the blood stream and enter the tissue by a process called neutrophil extravasation. This process consists of the attachment of neutrophils to the endothelial cells, rolling along the endothelium and firm attachment to the endothelial cells followed by transmigration into the tissue (Ley et al., 2007; Zarbock and Ley, 2008). During recruitment neutrophils are activated by selectin bound chemokines, which are produced by endothelial cells, by integrins and G-protein coupled receptors. Furthermore activation of neutrophils is

possible through Fc γ receptors (Fc γ R), the receptors for IgG immune complexes. Crosslinking of antibodies to Fc γ Rs leads to an activation of the cellular functions of neutrophils (McKenzie and Schreiber, 1998). After reaching the site of infection, the main function of activated neutrophils is the elimination of pathogens. This is mainly carried out by phagocytosis of the pathogen. In the endosome pathogens are killed by the production of highly toxic reactive oxygen species (ROS), generated by the NADPH-oxidase and by hypochlorous acid, which MPO produces from hydrogen peroxide. Furthermore fusion of the granules with the pathogen-containing endosome and release of the granule content (bactericidal peptides and proteases) into the endosomal lumen leads to the destruction of the engulfed pathogens. Neutrophil activation can also lead to an extracellular release of the granule content after fusion of the granules with the plasma membrane. This fusion can cause further neutrophil recruitment. Additionally, activation of neutrophils can result in the formation of neutrophil extracellular traps (NETs), an extracellular mechanism of bacterial killing. Here the pathogen is killed by the release of chromatin fibers which are decorated with antimicrobial peptides and enzymes (Brinkmann et al., 2004).

1.3.3 Neutrophil serine proteases (NSPs)

Besides the three neutrophil serine proteases (NSPs) proteinase 3 (PR3), neutrophil elastase (NE) and cathepsin G (CG), which are already known since over 30 years (Baggiolini et al., 1978), a fourth NSP, the neutrophil serine protease 4 (NSP4), was recently discovered (Perera et al., 2012). The genes for PR3 (PRTN3) and NE (ELA2/ELANE) are tightly linked together and form a gene cluster together with complement factor D (adipsin, AND or CFD) and azurocidin (AZU1) on the short arm of chromosome 19 (19p13.3) (Zimmer et al., 1992). The gene for NSP4 (PRSS57) is also located on the short arm of chromosome 19 (19p13.3), but outside of the AZU1-PRTN3-ELANE-CFD cluster (Perera et al., 2012). The CG gene (CTSG) belongs to a different gene cluster on chromosome 14 (14q11.2), containing the genes for chymase, granzyme H and granzyme B (Caughey et al., 1993). All four NSPs are synthesized as inactive zymogens. Only upon cleavage of the propeptide by the dipeptidyl aminopeptidase I (cathepsin C) NSPs are converted into a mature enzyme and adopt an enzymatically active conformation. After cleavage, the now accessible new N-terminus Ile16 can interact with Asp194 in the interior of the molecule and substrates can productively interact with the substrate binding pockets, in particular the S1 pocket (Freer et al., 1970). After biosynthesis, transport through a slightly acidic compartment and conversion by

cathepsin C, NSPs are stored as mature enzymes in the azurophilic granules in the neutrophil (Adkison et al., 2002; Korkmaz et al., 2010; Perera et al., 2013).

NSPs are released from azurophilic granules into the phagolysosome after phagocytosis of bacteria and neutrophil activation. In this way NSPs can participate in intracellular killing of pathogens in the pathogen-containing phagolysosome (Kobayashi et al., 2005). NSPs can further be involved in the extracellular killing after release of the granule content into the extracellular space. Here they can build a defense barrier against fungi, Gram-positive and Gram-negative bacteria. The important role of NSPs in the defense against pathogens has been confirmed in several studies. It could for instance be shown that NE and CG deficient mice are more susceptible to infections (Reeves et al., 2002). Furthermore NSPs are involved in the regulation of inflammation by proteolytic cleavage of chemokines, cytokines, growth factors and cell surface receptors. The proform of the inflammatory cytokines TNF α and IL-1 β , for example, can be cleaved and released via PR3 (Coeshott et al., 1999; Robache-Gallea et al., 1995). PR3, besides MMP-8 and MMP-9, also processes the pro-inflammatory cytokine IL-8 (Padrines et al., 1994). In addition PR3 and NE are able to proteolytically cleave the anti-inflammatory progranulin. This cleavage abolishes the anti-inflammatory effect of progranulin and thus has an enhancing effect on inflammation (Kessenbrock et al., 2008).

1.3.4 Protease specificity – The Schechter and Berger nomenclature

The degradation of proteins by proteases is limited by the specificity of the respective protease. This specificity is determined by the amino acid sequences of substrates that are cleaved by the protease. A nomenclature for the interaction of a protease and its substrates was introduced by Schechter and Berger (Schechter and Berger, 1967). To guarantee a successful cleavage of the peptide bond (scissile bond), a close interaction of the peptide and the active site cleft of the protease is necessary. Thus the active site of the protease mediates both the binding of the substrate as well as the catalyzing reaction, the cleavage of the amide peptide bond. The active site cleft in serine proteases contains the catalytic triad His57, Asp102 and Ser195 (numbering according to bovine chymotrypsinogen). In the context of the active site cleft, the hydroxyl group of the serine 195 is able to attack as a nucleophile the carbonyl carbon of the scissile peptide bond of the substrate, resulting in the hydrolysis of the peptide bond (Blow et al., 1969). The amino acid residues of the peptide, which are flanking the scissile bond, are designated as P-residues. The peptide is cleaved between the P1 and P1' residue (scissile bond). The residues, which are located on the N-terminal side of the scissile

bond are called P1, P2, P3, P4 etc. and the residues on the C-terminal side P1', P2', P3', P4' etc. The subsites in the protease close to the active site cleft, which take up the amino acids are numbered accordingly S1, S2, S3, S4 and S1', S2', S3', S4' etc. (Figure 1.1).

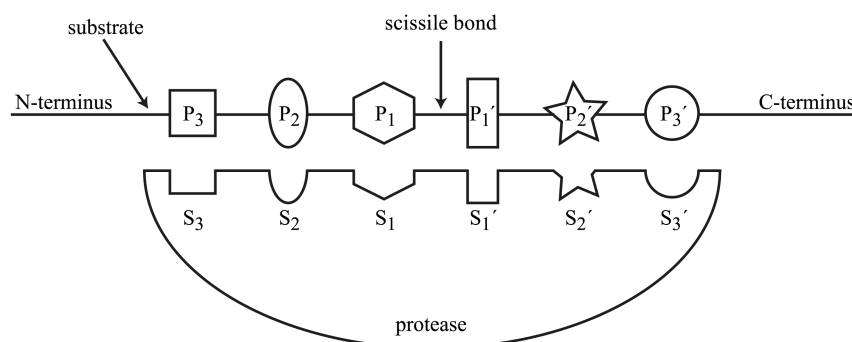


Figure 1.1: Schechter and Berger nomenclature. A tight interaction between the active site cleft of the protease and its substrate is necessary for proteolytic cleavage. The amino acid residues of the substrate, which are close to the cleavage site (scissile bond), are designated as P-residues. The P-residues on the N-terminal side of the scissile bond are called P1, P2, P3 etc.; on the C-terminal side the amino acids are called P1', P2', P3' etc. Cleavage takes place between the P1 and the P1' residue. The respective subsites in the protease, which interact with the amino acid residues of the substrate, are numbered accordingly S1, S2, S3, S1', S2', S3' etc.

1.3.5 Proteinase 3 (PR3)

PR3 is a multifunctional serine protease, formerly also known as p29b (Campanelli et al., 1990) and myeloblastin (Bories et al., 1989). It is a protein of 29 kDa. The crystal structure of PR3 consists of two β -barrels (Fujinaga et al., 1996), which is typical for serine proteases. After biosynthesis and cleavage of the propeptide by the dipeptidyl aminopeptidase I, PR3 is stored in azurophilic granules of neutrophils. Upon neutrophil activation in response to for instance infections, it is released into the phagolysosome or into the extracellular space. There it is involved in the clearance of pathogens with its antimicrobial activity. Additionally it is expressed on the surface of neutrophils (Halbwachs-Mecarelli et al., 1995). This surface expression occurs via a hydrophobic patch on the surface of the molecule, which can bind to the NB1 (CD177) receptor on neutrophils (Korkmaz et al., 2008). Besides antimicrobial activity, PR3 also exhibits proteolytic activity. Initially PR3 was described as a elastin degrading protein, which can cause pulmonary emphysema in hamsters (Kao et al., 1988). Apart from elastin, it is able to degrade matrix proteins, such as laminin, vitronectin, fibronectin and collagen type IV (Rao et al., 1991). Activity studies revealed an elastase-like P1 specificity of PR3 for small aliphatic residues like Ala, Val, Ser or Met (Rao et al., 1991). The proteolytic activity of PR3 is regulated by specific endogenous inhibitors, like α 1-proteinase inhibitor (α 1PI), elafin and α 2-macroglobulin.

Besides the role in emphysema, PR3 is associated with a number of other human diseases. Most important for this study is the role of PR3 in GPA. PR3 is the target antigen of ANCA (Jenne et al., 1990), which can be detected in the blood of patients with GPA. Additionally Bories et al. for example postulated an involvement of PR3 in the growth and differentiation of leukemia cells (Bories et al., 1989).

1.4 Anti-neutrophil cytoplasmic antibodies (ANCA)

The presence of ANCA has been first reported in patients with necrotizing glomerulonephritis in 1982 by Davies and Colleagues (Davies et al., 1982). A few years later van der Woude et al. observed a diffuse granular cytoplasmatic staining pattern of PR3-ANCA on ethanol fixed neutrophils (cANCA) and characterized PR3-specific ANCA as a clear marker for GPA (van der Woude et al., 1985). In contrast, ANCA, which are directed against MPO and associated with microscopic polyangiitis, usually display a perinuclear staining pattern (pANCA) (Falk and Jennette, 1988). About 80% to 90% of ANCA, found in GPA, are cANCA. As the target antigen of cANCA is in most cases PR3, a clear association of PR3-ANCA with GPA has been established (Hoffman and Specks, 1998). Due to this PR3-specificity of ANCA in GPA patients, PR3 autoantibodies as determined by ELISA are regarded and utilized as a highly reliable laboratory biomarker for the diagnosis of GPA. Besides systemic vasculitides, ANCA also appear at least transiently and occasionally in a number of other diseases, for example in rheumatic autoimmune disease, inflammatory bowel disease, autoimmune liver disease or infections (Hoffman and Specks, 1998).

1.5 The role of PR3, ANCA and the neutrophil immune response in GPA

As already mentioned in chapter 1.3.5 PR3 can be found on the outer membrane surface of neutrophils. The amount of surface accessible PR3, however, is heterogeneous and varies among individuals. In comparison to healthy control persons a higher proportion of neutrophils express PR3 on their surface in patients with GPA and this elevated proportion can influence the frequency of relapses (Kallenberg et al., 2006). This minor membrane-bound fraction of PR3 is the reason why ANCA are able to directly interact with neutrophils. ANCA binding then leads to activation of the neutrophils. Especially after priming of

neutrophils, for example with $\text{TNF}\alpha$, the membrane expression of PR3 is upregulated (Csernok et al., 1994), resulting in an augmentation of ANCA activation (Charles et al., 1991). Hence, membrane expression of PR3 is able to directly enhance neutrophil activation via ANCA. Besides the binding of the Fab (CDR) region of ANCA to PR3, the Fc domain of ANCA interacts with $\text{Fc}\gamma\text{Rs}$ and activates neutrophils via immunoglobulin receptors. Neutrophils express $\text{Fc}\gamma\text{RIIa}$ (CD32) and $\text{Fc}\gamma\text{RIIIb}$ (CD16) on their surface (Kocher et al., 1998; Porges et al., 1994). Interaction of the Fc domain of ANCA with $\text{Fc}\gamma\text{RIIa}$, for example, triggers neutrophil oxidative burst (Reumaux et al., 1995). Furthermore ANCA stimulation of neutrophils increases neutrophil adherence to endothelial cells (Ewert et al., 1992), leads to the generation of reactive oxygen species (ROS), the release of proteolytic enzymes (Falk et al., 1990) and secretion of proinflammatory cytokines (Brooks et al., 1996). Thus ANCA-mediated neutrophil activation causes inflammation of the vessel walls and the surrounding tissue and results in the development of necrotizing small-vessel vasculitis (Kallenberg et al., 2006). Besides the histopathological features of a necrotizing vasculitis, GPA is also characterized by granuloma formation and the role of ANCA in the development of these symptoms is still unclear. *In vivo* data rather suggest that this granulomatous inflammation is caused by cell mediated immune reactions rather than by ANCA-dependent mechanisms (Kallenberg, 2011). Furthermore, also microbial factors can play a role in GPA. 60% to 70% of patients are chronic carriers of *Staphylococcus aureus* and display an increased risk for relapses (Stegeman et al., 1994). Due to these facts, the role of PR3-ANCA on the pathogenesis of GPA still remains a matter of controversy and needs further clarification.

1.5.1 ANCA with inhibitory capacity towards PR3

Up to now, there is some disagreement as to whether changes in ANCA levels are a predictor for relapses in GPA patients. Rising levels of ANCA were found to be only weakly associated with disease activity (Finkelmann et al., 2007). Less than 10% of the variation in disease activity was shown to be correlated with changes in ANCA titers. A particular subset of ANCA, however, seemed to be a more promising indicator for the prediction of relapses. Some studies focused on the presence of ANCA, which reduced the catalytic activity of PR3 and impaired the inhibition of PR3 by α1PI . As a result of these studies, a close correlation of disease activity and the presence of inhibitory ANCA was repeatedly postulated (Daouk et al., 1995; Dolman et al., 1993; van der Geld et al., 2002). The outcome of these previous studies, however, has not been widely accepted. ANCA in all these studies clearly interfered with PR3

activity or PR3- α 1PI-complexation *in vitro*. Only Daouk et al. reported on data suggesting a correlation of inhibitory ANCA and disease activity (Daouk et al., 1995). Dolman et al. confirmed the inhibitory properties of ANCA with regard to the complexation of PR3 with α 1PI (Dolman et al., 1993). In a larger study with more patient samples (van der Geld et al., 2002), a correlation of ANCA, which interfered with the cleavage activity of PR3 towards casein, a macromolecular substrate, and disease activity was noticed. Inhibition of PR3 activity towards small synthetic substrates, however, did not occur in parallel with phases of active disease. Unexpectedly, during stable remission an even stronger inhibitory capacity of inhibitory ANCA was observed, indicating that these activity changing ANCA do not contribute to the pathogenesis of GPA (van der Geld et al., 2002). In view of these inconsistent and contradictory observations the significance of inhibitory ANCA and their impact on disease activity, clinical course and prognosis of the disease is still uncertain.

1.6 The role of protease inhibitors in GPA

1.6.1 Alpha-1-proteinase inhibitor (α 1PI)

The alpha-1-proteinase inhibitor (α 1PI) is an irreversible serine protease inhibitor and belongs to the serpin superfamily (serine protease inhibitor). As an acute phase plasma protein, it also plays an important role in acute inflammatory responses and immune defense reactions. Alpha-1PI consists of nine α -helices, three β -sheets and carries a flexible reactive center loop (RCL) on their surface. This loop is formed by 20 amino acid residues and acts as a pseudosubstrate for various target proteases (Gooptu and Lomas, 2009). Inhibition of proteases can be conducted in three different ways. Initially the protease binds to the RCL of the inhibitor and forms a Michaelis complex. In this complex the protease is only reversibly bound and is able to dissociate from the inhibitor. This form of complexation is called canonical inhibition. After formation of the Michaelis complex, the protease is able to catalyze the hydrolysis of the scissile bond in the RCL. After this cleavage, the protease can be released from the inhibitor, and is then free to cleave other substrates. In many instances, however, the protease is trapped and forms an ester bond with the P1 residue of the RCL after cleavage of the RCL. During this productive inhibitory reaction, the protease is translocated from one pole of the inhibitor to the other, opposite pole of the inhibitor. While the protease is covalently linked to the inhibitor, it undergoes a conformational change and adopts an

inactive zymogen-like conformation in the resulting complex. This complex exposes a new binding site, which is recognized by members of the lipoprotein receptor family. Protease-inhibitor complexes are rapidly cleared from the neutrophil membrane and removed from the interstitial fluids and the circulation (Gooptu and Lomas, 2009).

Up to now, more than 100 genetic variants of α 1PI have been identified. The most important genetic variants are the Z-allele, the S-allele, and the M-allele, which are named according to their migration position in a native gel after isoelectric focusing in the pH range between 4.5 and 5.5. Another well-known variant is the so-called null-variant. Those four alleles are associated with three major clinical categories according to their pathogenic potential. The by far most prevalent M-allele gives rise to normal plasma levels of α 1PI and is not associated with any risk for lung or liver diseases. In contrast the Z- and the S-allele are the most common deficiency alleles in the Caucasian population and lead to an increased risk for lung and liver diseases. Alpha-1PI levels in carriers of these alleles are reduced, but still detectable. The last group comprises patients which are homozygous for the null-variant. Here no plasma- α 1PI levels can be detected and the variant is associated with an increased risk for emphysema (Luisetti and Seersholm, 2004).

1.6.2 The role of α 1PI in GPA

In a recent genome wide association study (GWAS) both the gene locus of PR3 as well as the locus for its natural inhibitor, α 1PI, were identified as a genetic risk factor for GPA, but not for MPA. In particular, the Z-allele of α 1PI was confirmed as a risk factor in this GWAS (Lyons et al., 2012), which is consistent with a role of this protease inhibitor in GPA. In earlier studies, Segelmark et al. already reported a negative impact of the Z-allele on the disease outcome in GPA patients. A more disseminated disease and a worse prognosis in patients with the Z-allele, and thus with lower levels of functional α 1PI, was observed (Segelmark et al., 1995). Such a protease-antiprotease imbalance could also be detected in other studies on patients with GPA and thus a pathogenic role of α 1PI deficiency in conjunction with ANCA has been postulated (Esnault et al., 1993; Griffith et al., 1996; Savage et al., 1995). While inherited defects of the α 1PI gene were identified as a risk factor for GPA, PR3-ANCA acquired as a result of unknown environmental factors were also found to weaken the biological function of α 1PI. In both settings the PR3- α 1PI complexation reaction is affected. On the one hand ANCA can interfere with the complexation of PR3 with α 1PI,

which was found to be positively correlated with disease activity (Dolman et al., 1993). On the other hand low levels of α 1PI favor the binding of ANCA to surface-bound PR3 and thus neutrophil-mediated tissue damage. These observations are the basis of our current view about a beneficial effect of normal α 1PI levels in GPA patients (see e.g. Rooney et al., 2001).

1.7 Animal models for GPA

The pathogenesis of GPA is still a topic of controversial discussions. The significance of ANCA for the development of GPA, as well as their capacity to trigger GPA is still uncertain. The high mortality rate of GPA patients and limited treatment options has prompted many researchers to clarify the pathogenic basis of the disease process in GPA patients. Several animal models have already been developed, to study the pathogenicity of ANCA *in vivo*. Considering the differences in the structure and expression pattern of human and murine PR3, developing appropriate mouse models for GPA turned out to be difficult. On one hand, antibodies against human PR3 (hPR3) did not crossreact with murine PR3 (mPR3) (Jenne et al., 1997). On the other hand, the mPR3 molecule, in contrast to hPR3, was not found on the surface of naïve and primed mouse neutrophils (Pfister et al., 2004). In line with these findings, transfer of mouse PR3-specific antibodies, which were generated in PR3/NE deficient mice, into wildtype mice did not induce pathological changes (Pfister et al., 2004). Immunization of wildtype mice with a chimeric human/mouse PR3 molecule led to the production of antibodies against the chimeric PR3, but did not result in vascular lesions (van der Geld et al., 2007). To overcome the species barrier between human and murine neutrophils, a few models with humanized mice were evaluated. One approach was to reconstitute immunodeficient mice with the human immune system by injecting human hematopoietic stem cells. Transfer of PR3-specific antibodies from GPA patients into these mice did indeed lead to a mild pauci-immune proliferative glomerulonephritis, supporting the pathogenicity of ANCA in GPA (Little et al., 2012). However, expression of hPR3 at protein level and the presence of hPR3 on the neutrophil surface were not demonstrated in this model. Hence the mechanism for the development of glomerulonephritis in these mice remained unclear and obscure. Another humanized model was generated by Relle et al. Here the hPR3 cDNA was expressed with the help of the podocin promotor in transgenic mice. Expression of hPR3 was restricted to the kidneys. Injections of hPR3-specific antibodies, however, did not elicit renal pathology in these mice (Relle et al., 2013).

1.8 Objective

Despite numerous attempts to determine the role of ANCA at the onset and during progression of GPA with the help of animal models and large patient cohorts, the pathogenicity of ANCA is still a controversial topic. The aim of this thesis was to explore the mechanisms by which ANCA contribute to the development of GPA and influence disease progression and severity. For this purpose, two different approaches were chosen.

On one hand, the induction of small-vessel vasculitis by the action of ANCA was investigated using a newly developed humanized mouse model. As all initial attempts to generate an animal model of PR3-ANCA induced systemic vasculitis were inconclusive, a new mouse model on the basis of an hPR3 knock-in mouse was created. Transfer of mAbs and ANCA from patients should provide new insights into the pathogenicity of ANCA in GPA. Before transfer of antibodies into the humanized mouse line, expression of hPR3 in the knock-in mice had to be characterized. Removal of the neomycin cassette after insertion of the humanized PR3 locus was planned to improve the expression of the hPR3. However, this step necessitated the backcrossing of the knock-in mice onto a pure background. Furthermore the binding properties of different PR3-specific mAbs had to be analyzed to evaluate their potential as transfer antibodies. Antibodies of different subclasses were transferred into the hPR3 knock-in mice, to establish the animal model, and their potential to induce vasculitis-like and pulmonary lesions was explored.

In the second part of this thesis the question as to whether distinct subtypes of ANCA are able to modulate the activity of PR3, determine relapses, overall disease activity and organ involvement was addressed. The influence of ANCA, which inhibit PR3 activity, on the course of disease was often postulated. To determine if a relationship between activity modulating ANCA and disease activity exists, a large GPA patient cohort was analyzed. Therefore a new small scale approach to analyze the inhibitory properties of ANCA directly with small volumes of serum or plasma from GPA patients was developed. The activity modulating capacity of ANCA in the plasma samples from the patient cohort was determined with this new approach and correlated to disease severity and organ involvement. Furthermore potential activity modulating mechanisms of these ANCA were determined.

2. Material and Methods

2.1 Material

2.1.1 Chemicals and consumables

Chemicals were purchased from the companies Biozym (Hessisch Oldendorf, Germany), Merck (Darmstadt, Germany), Millipore (Billerica, MA, USA), Roth (Karlsruhe, Germany) and Sigma-Aldrich (St. Luis, MO, USA), unless mentioned otherwise. Consumables such as pipette tips, centrifuge tubes, reaction tubes and microwell plates were obtained from BD Biosciences (Franklin Lakes, NJ, USA), Biozym, Eppendorf (Hamburg, Germany), Millipore and Nunc/Thermo-Scientific (Waltham, MA, USA). Cell culture flasks were procured from Corning (Corning, NY, USA) and cell culture media from Gibco® Life Technologies (Carlsbad, CA, USA).

2.1.2 Plasmids

Plasmid	Construct	Origin
PR3-precursor(human)-pcDNA5	SigIgκ-proPR3-H ₆	Angelika Kuhl, AG Jenne
PR3-inactive(human)-pTT5	ΔhPR3-S195A	Heike Kittel, AG Jenne

The vector maps are provided in the Appendix (7.1).

2.1.3 Cell lines

The cell line HEK 293EBNA-1 was purchased from the NRC Biotechnology Research Institute, which is part of the National Research Council in Montreal, Canada.

2.1.4 Recombinant and purified proteins

Protein	Origin
α 1PI, human	Athens Research & Technology (Athens, GA, USA)
Elafin, human	Proteo Biotech AG (Kiel, Germany)
Neutrophil elastase, human	Elastin Products (Owensville, MO, USA)
Neutrophil elastase, mouse	Therese Dau, AG Jenne
Proteinase 3, human	Diarect AG (Freiburg, Germany)
Proteinase 3, mouse	Therese Dau, AG Jenne

2.1.5 Antibodies

Primary Antibodies

Antigen / Isotype control	Species	Clone	Provider	Cat. No.
Human PR3	Mouse	MCPR3-2	Ulrich Specks, Rochester, USA	-
		MCPR3-3	Ulrich Specks, Rochester, USA	-
		MCPR3-7	Ulrich Specks, Rochester, USA	-
		CLB-12.8	Sanquin	M9050
		4B12	AG Jenne/AG Kremmer IMI	-
		5B11	AG Jenne/AG Kremmer IMI	-
		7D12	AG Jenne/AG Kremmer IMI	-
Human PR3-biotin	Mouse	WGM2	Hycult Biotech	HM217BT
Human PR3-FITC	Mouse	WGM2	Hycult Biotech	HM217F
Mouse PR3	Goat	α -mPR3	AG Jenne/Animal facility MPI	-
IgG1 Isotype	Mouse	-	BD Biosciences	349040
IgG1 Isotype-FITC	Mouse	-	MACS Miltenyi Biotech	130-098-847
Mouse Ly6G-FITC	Rat	RB6-8C5	BD Biosciences	553126
IgG2b Isotype-FITC	Rat	-	BD Biosciences	553988

Secondary Antibodies

Antigen	Species	Label	Provider	Cat. No.
Mouse IgG+IgM	Goat	Peroxidase	Pierce (Thermo Scientific)	31444
Mouse Ig	Goat		Dako	Z0420
Goat IgG	Mouse	Peroxidase	Chemicon	AP186P
Human k-light chain	Goat	Peroxidase	Sigma-Aldrich	A-7164

Other

Protein	Label	Provider	Cat. No.
Avidin	Peroxidase	Invitrogen, Life Technologies	434423

2.1.6 Synthetic substrates

FRET substrates

Sequence	Cleaving protease	Provider
Abz-YYAbu-ANBNH ₂	PR3, NE	Adam Lesner, Gdansk, Poland
Abz-VADCADRQ-EDDnp	PR3	Brice Korkmaz, Tours, France
TAMRA-VADnVVADYQ-Dap(CF)	PR3, NE	EMC Microcollections
TAMRA-VADnVRDYQ-Dap(CF)	PR3	EMC Microcollections

Lipid anchored FRET substrate

Sequence	Cleaving protease	Provider
TAMRA-doo-VADnVRDRQ-doo	PR3	EMC Microcollections

SBzl substrates

Sequence	Cleaving protease	Provider
Boc-APnV-SBzl	PR3, NE	Bachem
For-AAPAbu-SBzl	PR3, NE	Bachem

pNA and ONp substrates

Sequence	Cleaving protease	Provider
Ahx-PYFA-pNA	PR3	Brice Korkmaz, Tours, France
Boc-A-ONp	PR3, NE	Sigma-Aldrich

2.1.7 Oligonucleotides

Oligonucleotides were synthesized by Metabion (Martinsried, Germany).

DJ3446	5'-TTA GCT GTG TGG CTT CAT GC-3'
DJ3447	5'-TAC CTT GAA CCT GGG AGG TG-3'
DJ3465	5'-TAC ACC CGC TGT GACCAT AA-3'
DJ3466	5'-AGC CAT GCT GGA CTC CTC TA-3'
DJ3467	5'-GTG GCT AGC TTG AGG TTT GG-3'
DJ3468	5'-CTG TGC AGA GCT TCA AAA CG-3'
DJ3536	5'-AGC TAC CCA TCC CCC AAG-3'
DJ3538	5'-ATG GCC AGG CAC TGG GT-3'
mActin-fw	5'-CTG GGC CGC CCT AGG CAC CA-3'
mActin-rev	5'-TGG CCT TAG GGT TCA GGG-3'

2.1.8 Mouse strains

Mouse strain	Background	Origin
129S6/SvEv wildtype	129S6/SvEv	-
PR3/NE knockout	129S6/SvEv	Markus Moser, MPI Biochemistry
hPR3 knock-in	129S6/SvEv	Markus Moser, MPI Biochemistry

2.1.9 Laboratory equipment

Balances	PM 4800 Delta Range, Mettler Toledo, Columbus, OH, USA XS205 Dual Range, Mettler Toledo, Columbus, OH, USA
Centrifuges	5417R, Eppendorf, Hamburg, Germany 5417C, Eppendorf, Hamburg, Germany Rotana 460R, Hettich, Tuttlingen, Germany Rotana/R, Hettich, Tuttlingen, Germany
Flow Cytometer	BD LSR II, BD Biosciences, Franklin Lakes, NJ, USA
FPLC	ÄKTAprime TM , GE Healthcare, Chalfont St Giles, Great Britain
Gel electrophoresis chambers/power supplies	Bio-Rad, Amersham-Pharmacia, MPI workshop
Incubation shaker	HAT Multitron, Infors, Bottmingen, Switzerland
Incubator	Heraeus B6, Thermo Scientific, Waltham, MA, USA
Ice machine	Ziegra, Isernhagen, Germany
Magnetic Stirrer	KMO2 basic, IKA, Staufen, Germany RCT basic IKAMAG, IKA, Staufen, Germany
Microplate reader	FLUOStar Optima, BMG Labtech, Offenburg, Germany Sunrise TM , TECAN, Maennedorf, Switzerland
Microscope	Leica DM IL, Leica Microsystems, Wetzlar, Germany
Molecular Imager	ChemiDoc TM XRS+, Bio-Rad, Hercules, CA, USA
PCR cycler	T3 Thermocycler, Biometra, Göttingen, Germany
Rotator	Fröbel Labortechnik, Lindau, Germany
Semidry Blotter	FastBlot, Biometra, Göttingen, Germany
Shakers	KS 260 basic, IKA, Staufen, Germany Polymax 1040, Heidolph, Schwabach, Germany
Spectrophotometer	BioPhotometer, Eppendorf, Hamburg, Germany
Stirring Cell	MPI workshop
Thermoblock	Thermomixer 5436, Eppendorf, Hamburg, Germany
Ultrasonic bath	Sonorex digital 10P, Bandelin, Berlin, Germany
Water bath incubator	MA6, LAUDA, Lauda-Königshofen, Germany
Water preparation	Milli Q Advantage, Millipore, Billerica, MA, USA

2.2 Molecular biological methods

2.2.1 Plasmid DNA purification from *E.coli*

Purification of Plasmid DNA from 2-5 ml overnight culture of *E.coli* was carried out with the QIAprep Spin Miniprep Kit from Qiagen. After alkaline lysis of the bacterial cells the DNA was bound to a silica membrane in high salt. For the purification of higher amounts of Plasmid DNA out of larger overnight cultures the PureYield™ Plasmid Maxiprep System (Promega) was used. Here the DNA was also bound to a silica membrane after alkaline lysis of the bacterial cells. Furthermore this purification procedure included an endotoxin removal step to remove protein, RNA and endotoxin contaminants from the DNA preparation. Both kits were used according to the manufacturer's instructions. The purified and endotoxin free Plasmid DNA was used for transfection of mammalian cells (HEK 293EBNA) in cell culture. Removal of endotoxin was necessary to avoid reduced transfection efficiency.

2.2.2 Polymerase chain reaction (PCR)

Polymerase chain reaction (PCR) is a method to amplify defined short DNA fragments from a larger DNA fragment. Therefor two oligonucleotides are used, flanking the two ends of the DNA strand, which should be amplified. These two primers contain a free 3'-OH at one end, ensuring the synthesis of the new strand in only one direction. The synthesis is carried out by a polymerase, which is adding and linking new nucleotides to the primers, generating the amplificate. One PCR cycle consists of denaturation of the DNA strand, in which the double helix is separated into single stranded DNA, annealing of the primers to the single strands and extension of the primers by the DNA-polymerase to generate the new strand. Replication of this cycle leads to an amplification of the required DNA fragment. For all PCRs the HotStarTaq DNA Polymerase from Qiagen was used.

HotStarTaq PCR reaction (25 µl):	1×	PCR buffer (Qiagen)
	0.2 mM	dNTP-mix
	0.4 µM	forward primer (10 pmol absolute)
	0.4 µM	reverse primer (10 pmol absolute)
	0.2 µl	HotStarTaq DNA polymerase
	1-2 µl	DNA template
		H ₂ O to 25 µl

Touchdown HotStarTaq PCR program:

15 min	95 °C	Denaturation	
30 s	94 °C	Denaturation	} 3 cycles
30 s	*	Annealing	
30 s	72 °C	Extension	
30 s	94 °C	Denaturation	} 3 cycles
30 s	**	Annealing	
30 s	72 °C	Extension	
30 s	94 °C	Denaturation	} 21 cycles
30 s	***	Annealing	
30 s	72 °C	Extension	
10 min	72 °C	Extension	

* primer specific annealing temperature + 6 °C

** primer specific annealing temperature + 3 °C

*** primer specific annealing temperature

2.2.3 Agarose gel electrophoresis

Due to their negatively charged backbone, DNA fragments can be separated in a gel matrix in an electric field according to their size. Depending on the size of the fragments the density of the agarose gels ranged from 0.7 to 2.0% (w/v). To visualize the DNA strands on the gels under UV ($\lambda = 254\text{-}366\text{ nm}$) SYBR safe (Life Technologies) or ethidium bromide was used. The agarose gels were prepared in TAE-buffer, adding SYBR safe 1:10 000 or 1 µg/ml ethidium bromide. After addition of DNA loading buffer, the samples were loaded into the gel slots and the gel was run in TAE-buffer at 80 V. To determine the size of the DNA fragments, the bands were compared to a molecular weight standard (Gene Ruler 1kb, Fermentas, Thermo Fisher Scientific).

TAE-buffer (50 ×):	242 g	Tris
	100 ml	0.5 M EDTA pH 8.0
	57.1 ml	acetic acid
		H ₂ O to 1 l

DNA loading buffer (10 ×):	0.25% (w/v)	bromphenol blue
	0.25% (w/v)	xylene cyanol
	50% (v/v)	glycerol

2.2.4 Restriction digest

DNA can be cleaved at specific recognition sites with restriction endonucleases. One unit of these restriction enzymes is defined as the amount of enzyme needed to digest 1 µg of DNA in one hour at an optimal temperature. The restriction enzymes were purchased from New England Biolabs (Ipswich, MA, USA) and the digests were carried out according to the manufacturer's instructions. 500 ng DNA were digested in a total volume of 20 µl for one hour at the temperature optimum of the respective enzyme.

2.3 Recombinant protein expression

Expression of the two different PR3-constructs was carried out in the HEK 293EBNA-1 (HEK 293E) cell line. This cell line carries a plasmid with the Epstein Barr Virus gene EBNA-1. The EBNA-1-gene is able to activate the episomal replication of plasmids, which carry the EBV origin of replication *oriP*, e.g. pTT5 (Durocher et al., 2002). Furthermore the plasmid contains a geneticin resistance marker (G418) for maintenance of this plasmid within the cell. The cells were cultured in suspension in HEK 293E medium in Erlenmeyer flasks at 37 °C, 8% CO₂ and 110 rpm in the incubation shaker.

HEK 293E medium:	1 ×	Freestyle™ 293 Expression Medium (Invitrogen)
	0.1% (v/v)	Pluronic® F-68
	25 µg/ml	Geneticin® G418

2.3.1 Transfection of HEK 293E

Prior to transfection HEK 293E cells were diluted to a concentration of 1×10^6 cells/ml in HEK 293E medium. Complexes of Polyethylenimin (PEI) and DNA were prepared in OptiPRO™ serum-free medium (Gibco® Life Technologies). Therefor 1 μ g DNA and 2 μ g PEI were used for 1 ml of cell culture suspension. Both were prediluted in OptiPRO™. The PEI dilution was added to the DNA dilution, incubated for 20 min at room temperature and then added to the cell suspension. After 5 to 24 hours Lactalbumin was added as an amino acid supply to a final concentration of 0.5%. The supernatant of the cells was harvested after four days.

2.4 Protein analysis

2.4.1 Purification of recombinant proteins

Proteins were purified from supernatants of transfected HEK 293E cells. Cell suspensions were centrifuged for 15 min at $2400 \times g$ and 4 °C. The supernatant was filtered through a 0.22 μ m membrane (Millipore), concentrated fivefold in a stirring chamber under nitrogen pressure (2.5×10^5 Pa) using an ultrafiltration membrane with 10 kDa cutoff and dialyzed in binding buffer overnight at 4 °C. Purification of 6 \times His-tagged Δ hPR3S195A and SigIgk-proPR3-H₆ was employed via nickel-affinity chromatography. HisTrap HP columns (GE Healthcare) were equilibrated in binding buffer. The protein solution was applied, the column washed with binding buffer and the proteins were eluted using a linear imidazole gradient ranging from 10 mM to 1 M imidazole in binding buffer. Fractions were collected and analyzed by SDS PAGE and silver staining to detect the protein of interest. Protein fractions were pooled and concentrated.

Binding buffer:	20 mM	Na ₂ HPO ₄
	500 mM	NaCl
	10 mM	imidazole
		pH 7.4

2.4.2 Determination of protein concentration

Spectrophotometric determination of protein concentration

To determine the protein concentration spectrophotometrically the absorbance of the protein solution was measured at $\lambda = 280$ nm and calculated with the following equation:

$$c = (A_{280} \times MW) / (\epsilon_{280} \times l)$$

(*c*, concentration; *A*, absorption; *MW*, molecular weight; ϵ , extinction coefficient; *l*, length of solution). To determine the extinction coefficient of each protein the program ProtParam (<http://us.expasy.org/tools/protparam.htm>) was used according to the respective amino acid sequence.

Determination of protein concentration by bicinchonic acid (BCA) assay

Protein concentration by BCA assay was determined by using the Uptima MicroBC Assay kit (Interchim, Montluçon Cedex, France) according to the manufacturer's instructions.

2.4.3 Sodium dodecyl sulfate polyacrylamide gel electrophoresis (SDS PAGE)

Discrimination of proteins according to their size was carried out by sodium dodecyl sulfate polyacrylamide gel electrophoresis (SDS PAGE). A discontinuous gel system was used, consisting of a stacking gel and a resolving gel. The stacking gel is slightly acidic and has a relatively low acrylamide concentration. Thus the protein sample is forming a thin sharp band before entering the resolving gel. In the resolving gel the higher concentration of polyacrylamide and a more basic pH lead to the separation of the proteins according to their size. The samples as well as the gels and the running buffer contained the detergent SDS. Binding of SDS to proteins unfolds their secondary structure. Furthermore it charges the proteins negatively according to their length, enabling a discrimination of the proteins relative to their size. The samples furthermore contained β -mercaptoethanol for the reduction of disulfide bridges. Prior to loading the samples were taken in sample buffer and boiled at 95 °C for 5 min. For comparison of protein sizes a molecular weight standard was used (Prestained Protein Marker, Broad Range, New England Biolabs).

	stacking gel	resolving gel
H ₂ O	13.6 ml	9.4 ml
30% polyacrylamide	3.32 ml	20 ml
1 M Tris HCl, pH 6.8	2.56 ml	
1.5 M Tris HCl, pH 8.8		10 ml
20% SDS	100 µl	200 µl
bromphenol blue	20 µl	
TEMED	14 µl	16 µl
10% APS	200 µl	400 µl

Running buffer (10 ×):	250 mM	Tris HCl
	1.92 M	glycine
	1% (w/v)	SDS

Silver nitrate staining

Fixation solution:	50% (v/v)	methanol
	12% (v/v)	acetic acid
	0.5 ml/l	37% formaldehyde

22

Silver nitrate solution: 2 g/l AgNO₃
 750 µl/l 37% formaldehyde

Development solution: 60 g/l Na₂CO₃
 4 mg/l Na₂S₂O₃ × 5 H₂O
 0.5 ml/l 37% formaldehyde

Coomassie staining

After SDS PAGE proteins were detected by staining the gels in Coomassie Blue staining solution for at least 30 min. To remove unspecific staining the gel afterwards was incubated in Coomassie Blue destaining solution until the protein bands became visible.

Coomassie Blue staining solution: 0.25% (w/v) Coomassie Brilliant Blue
 45% (v/v) methanol
 10% (v/v) acetic acid

Coomassie Blue destaining solution: 45% (v/v) methanol
 10% (v/v) acetic acid

2.4.5 Processing of proPR3 by enterokinase

ProPR3 was converted into its active conformation by calf enterokinase (Roche, Basel, Switzerland). After dialysis of the proteins against enterokinase buffer, the proteins were cleaved at an enzyme/substrate ratio of 1/40 at room temperature overnight.

Enterokinase buffer: 20 mM Tris HCl
 50 mM NaCl
 2 mM CaCl₂
 pH 7.4

2.4.6 Measurement of enzymatic activity

FRET-based activity assay

Activity of PR3 was measured over time by diluting PR3 to a final concentration of 50 nM in the respective buffer. After adding antibodies at a 2- to 15-fold molar excess the FRET-substrates were added and fluorescence was measured over time in the FLUOStar optima. For the substrate Abz-YYAbu-ANBNH₂ the proteins were diluted in Tris-HCl buffer, the FRET substrate was added at a concentration of 800 nM and the fluorescence was measured at $\lambda_{Ex} = 320$ nm and $\lambda_{Em} = 405$ nm. TAMRA-VADnVVADYQ-Dap(CF) or TAMRA-VADnVRDYQ-Dap(CF) was measured in activity assay buffer. 5 μ M of the FRET substrates were used and the fluorescence was determined at $\lambda_{Ex} = 485$ nm and $\lambda_{Em} = 520$ nm. Measurements with the substrate Abz-VADCADRQ-EDDnp (5 μ M) were carried out in activity assay buffer, and fluorescence was obtained at $\lambda_{Ex} = 320$ nm and $\lambda_{Em} = 405$ nm.

Absorbance-based activity assay

The activity of 50 nM PR3 in activity assay buffer was measured in absence and presence of a three-fold molar excess of MCPR3-7. Prior to measurement 1 mM Ahx-PYFA-*p*NA, Boc-A-ONp, Boc-APnV-SBzl or For-AAPAbu-SBzl were added and absorbance was determined at $\lambda_{Ab} = 405$ nm. In case of the thiobenzyl ester substrates 500 μ M 5,5'-dithiobis(2-nitrobenzoic acid) was added to the samples before measurement.

Tris-HCl buffer:	100 mM	Tris
	500 mM	NaCl
	0.01% (w/v)	Brij 39
		pH 7.5
Activity assay buffer:	50 mM	Tris
	150 mM	NaCl
	0.01% (v/v)	Triton X-100
		pH 7.4

2.5 Mouse model analysis

2.5.1 Isolation of genomic DNA from mouse tails

Tail biopsies (2-5 mm of the distal tail) were taken from mice at the age of 4-5 weeks. DNA was isolated out of these biopsies by Phenol/Chloroform extraction. After a Proteinase K digestion in 500 µl Tails buffer with 1 mg/ml Proteinase K overnight at 56 °C while shaking, the DNA was precipitated by adding 1 volume of Roti®-Phenol/Chloroform/Isoamyl alcohol, mixing and centrifugation at $20\,000 \times g$ for 10 min. The DNA was precipitated out of the aqueous phase by adding 1 ml 100% ethanol. After centrifugation at $20\,000 \times g$ for 10 min the DNA was washed with 400 µl 70% ethanol and again pelleted. The pellets were dried briefly at 37 °C and solved in 100 µl Tails buffer at 56 °C for 30 min while shaking.

Tails buffer: 20 mM Tris
 150 mM NaCl
 pH 7.5

2.5.2 Mouse-genotyping

After isolation of the DNA from mouse tail biopsies the genotypes were analyzed by PCR with HotStarTaq DNA polymerase (see chapter 2.2.2). With the primers DJ3446 and DJ3447 the hPR3-allele was amplified at the annealing temperatures 59 °C, 56 °C and 53 °C, represented by a band of 400 bp. The wildtype mPR3-allele was amplified with the primers DJ3467 and DJ3468 leading to a band of 450 bp (annealing temperatures: 61 °C, 58 °C and 55 °C). After cre-recombination the successful deletion of the neomycin cassette was verified with the primers DJ3465 and DJ3466, with 3 cycles at 59 °C, 3 cycles at 56 °C and 30 cycles at 53 °C. The result of this amplification was a band with 400 bp.

2.5.3 Isolation of bone marrow leukocytes

Bone marrow leukocytes were isolated from mouse femurs. After sacrificing the mice by CO₂ inhalation, both femurs were dissected, the ends of the bones were cut off and the bone marrow cells were flushed out of the bone with 5 ml PBS by using a syringe with a 21-gauge needle. After centrifugation ($500 \times g$, 5 min) the erythrocytes were lysed in 10 ml erythrocyte lysis buffer for 1-3 min at room temperature. The remaining bone marrow cells were again pelleted and then washed with 10 ml PBS.

Erythrocyte lysis buffer:	9 ml	0.8% NH ₄ Cl
	1 ml	0.2 M Tris HCl, pH 7.5

2.5.4 Isolation of neutrophils

Neutrophils were purified out of bone marrow cells from 2-4 mice. Therefor the bone marrow cells were flushed out of the femurs as described above with 5 ml RPMI 1640 (Gibco®, Life Technologies). The bone marrow solution was sent through a cell strainer to disperse the cells. The cell suspension was underlaid with 62.1% Percoll (GE Healthcare) in 3 × HBSS and centrifuged for 30 min at 500 × g and 4 °C without brake. The cell pellet, containing PMNs and erythrocytes, was resuspended in 10 ml erythrocyte lysis buffer (see chapter 2.5.3) and after 1-3 min at room temperature centrifuged for 5 min at 500 × g and 4 °C. The remaining PMNs were washed with RPMI 1640.

62.1% Percoll (15 ml):	5.69 ml	10 × HBSS
	9.32 ml	Percoll (GE Healthcare)

2.5.5 Reverse transcriptase (RT) PCR

Isolation of mRNA

After isolation of bone marrow leucocytes from mice, the cells were resuspended in 1 ml TRIzol® (Life Technologies) and incubated for 5 min at room temperature. 200 µl Chloroform were added to the solution, the solution was mixed and incubated at room temperature for 15 min. After centrifugation for 10 min at 13 000 × g and 4 °C, 500 µl of isopropanol were added to the aqueous phase. The solution was incubated at room temperature for 15 min. Afterwards it was centrifuged for 10 min at 13 000 × g and 4 °C, the pellet was resuspended in 1 ml 70% ethanol and again centrifuged for 5 min at 5000 × g and 4 °C. The pellet was dried for 10 min and then resolved in 20 µl RNase free water. To determine the RNA concentration, absorbance at $\lambda = 260$ nm was measured. For storage the RNA was frozen at – 80 °C.

Reverse transcription of mouse bone marrow mRNA

The transcription of mouse bone marrow mRNA into cDNA was carried out with the Verso cDNA synthesis kit (Thermo Fisher Scientific). One μg of mRNA and 0.5 μM reverse primer (Oligo dT) in a total volume of 12 μl were incubated at 65 °C for 10 min. Afterwards the solution was immediately chilled on ice. After adding 4 μl of 5 \times synthesis buffer, 2 μl 20 mM dNTPs, 1 μl RT-Enhancer and 1 μl Verso enzyme mix the transcription was performed at 42 °C for 30 min followed by 2 min at 95 °C.

PCR of mouse bone marrow cDNA

A homologous mouse/human PR3 transcript from bone marrow cDNA of heterozygous hPR3 knock-in mice was amplified by PCR as described in chapter 2.2.2. The HotStarTaq PCR was carried out with 1 μl of cDNA and the primers DJ3536 and DJ3538. The amplification consisted of 3 cycles at 58 °C annealing temperature, 3 cycles at 55 °C and 30 cycles at 52 °C. As a positive control β -actin was amplified with mouse β -actin primers. Here the program consisted of 3, 3 and 24 cycles with annealing temperatures at 65 °C, 62 °C and 59 °C.

2.5.6 Transfer of mAb into hPR3^{+/+} mice

Monoclonal antibodies against hPR3 were injected into 12-14 week old hPR3^{+/+} mice, to evaluate the potential of hPR3 antibodies to induce a GPA-like phenotype. Groups of three mice were used for each antibody. 300 μg anti-hPR3 mAb or isotype control antibody in 200 μl PBS were injected into the mice intraperitoneal. An hour later a mild inflammation was induced in the lungs of the mice by administration of LPS. Therefore the mice were anesthetized with isoflurane and 3 ng LPS in 50 μl PBS were applied intratracheally. At this concentration LPS alone or in combination with the isotype control did not induce an inflammatory phenotype. Seven days after the LPS administration the mice were sacrificed and the extent of inflammation in the lungs was analyzed. The antibody injection and the following analysis of the mice were carried out by André Tittel (Institutes of Molecular Medicine and Experimental Immunology, Rheinische Friedrich-Wilhelms Universität, Bonn, Germany).

2.5.7 Immune cell analysis after mAb transfer

Seven days after injection of the mAbs and LPS the mice were sacrificed and the lungs were dissected. The lung tissue of the left lung was used for the analysis of immune cell infiltration by flow cytometry. The tissue was digested in collagenase/DNase digestion media for 45 min at 37 °C. The solution was filtrated through a 100 µm filter and centrifuged at 300 × g and 4 °C for 5 min. All following centrifugation steps were carried out under these conditions. The cells were washed in FACS-buffer and the erythrocytes were lysed by incubation in RCB-buffer for 3 min. After another washing step 10% of the cells were used for FACS staining. The FcγR were blocked with 5 µg/ml Fc-block (2.4G2 hybridoma) for 15 min at 4 °C. The cells were washed and stained for 15 min at 4 °C with 100 µl antibody-dilution (1:200). A list of the used antibodies, labels and target cells is given below. After another washing step the cells were taken in 300 µl FACS-buffer and 20 000 APC-beads were added for correlation of the cell count. Data were collected at a BD Cantoll or BD Fortessa (BD Bioscience) and analyzed with the FlowJo software. Analysis of the immune cell infiltration was carried out by André Tittel (Institutes of Molecular Medicine and Experimental Immunology, Rheinische Friedrich-Wilhelms Universität, Bonn, Germany).

Antibodies:	FITC-MHCII	B cells, monocytes, macrophages, dendritic cells, activated T cells
	PE-F4/80	macrophages
	PE-Cy7-CD19	B cells
	PerCP-Cy5.5-Ly6C	macrophages and granulocytes
	APC-Ly6G	granulocytes
	APC-Cy7-CD45	hematopoietic cells
	BV421-CD11c	macrophages, dendritic cells, granulocytes, NK cells, T cells, B cells
	FITC-TCRβ	T cells
	PE-CD4	CD4 ⁺ T cells
	PerCP-Cy5.5-NK1.1	NK cells
	APC-CD8	CD8 ⁺ T cells
	BV421-CD45	hematopoietic cells

Antibodies were purchased from eBioscience or Biolegend.

Collagenase/DNase digestion media:	1 ×	RPMI 1640
	0.5 mg/ml	collagenase
	100 µg/ml	DNase
	20 mM	HEPES
	2 mM	L-Glutamine
	10% (v/v)	FCS
	0.1% (w/v)	β-mercaptoethanol
	10 ⁵ U	Penicillin
	0.1 g/l	Streptomycin
RCB-buffer:	145 mM	NH ₄ Cl
	12 mM	NaHCO ₃
	127 µM	EDTA disodium salt
		pH 7.3
FACS-buffer:	1 ×	PBS
	1% (v/v)	FCS (heat inactivated)
	0.5% (w/v)	NaN ₃

2.5.8 Periodic acid-Schiff (PAS) staining of lung slices

Seven days after injection of mAbs and LPS the mice were sacrificed, the lungs were dissected and the right lung was used for histology. The right lung was rinsed in PBS to remove the spilled blood and then fixated in 10% formalin for 2-3 days. The fixated tissue was embedded into paraffin cassettes and rinsed under running water for 2-3 hours. After dehydration of the organs with an ethanol row (50%, 75%, 96%, 100%) they were paraffinized. The paraffin blocks were cut with the microtome. The resulting slices were dried overnight to prevent solubilization of the slices during the staining process. For the PAS-staining the slices were incubated in xylol for 15 min and rehydrated with a decreasing ethanol row (100%, 96%, 75%, 50%). After one minute in water the slices were oxidized by 0.5% periodic acid for 5 min. The generated aldehyde groups were stained with Schiff reagent for 10 min. In the following the slices were incubated for 5 min in sulfite water, 5 min under running cold water, 5 min in hematoxylin and 5 min under running warm water. After shortly rinsing the slices in water they were again dehydrated with an increasing ethanol row and afterwards incubated in xylol for 5 min. After the staining the slices were mounted with Histomount, dried overnight and then analyzed with an IX71 microscope (Olympus). Staining and analysis were carried out by André Tittel and Magdalena Esser (Institutes of Molecular Medicine and Experimental Immunology, Rheinische Friedrich-Wilhelms Universität, Bonn, Germany).

2.6 Cell biological methods

2.6.1 Determination of cell count and viability

To determine the number of viable cells a hemocytometer (Neubauer-improved) was used. Cells were mixed in a 1:1 ratio with trypan blue solution. Trypan blue is able to enter perforated membranes of dead cells enabling discrimination of living and dead cells. The cells in the four quadrants of the hemocytometer were counted, the average was build and multiplied with the dilution factor. As the volume of one quadrant equates 100 nl the result was multiplied with 10^4 to determine the concentration of cells/ml.

Trypan blue solution: 0.1% (w/v) trypan blue
 1 × PBS pH 7.4

2.6.2 Isolation of PMNs from human blood

Blood was taken from volunteering healthy donors into 9 ml EDTA tubes to prevent clotting. The blood was transferred into a 50 ml tube and PBS was added to a total volume of 40 ml. The solution was carefully underlaid with Pancoll human (Pan Biotech, Aidenbach, Germany). After gradient centrifugation for 20 min at $500 \times g$ and 20 °C without brake, the PMNs and erythrocytes can be found at the bottom of the tube. Plasma, thrombocytes, and peripheral blood mononuclear cells (PBMCs) remain on top of the Pancoll layer. Plasma, thrombocytes, PBMCs and Pancoll were removed and the tube was filled with PBS to 40 ml. The solution was mixed with 8 ml of 6% dextran in PBS to sediment the erythrocytes. After 30 min incubation at room temperature, the PMNs in the supernatant were taken and centrifuged for 5 min at $500 \times g$. The remaining erythrocytes in the pellet were lysed by adding 5 ml 0.2% NaCl for 1 min. Five ml 1.6% NaCl were added for another minute. Then the solution was filled with PBS to 30 ml and again centrifuged for 5 min at $500 \times g$. PMNs were resuspended in PBS.

2.6.3 Preparation of total cell lysates

To lyse neutrophils isolated from mouse bone marrow or human blood, the cell pellets were resuspended in cold RIPA-buffer. 60 µl of RIPA-buffer were used for 5×10^6 cells. The cells were transferred into thin-walled PCR-tubes and incubated five-times for 5 min in the

ultrasonic bath. In between the solution was incubated on ice for 1 min. Afterwards cell debris and DNA was pelleted for 10 min at $20\,000 \times g$ and $4\text{ }^{\circ}\text{C}$.

RIPA buffer:	50 mM	Tris
	150 mM	NaCl
	0.5 M	EDTA
	0.5% (w/v)	deoxycholic acid
	0.1% (w/v)	SDS
	0.5% (w/v)	Nonidet P-40
		pH 8.0

2.7 Immunological methods

2.7.1 Western blot

Western blot analysis provides a method to detect specific proteins after SDS PAGE by applying specific antibodies. After separation of proteins according to their size by SDS PAGE, the proteins were transferred on a PVDF membrane by semidry electroblotting. The PVDF membrane was activated for 15 seconds in 100% methanol and then the gel and the membrane were equilibrated in western transfer buffer for 5 min. The transfer was carried out between four sheets of blotting paper, soaked in western transfer buffer. Proteins were transferred for 30 min at 5 mA/cm^2 . After the transfer the membrane was washed in H_2O and blocked to avoid unspecific binding. Therefor the membrane was incubated in blocking milk for one hour at room temperature. After three washing steps in PBS with 0.05% Tween 20 (PBS-T), the first antibody was applied in PBS-T at $4\text{ }^{\circ}\text{C}$ overnight. The membrane was washed three times with PBS-T and incubated for one hour at room temperature in the secondary antibody while shaking. The secondary antibody was coupled to horseradish peroxidase (HRP) and diluted in PBS-T. After another washing step the bound HRP-conjugates were visualized with chemiluminescence substrate (SuperSignal West Pico Chemiluminescent Substrate, Pierce). For development the ChemiDoc imaging system was used (Bio-Rad).

Antibody dilutions:	Goat anti-mPR3	1:1000
	Mouse anti-goat-HRP	1:1000

Further information on antibodies is provided in 2.1.7.

Western transfer buffer:	10% (v/v)	methanol, p.a.
	150 mM	glycine
	35 mM	Tris
		pH 8.3
Blocking milk:	1 ×	PBS-T
	5% (w/v)	Non-Fat Dry Milk Blocker, Bio-Rad
		pH 7.4

2.7.2 Enzyme-linked immunosorbent assay (ELISA)

ELISA with His-tagged proteins

The detection of His-tagged proteins or protein complexes was carried out by using nickel-coated 96-well plates. Proteins were coated in PBS with 0.05% Tween 20 (1 µg/ml; 100 µl/well) overnight at 4 °C. Between all following steps, the plates were washed three times with washing-buffer (Utecht & Lüdemann). All incubation steps were carried out by room temperature. The primary antibody was diluted in diluent-buffer (Utecht & Lüdemann) and incubated for one hour. After washing, a secondary, HRP-coupled antibody was added, also diluted in diluent-buffer and incubated for one hour. The reaction was developed using ABTS[®] peroxidase substrate (KPL, Gaithersburg, MD, USA) and OD values were obtained at $\lambda_{Ab} = 405 \text{ nm}$.

Capture ELISA

For the detection of antigen in solution a capture ELISA approach was used. An antigen specific antibody was coated on 96-well maxisorp plates. The antibody was diluted in coating buffer, yielding a concentration of 100 ng/well and incubated overnight at 4 °C. Between all following steps, the plate was washed three times in PBS with 0.05% Tween 20 and all incubation steps were carried out at room temperature. To prevent unspecific binding the wells were blocked for one hour in blocking buffer. The solution containing the antigen was diluted in blocking buffer and incubated for one hour. Afterwards the primary antibody (1 µg/ml in blocking buffer) was added and also incubated for one hour. As primary antibody a biotinylated antibody was used, to enable discrimination of coating antibody and primary antibody. Avidin-HRP was added and incubated for one hour. The reaction was developed with ABTS[®] peroxidase substrate (KPL, Gaithersburg, MD, USA) and OD values were measured at $\lambda_{Ab} = 405 \text{ nm}$.

Antibody dilutions:	MCPR3-2	1:5000
	MCPR3-7	1:200
	CLB-12.8	1:1000
	IgG1 Isotype control	1:50
	WGM2-biotin	1:700
	Goat anti-mouse-HRP	1:2500
	Human k-light-chain-HRP	1:1000
	Avidin-HRP	1:20000

Further information on antibodies is provided in 2.1.7.

Coating buffer:	10 mM	Na ₂ CO ₃
	10 mM	NaHCO ₃
		pH 9.4

Blocking buffer:	140 mM	NaCl
	3 mM	KCl
	8 mM	Na ₂ HPO ₄
	1 mM	KH ₂ PO ₄
	0.05% (v/v)	Tween 20
	2% (w/v)	BSA
		pH 7.4

2.8 Flow cytometry

2.8.1 Cell surface staining of PR3

Neutrophils isolated from human blood or mouse bone marrow were stained for PR3 expression on their surface. 2×10^5 cells were taken in 200 μ l PBS. After centrifugation for 10 min at $300 \times g$ and 4 °C the cells were activated by adding 10 ng/ml TNF α or 200 ng/ml PMA for 15 min at 37 °C. Prior to activation with PMA cells were incubated with cytochalasin B (5 μ g/ml) for 5 min at 37 °C. The primary antibody, diluted in PBS, was added and incubated for 30 min at 4 °C. Cells were washed three times in PBS. The FITC-coupled secondary antibody was diluted in PBS, added to the cells and incubated in the dark for 30 min at 4 °C. Cells were washed again in PBS and then fixated in PBS with 2% PFA. Between all steps cells were centrifuged for 10 min at $300 \times g$ and 4 °C. Until measurement, fixated cells were kept in the dark at 4 °C. Data were collected at LSRII (BD Bioscience) and analyzed with the FlowJo software.

2.8.2 Measurement of PR3 activity on the cell surface

For measurement of PR3 activity on the surface of PMNs, a FRET substrate bound to a lipid-anchor was inserted into the membrane of the cells. Cleavage of the FRET substrate by membrane-bound PR3 results in a fluorescence signal on the cell surface. First 2×10^5 freshly isolated neutrophils were activated with 10 ng/ml TNF α for 15 min at 37 °C or with 5 μ g/ml cytochalasin B for 5 min at 37 °C followed by 200 ng/ml PMA for 15 min at 37 °C. The cells were centrifuged at $300 \times g$ and 4 °C for 10 min and 1 μ M lipidated FRET substrate in PBS was added on ice. The cells were incubated in the dark for 30 min at 4 °C or 37 °C. After another centrifugation step, the cells were washed with PBS and fixated in PBS with 2% PFA. Until measurement at LSRII fixated samples were kept at 4 °C in the dark.

2.9 Thermophoresis

2.9.1 Fluorescent labeling of proteins

Proteins were labeled with the fluorescent dye NT-647 by attaching the dye via its *N*-hydroxysuccinimide ester to primary amines of lysine residues. Prior to labeling proteins were dialyzed overnight at 4 °C in PBS. Labeling was carried out by adding a 6.5-fold molar excess of NT-647 to the protein and incubation for 30 min at room temperature. Free dye was removed afterwards by dialyzing in PBS overnight at 4 °C.

2.9.2 Thermophoretic quantification

Thermophoretic quantification was carried out together with Susanne A. I. Seidel (Systems Biophysics and Functional Nanosystems, Ludwig-Maximilians-Universität München, Germany). By thermophoresis movement of molecules along a temperature gradient can be measured. Thus changes in charge or size can be detected, enabling the measurement of binding affinities between different molecules. To quantify affinities between two proteins or protein complexes, a dilution series of the unlabeled protein was prepared. The dilution series always started at a concentration above the estimated affinity constant of the two proteins of interest. Consistent amounts of labeled protein were added to the samples of the dilution series and the samples were filled into standard treated enhanced gradient capillaries (NanoTemper Technologies, Munich, Germany). To avoid adsorption to the capillary walls, BSA was added to all samples at a final concentration of 1% (w/v). Measurements were

performed at a constant ambient temperature of 20 °C on a Monolith NT.115 system (NanoTemper Technologies). Analysis of the obtained data was carried out by Susanne A. I. Seidel as recently published (Seidel et al., 2013).

2.10 Patient material analysis

2.10.1 Precipitation of total IgG from plasmapheresis material

Purification of IgGs from plasmapheresis material was carried out by ammonium sulfate precipitation. Plasmapheresis material from GPA patients was mixed with a saturated $(\text{NH}_4)_2\text{SO}_4$ solution to a final concentration of 50%. Precipitation of immunoglobulins takes place at a final ammonium sulfate concentration of 40-50%. For precipitation the solution was stirred one hour at room temperature. Afterwards the precipitated antibodies were pelleted for 20 min at $4000 \times g$. The pellet was resuspended in PBS and dialyzed in dialysis tubes with 50 kDa cutoff in PBS for 72 hours at 4 °C. During the first 24 hours PBS was exchanged every 4-6 h and dialysis was carried out without stirring. After 24 hours the buffer was only exchanged every 8-12 hours and the solution was stirred. The antibody solution was concentrated three-fold in a stirring chamber under nitrogen pressure (2.5×10^5 Pa) using an ultrafiltration membrane with 100 kDa cutoff.

2.10.2 Affinity purification of PR3-specific ANCA

Chemical biotinylation of PR3

N-hydroxysuccinimide ester coupled biotin (NHS-biotin) was used for the labeling of recombinant PR3. NHS-biotin reacts with primary amines and labels proteins for example by binding to the side-chain of lysine residues. Prior to labeling recombinant PR3 was dialyzed in PBS at 4 °C overnight. The NHS-biotin was added to the protein in a 20-fold molar excess, and the solution was incubated for two hours on ice. Unbound NHS-biotin was removed by another dialysis step in PBS at 4 °C overnight.

Affinity purification

Total IgG solutions, precipitated from plasmapheresis material of patients with GPA (see chapter 2.10.1), were used to extract PR3-specific ANCA. To remove precipitated proteins from the IgG solutions, the IgGs were ultracentrifuged for one hour at $166\,880 \times g$ and filtered through a $0.5\,\mu\text{M}$ syringe filter. All solutions were kept at room temperature during the purification, to avoid further precipitation of proteins. Purification of PR3-specific ANCA was carried out by streptavidin-affinity chromatography. HiTrap Streptavidin HP columns were equilibrated in solubilization buffer. Biotinylated PR3 was taken in solubilization buffer, by adding 1/10 volume $10 \times$ solubilization buffer and bound to the columns. After washing the column the IgG solution was applied after adding 1/10 volume $10 \times$ solubilization buffer. Another washing step was carried out before PR3-specific ANCA were eluted from the column with 0.1 M Glycin/HCl pH 2.5. Eluted antibodies were immediately neutralized by adding 1/4 volume Tris HCl pH 9.0. Presence of PR3 reactive antibodies in the elution fractions was tested via ELISA.

Solubilization buffer ($10 \times$):

5% (w/v)	Na-deoxycholate
10% (v/v)	NP-40
0.2% (w/v)	NaN_3
	in PBS pH 7.4

2.10.3 Protein G purification of antibodies from patient plasma

For the purification of total IgGs out of patient plasma, the plasma was mixed with 1 volume of PBS with 0.05% Tween 20 (PBS-T). One μl magnetic Protein G dynabeads (life technologies) per 2.5 μl patient plasma was added. After rotation of the mixture for one hour at room temperature the beads were washed three times with PBS-T. IgGs were eluted from the beads by adding 0.1 M Glycin/HCl pH 2.5. The amount was geared to the original plasma volume, enabling an estimation of the IgG concentration in the eluted fractions. 9/10 volume Glycin/HCl of the original plasma volume was used for the elution. After incubation for one minute the fluid was separated from the beads with a magnetic rack. The pH of the elution fraction was neutralized by adding Tris HCl, pH 9.0 (1/10 volume of the original plasma volume).

2.10.4 Measurement of inhibitory capacity of ANCA from patient plasma

The effect of ANCA from patient material on the activity of PR3 was measured with the FRET-substrate TAMRA-VADnVRDYQ-Dap(CF) (2.5 μ M; λ_{Ex} = 485 nm, λ_{Em} = 520 nm). PR3 was diluted in activity buffer to a concentration of 10 nM. The concentration of total IgGs in our elution fraction was similar to the IgG concentration in plasma. Thus the concentration of total IgGs was estimated to be 100 μ M. Based on the assumption, that approximately 0.1% of the total IgGs are PR3-specific ANCA, the expected concentration of ANCA in our IgG fraction was 100 nM. ANCA were added to PR3 at an about four-fold molar excess. As control IgGs purified from healthy control persons were used. The relative PR3 activity was calculated in relation to PR3 activity in presence of control IgGs, which was set to 1. To reduce the amount of patient sample needed for the assay the measurements were carried out in black 384-well plates. All tests were performed in duplicates and the inter- and intra-assay variances were calculated.

Activity buffer:	50 mM	Tris
	150 mM	NaCl
	0.01% (v/v)	Triton-X100
		pH 7.4

2.11 Statistical analysis

Results are given as the average with the standard error of the mean (SEM) or in case of the thermophoretic measurements as the mean with standard deviation (SD). In case of the patient data, the median values of BVAS and PR3 inhibition were calculated and displayed with the range of the respective values. Statistical differences of the groups of patient samples were tested by Mann-Whitney U-test. The statistical differences in the activity assay approach with proPR3 were determined with OneWayAnova. Correlation between ANCA binding to PR3 and PR3-elafin complexes was analyzed by the Spearman rank correlation test. The level of significance was 0.05. Calculations were carried out with the GraphPad Prism software.

3. Results

3.1 Generation of hPR3 knock-in mice

To investigate the *in vivo* role of human autoantibodies in the development and progression of GPA a new transgenic mouse line was generated. In this line, the endogenous murine gene segment for PR3 was replaced by a human genomic fragment with four human exons covering the mature reading frame. This so-called hPR3 knock-in mouse line was created by homologous recombination of a targeting construct in murine embryonic stem cells. By transferring PR3-specific antibodies from patients (ANCA), as well as monoclonal antibodies (mAbs) against PR3 into these knock-in mice, new insights in their pathogenicity can be obtained.

The first step in the generation of the hPR3 knock-in mice (hPR3^{+/+} mice) was the design of a humanized PR3/NE targeting vector. This was already carried out by Leopold Fröhlich and Therese Dau prior to the work presented here. In the humanized PR3/NE locus exon 2 to 5 of the mPR3 were replaced by the hPR3 gene (Figure 3.1). To ensure the expression of hPR3 under natural conditions the humanized locus still consists of the promoter region up to exon 1 and the major portion of intron 1 of the wildtype murine gene. As the exon 1 only contains the murine signal peptide, the resulting protein represents the complete human proform of the hPR3 gene. At the 3' end of the humanized PR3 gene segment a neomycin cassette was inserted. The neomycin cassette was flanked by two loxP sites, enabling a later removal of the cassette by cre-recombinase. The first chimeric founder animals were generated by Markus Moser (Max Planck Institute of Biochemistry, Munich, Germany) and then bred by me to homozygosity. Initial attempts to detect the expressed PR3 protein in these hPR3^{+/+} knock-in mice were made, but only very low levels were found (carried out by Therese Dau).

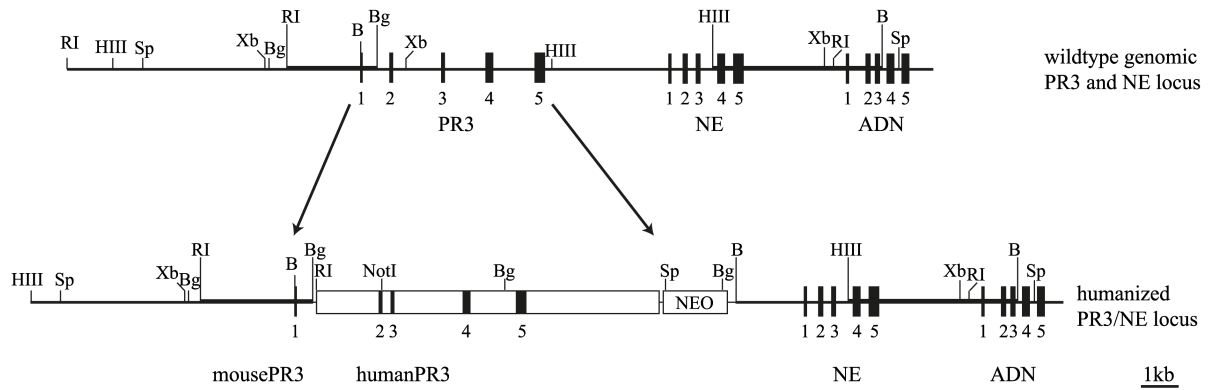


Figure 3.1: Humanized knock-in locus, used for the generation of hPR3^{+/+} mice. In the wildtype genomic PR3 and NE locus exon 2 to exon 5 was replaced by the human PR3 gene locus. The promotor region up to exon 1 still consists of the murine gene in the humanized locus, to ensure expression of hPR3 under wildtype conditions. A neomycin cassette flanked by two loxP sites was inserted downstream from the humanized PR3 gene.

3.1.1 Removal of the neomycin and backcrossing to 129S6/SvEv background

To improve the expression of hPR3 in the knock-in mice, the neomycin cassette was removed via cre-mediated recombination at an early embryonic cell stage. For this purpose C57BL/6 mice with an X-linked cre-recombinase gene were mated to the homozygous hPR3^{+/+} 129S6/SvEv mice. These pairings only resulted in heterozygous female offspring, carrying the rearranged hPR3 knock-in locus. The reason for this gender bias is that male offspring with the cre-recombinase locus on the X chromosome is not viable. Due to this crossing with a C57BL/6 mouse line, the knock-in locus was on a mixed background. The females with the rearranged hPR3 knock-in locus were, therefore, crossed back to wildtype 129S6/SvEv mice, to obtain heterozygous knock-in mice of both genders. This first breeding step was the first in a series of backcrossing steps, in order to receive mice on a pure 129S6/SvEv background. In total the mice were backcrossed to 129S6/SvEv wildtype mice for seven generations. The heterozygous offspring of the seventh generation on an almost pure 129S6/SvEv background were then bred to homozygosity and maintained as an inbred line.

3.2 Characterization of hPR3 expression in hPR3^{+/+} mice

3.2.1 Human PR3^{+/+} mice express hPR3

To examine, if hPR3 is expressed in hPR3^{+/+} mice to the same extend as the endogenous murine PR3 gene (mPR3) in wildtype mice, RNA transcription in heterozygous knock-in mice was determined. RNA isolated from bone marrow cells was transcribed into cDNA and a highly homologous part of mPR3 and hPR3 was amplified with primers that perfectly matched both the murine and the human sequence. With an hPR3 specific digest the amount of human and mouse DNA could be compared (Figure 3.2 A). The 440 bp amplicate was digested with *SacI*, resulting in two bands of 270 bp and 170 bp, representing the hPR3. The mPR3 gene remained uncut. In comparison to undigested DNA, the amount of uncut mPR3 after *SacI* digest equaled about half the amount of undigested DNA. Furthermore the two digested bands of hPR3 when taken together made up approximately the same amount of DNA as the uncut mPR3 band. In Figure 3.2 B the expression of hPR3 in knock-in mice at protein level was compared to the expression of hPR3 in human PMNs (hPMNs) and mPR3 in wildtype murine PMNs (mPMNs). Using recombinant hPR3 and mPR3 as protein standards, the PR3 amount in hPMNs and wildtype mPMNs was determined semi quantitatively by western blotting. Human PR3 from hPR3^{+/+} PMN lysate could not be detected by western blotting. The antibody used for detection of PR3 by western blotting, was originally raised against mPR3. Therefore cross reactivity with hPR3 was weaker and detection of low amounts of hPR3 was not possible. For that reason protein expression of hPR3 in hPR3^{+/+} mice was analyzed by capture ELISA. PR3 from hPR3^{+/+} PMN lysates was captured with a PR3-specific antibody and then detected with a biotinylated PR3-specific antibody. For quantitative comparisons a specified quantity of recombinant hPR3 was captured. The total amount of PR3 in lysates obtained from 1×10^6 cells was calculated in all three cases. This comparison revealed much higher protein expression in humans ($1.5 \mu\text{g}/1 \times 10^6$ cells) than in wildtype mice ($500 \text{ ng}/1 \times 10^6$ cells). Moreover, the expression of the hPR3 knock-in gene in mice was found to be reduced further in comparison to the endogenous mouse protein, mPR3. Only 75 ng hPR3 were detected in 1×10^6 cells.

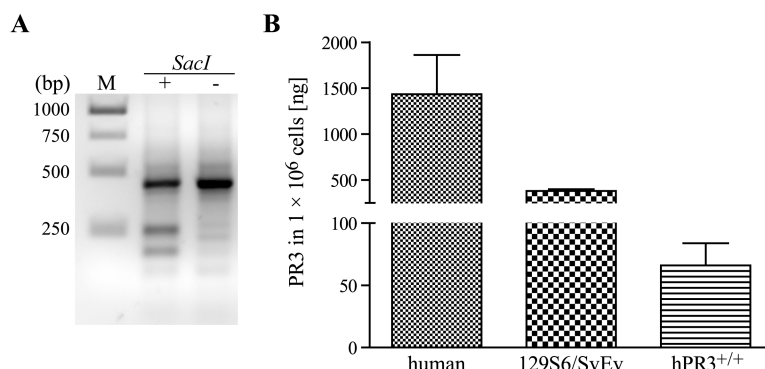


Figure 3.2: Human PR3 is expressed in hPR3^{+/+} PMNs. A, RNA isolated from neutrophils of heterozygous hPR3 knock-in mice was translated into cDNA and a homologous genomic segment of 440 bp was amplified. Differences in transcription of human and mouse PR3 were detected by *SacI* digestion. *SacI* solely digests the human fragment, resulting in two smaller bands (270 bp and 170 bp). Total amounts of mouse and human cDNA have been compared. One example of three independent experiments is shown. B, Expression levels of hPR3 in hPMNs and mPR3 in wildtype mPMNs were determined by western blotting. Freshly isolated neutrophils were lysed and analyzed by SDS PAGE and immunoblotting. Human and mouse PR3 were detected with a goat anti-mPR3 polyclonal antibody. Expression levels were determined semi quantitatively in comparison to increasing amounts of recombinant human PR3. PR3 expression in hPR3^{+/+} PMNs was examined by ELISA. PR3 from neutrophil lysates was captured with immobilized MCPR3-2 and detected via WGM2-biotin. The amount of PR3 in 1×10^6 PMNs was calculated in all three cases in comparison to specified amounts of recombinant human PR3 ($n = 3$, \pm SEM). (M, molecular weight standard)

3.2.2 Human PR3 expressed in hPR3^{+/+} mice is catalytically active

Successful generation of an animal model for GPA not only demands expression of hPR3 in neutrophils of the knock-in mice but also correct folding, integrity and functionality of hPR3 in mouse neutrophils. The hPR3 expressed in hPR3^{+/+} knock-in PMNs was tested for its catalytic activity in an *in vitro* activity assay. Cleavage of the PR3-specific FRET substrate Abz-VADCADRQ-EDDnp by PR3 was determined in different neutrophil lysates prepared for human and mouse neutrophils (Figure 3.3). Added to lysates of human PMNs the substrate was cleaved rapidly, due to the high amount of hPR3 present in human PMNs. Besides hPR3, mPR3 is also able to cleave the FRET substrate. However, mPR3 cleaves the substrate with more than ten-fold lower efficacy. Hence, a fluorescence signal was also obtained by adding the FRET substrates to a lysate of 129S6/SvEv wildtype PMNs. But more importantly, the hPR3 present in lysates of homozygous hPR3^{+/+} PMNs also cleaved the FRET substrate, indicating the presence of a catalytically active human enzyme. The fluorescence detected in hPR3^{+/+} lysates, however, was only slightly higher than the signal in 129S6/SvEv lysates, despite the better cleavage by hPR3. This result is explained by the much lower expression levels of hPR3 in hPR3^{+/+} PMNs in comparison to mPR3 in 129S6/SvEv PMNs as

demonstrated in Figure 3.2 B. As negative control, lysates of PR3/NE double knock-out PMNs (PR3/NE^{-/-}) were used, to exclude cleavage of the substrate by other proteases.

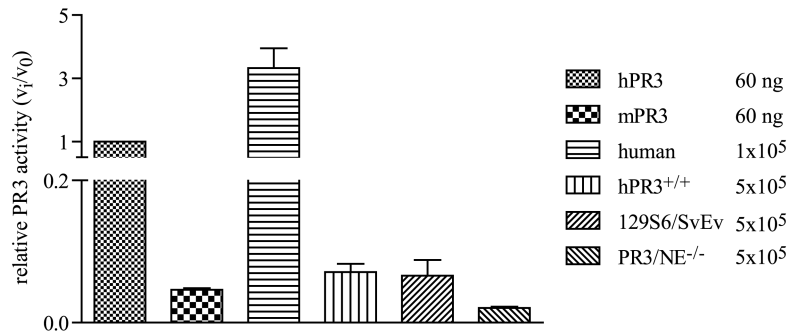


Figure 3.3: Human PR3 in hPR3^{+/+} PMNs is catalytically active. Functional activity of PR3 from hPR3^{+/+} mice was assessed with a PR3 specific FRET substrate (Abz-VADCADRQ-EDDnp, $\lambda_{Ex} = 320$ nm, $\lambda_{Em} = 405$ nm). Five μ M of FRET substrate were added to 50 nM PR3 and to lysates of 1×10^5 hPMNs or 5×10^5 mPMNs. PR3 activity was measured over time ($n = 3$, \pm SEM). The fluorescence signal obtained in 129S6/SvEv mice can be traced back to mPR3 activity. Murine PR3 is also able to cleave this FRET substrate, but with much lower efficacy than hPR3.

3.2.3 Human PR3 in hPR3^{+/+} mice is transported to the neutrophil surface

ANCA binding to PR3 on the surface membrane of neutrophils is thought to be one of the key steps for the pathogenicity of ANCA in GPA. In humans PR3 is clearly expressed on the surface of unprimed and primed neutrophils. Flow cytometry analysis revealed a surface signal of PR3 in about 90% of unstimulated hPMNs after purification (Figure 3.4 A). TNF α did barely increase the proportion of cells, expressing PR3 on their surface in comparison to unstimulated cells (Figure 3.4 B). Stimulation with PMA, however, led to activation and stronger membrane exposure of PR3 in all neutrophils (Figure 3.4 C and D).

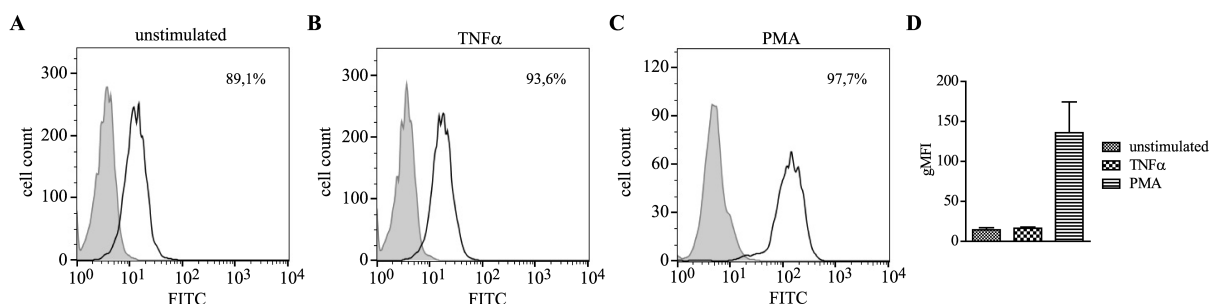


Figure 3.4: Human PR3 is strongly expressed on the surface of hPMNs. Surface expression of PR3 in hPMNs was analyzed by FACS staining. Unstimulated PMNs (A), TNF α -primed (B) and PMA activated (C) PMNs were stained for PR3 with WGM2-FITC (black line). As negative control, cells were stained with a FITC-labelled IgG1 isotype control antibody (gray curve). One representative example for each condition is shown. D, Geometric mean fluorescence (gMFI) of PR3 positive cells was calculated ($n = 3$, \pm SEM).

Due to a lack of mPR3 on the surface of mPMNs (Pfister et al., 2004), the question arises as to whether hPR3 in hPR3^{+/+} mice is able to bind to the plasma membrane of mouse neutrophils. Human PR3 is known to bind to the NB1 receptor on the neutrophil surface and to lipid bilayers via a hydrophobic patch on the surface of hPR3 (Goldmann et al., 1999; Korkmaz et al., 2008). In mice, surface expression of hPR3 was tested by FACS analysis. No hPR3 could be detected on the surface of unstimulated or TNF α -primed hPR3^{+/+} PMNs (Figure 3.5 A and B). In PMA stimulated cells hPR3 was detected on the surface (Figure 3.5 C), but the antigen levels were much lower than those on the surface of hPMNs. To ensure correct gating of the cells, neutrophils were stained with anti-Ly6G as a positive control.

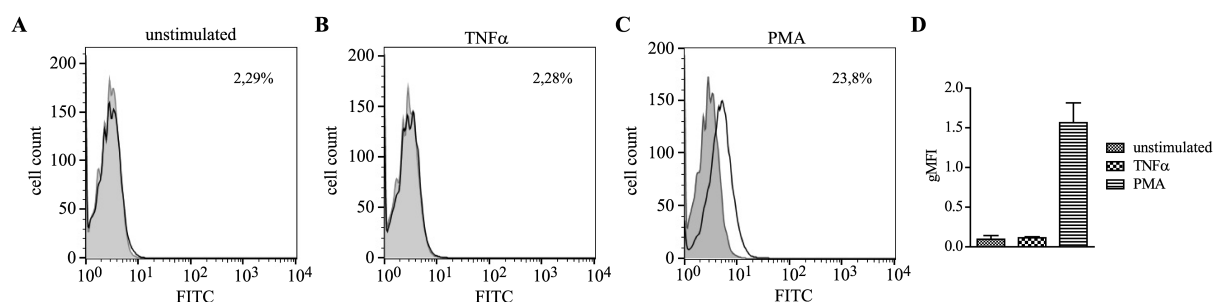


Figure 3.5: Surface expression of hPR3 on hPR3^{+/+} neutrophils after PMA stimulation. PR3 expression on the surface of hPR3^{+/+} PMNs was detected by FACS analysis. PR3 was stained with WGM2-FITC (black line) on the surface of unstimulated (A), TNF α -primed (B) and PMA activated (C) PMNs. An IgG1-FITC isotype control antibody (gray curve) was used as negative control. One representative example of three independent experiments is shown. D, Differences in fluorescence signals were obtained by calculating the geometric mean fluorescence (gMFI) of the PR3 positive cells (n = 3, \pm SEM).

3.2.4 PR3 on the surface of hPR3^{+/+} neutrophils is active

For membrane binding of PR3 and exposure of conformational epitopes it is not only important, that the PR3 antigen is detectable on the surface of the hPR3^{+/+} neutrophils. The protease on the surface should also be folded as a catalytically active, mature serine protease, exposing conformational epitopes. First of all the activity of PR3 on the surface of hPMNs was analyzed (Figure 3.6). For this purpose a FRET substrate linked to a lipid anchor was used. The lipid anchor of this substrate inserts into the membrane of neutrophils. Active PR3 on the neutrophil surface can then cleave the attached FRET substrate and thus a fluorescence signal associated to the cellular surface can be measured. On hPMNs a fluorescence signal could be detected in unstimulated, as well as in stimulated cells (Figure 3.6 A to C), indicating catalytic activity of membrane-bound PR3 in hPMNs. In PMA stimulated cells, active PR3 on the cell surface was reduced (Figure 3.6 E). Stimulation with PMA induces oxygen radicals and may lead to the inactivation of PR3 on the surface. Despite the possibility of recognizing

PR3 on the surface after PMA stimulation (see Figure 3.4 C), catalytic activity was probably reduced due to that fact. As a control the FRET substrate was incubated on unstimulated cells at 37 °C. Incubation at 37 °C leads to an internalization of the FRET substrate. Fluorescence signal obtained in these cells, reflects the expression of active PR3 in the cell. A high fluorescence signal could be obtained under these conditions (Figure 3.6 D).

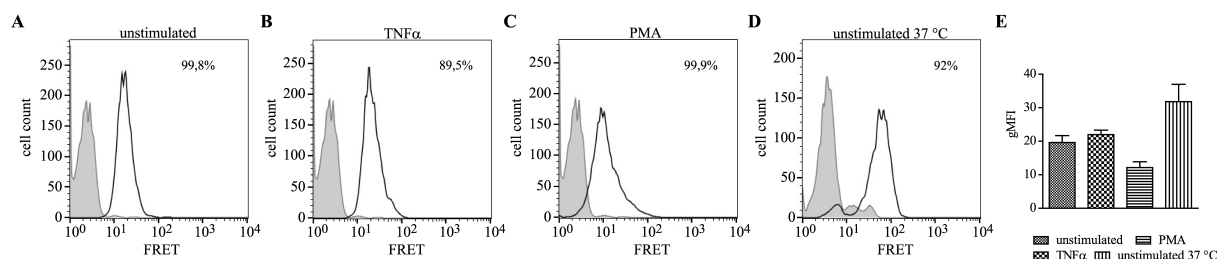


Figure 3.6: Human PR3 on the surface of hPMNs is catalytically active. To determine activity of membrane-bound PR3 on hPMNs, a FRET substrate with a lipid anchor was used (TAMRA-doo-VADnVRDRQ-doo). The FRET substrate anchors in the neutrophil membrane and cleavage by active PR3 on the cell surface leads to a fluorescence signal measurable by FACS analysis ($\lambda_{\text{Ex}} = 485$ nm and $\lambda_{\text{Em}} = 520$ nm). The lipid anchored FRET substrate (1 μM) was bound to the membrane of unstimulated (A), TNF α -primed (B) and PMA activated (C) hPMNs (black line) at 4 °C. As negative control neutrophils without FRET substrate were used (gray curve). D, Incubation of the FRET substrate at 37 °C leads to internalization and active PR3 in the neutrophils could be detected (one representative example for the different conditions shown). E, Geometric mean fluorescence (gMFI) for each experiment is given ($n = 3$, \pm SEM).

To determine the catalytic activity of hPR3 on the surface of hPR3^{+/+} PMNs, freshly isolated neutrophils were incubated with the lipid anchored FRET substrate. In unstimulated cells only a relative low amount of PMNs with PR3 activity on their surface could be detected (Figure 3.7 A). The highest expression of active PR3 was obtained in TNF α -primed cells (Figure 3.7 B). In PMA activated cells the amount of active PR3 was slightly reduced in comparison to TNF α -primed PMNs (Figure 3.7 C and E). Despite the high signal for PR3 obtained with the surface staining (see Figure 3.5 C), the signal for active PR3 on PMA activated cells was reduced. These findings are consistent with the activity measurements on the surface of hPMNs after PMA-stimulation, suggesting a damage of catalytic PR3 activity by PMA. After incubation at 37 °C and subsequent internalization of the FRET substrate, a high fluorescence signal could be detected (Figure 3.7 D). With these experiments hPR3 expression and functionality detected in the lysates of hPR3 expressing mPMNs (see Figure 3.2 and 3.3) could be confirmed.

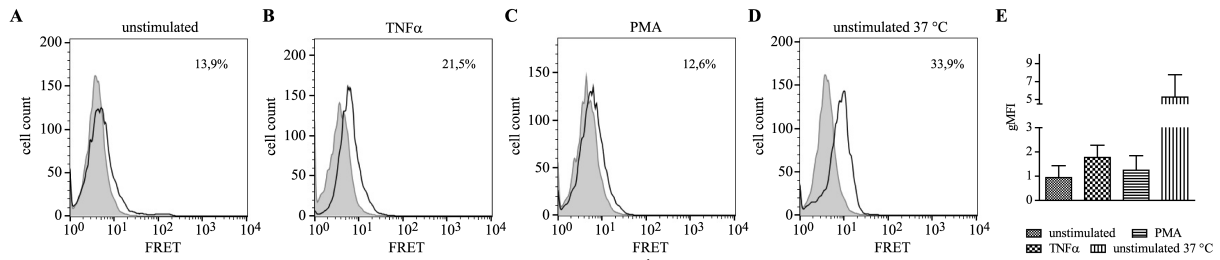


Figure 3.7: Catalytic activity of hPR3 on hPR3^{+/+} neutrophils. PR3 activity on the surface of hPR3^{+/+} PMNs was determined by FACS analysis with the lipidated FRET substrate TAMRA-doo-VADnVRDRQ-doo ($\lambda_{Ex} = 485$ nm, $\lambda_{Em} = 520$ nm). The FRET substrate was attached to the membrane of unstimulated (A), TNF α -primed (B) and PMA activated (C) hPR3^{+/+} PMNs (black line) at 4 °C. As a negative control the FRET substrate was inserted in the membrane of PR3/NE^{-/-} PMNs (gray curve). D, Activity of PR3 in hPR3^{+/+} PMNs was detected after incubation of the FRET substrate at 37 °C, which leads to internalization of the substrate (one representative example of each condition shown). E, The geometric mean fluorescence (gMFI), representing catalytically active PR3, is shown for the different conditions (n = 3, \pm SEM).

3.3 Characterization of monoclonal antibodies for transfer experiments

The impact of ANCA in general and of different subpopulations or subclasses in particular, on the pathogenesis of GPA is still uncertain. An animal model expressing hPR3 in mouse neutrophils should help solve this question. By transfer of monoclonal antibodies (mAbs) to these mice, the influence of antibodies on disease development and progression should be assessed. But which antibodies can be used for these transfer experiments? To answer this question, the binding properties of the mAbs MCPR3-2, MCPR3-7 and CLB-12.8 were examined in the following.

3.3.1 Interference of mAbs with catalytic activity of PR3

Some former studies suggest the hypothesis, that antibodies, which inhibit the activity of PR3, could be associated with disease development and progression (Daouk et al., 1995; van der Geld et al., 2002). Comparison of inhibitory with non-inhibitory antibodies in transfer experiments should answer the question as to how ANCA types determine the course and severity of the disease. Thus the inhibitory potential of mAbs was analyzed (Figure 3.8). Increasing amounts of mAbs were added to 50 nM PR3 and cleavage of Abz-YYAbu-ANBNH₂ (800nM) was measured. Whereas MCPR3-2 and CLB-12.8 did not influence the activity of PR3, MCPR3-7 strongly inhibited PR3. Already at a 1:1 ratio an effect on PR3

activity could be detected. At a three-fold molar excess of MCPR3-7 PR3 was completely inhibited.

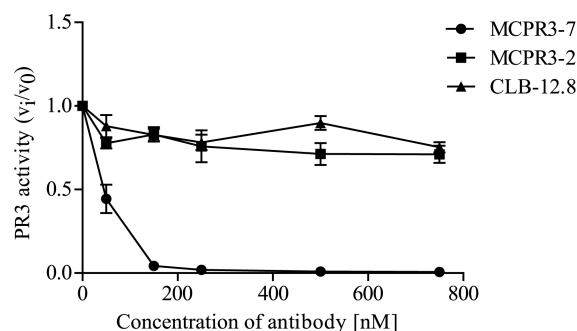


Figure 3.8: Interference of mAbs with catalytic PR3 activity. Influence of mAbs on the activity of PR3 was measured in a FRET-based activity assay. Cleavage of 800 nM FRET substrate (Abz-YYAbu-ANBNH₂, $\lambda_{Ex} = 320$ nm, $\lambda_{Em} = 405$ nm) by PR3 (50 nM) was measured in the presence of increasing concentrations of three different mAbs (0 – 750 nM) ($n = 3$, \pm SEM).

3.3.2 Interaction of mAbs with PR3 inhibitor complexes

Inhibition of PR3 plays an important role in the pathogenesis of GPA. In a recent genome wide association study, besides a SNP in the PR3 gene, a SNP in the gene of the alpha-1 proteinase inhibitor (α 1PI) was confirmed as risk allele for GPA (Lyons et al., 2012). As already outlined in the introduction (see chapter 1.6.1), binding of α 1PI to PR3 first leads to the formation of a canonical complex and after cleavage of the reactive center loop PR3 is covalently linked to the inhibitor. The covalent association with α 1PI induces a conformational change in PR3 resulting in an inactive zymogen-like conformation. As interaction of PR3 with its physiological inhibitors, plays an important role in the immune response, antibodies have to be able to interact with this PR3-inhibitor complexes to unfurl a pathogenic effect. Therefore the binding capability of mAbs to different PR3-inhibitor complexes was examined.

Covalent PR3-inhibitor complexes were formed using α 1PI and an AAPV-chloromethyl ketone (CMK). Furthermore canonical complexes were generated with elafin and α 1PI. To form the canonical α 1PI-PR3 complex the catalytically inactive PR3 variant Δ hPR3-S195A (labeled as PR3*) was used. In nearly all these complexes PR3 is present in its active conformation. Only covalent complexation to α 1PI leads to a conformational change of PR3 as described above and displays PR3 in a precursor-like conformation. The PR3 complexes were formed by adding a ten-fold molar excess of inhibitor to PR3 and incubation at 37 °C for one hour. After immobilization on nickel-plates via the $6 \times$ His-tag of PR3, the binding of mAbs to the different complexes was detected (Figure 3.9). MCPR3-7 (Figure 3.9 A) showed

a much stronger binding capability towards proPR3 in comparison to mature PR3. Furthermore MCPR3-7 was only able to bind to the covalent PR3- α 1PI complex. No binding to the other PR3-inhibitor complexes was observed. The strong binding to proPR3 and PR3- α 1PI complexes indicated a preferential binding of MCPR3-7 to the inactive conformation of PR3. In contrast CLB-12.8 (Figure 3.9 B) was able to bind to all different PR3-variants and complexes, except for the covalent PR3- α 1PI complex. The epitope of CLB-12.8, which lies close to the active site cleft (Silva et al., 2010), probably becomes inaccessible after binding of the inhibitor and the following conformational changes. As MCPR3-2 (Figure 3.9 C) is able to bind to all PR3-variants, it was chosen as an appropriate coating control. Thus equal coating of the different variants could be ascertained. No binding of the isotype control antibody to the different PR3-variants could be observed.

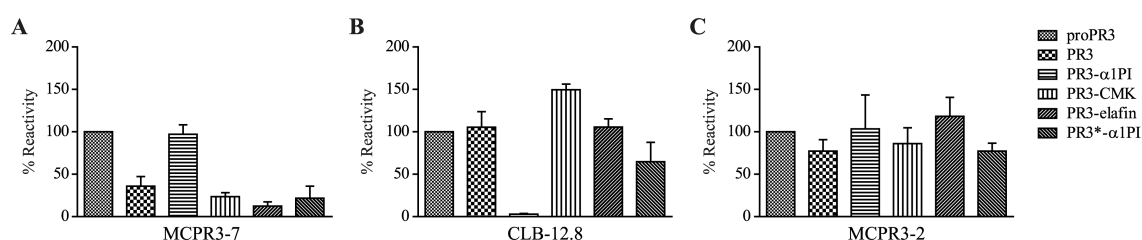


Figure 3.9: Binding of mAbs to different PR3 inhibitor complexes. Binding of mAbs to different PR3-inhibitor-complexes was assessed in an ELISA. Inhibitors were added to PR3 in solution at a ten-fold molar excess and incubated for one hour at 37 °C. The covalent PR3- α 1PI complex represents PR3 in its inactive conformation. In contrast the covalent complex with the AAPV-chloromethyl ketone (CMK) and the two canonical complexes PR3-Elafin and PR3*- α 1PI contain PR3 in its active conformation. The complexes, proPR3 and active PR3 were immobilized on nickel plates via the 6 \times His-tag of PR3 and binding of MCPR3-7 (A), CLB-12.8 (B) and MCPR3-2 (C) was determined with a HRP-conjugated goat-anti-mouse antibody. The recognition of the PR3 variants was normalized to the signal obtained with proPR3, which was set to 100% (n = 3, \pm SEM). As MCPR3-2 binds to the different PR3 variants at a similar level, MCPR3-2 was used as a coating control. (PR3*, catalytically inactive PR3)

3.3.3 MCPR3-7 impairs α 1PI-PR3 complexation

As already mentioned, inhibition and clearance of PR3 by α 1PI plays an important role in neutrophil-mediated tissue damage. Antibodies, which interfere with the complexation of PR3 with α 1PI, could reduce PR3 clearance and thus intensify the immune response. With regard to our animal model, it was important to investigate, whether mAbs with such properties exist. Transfer of such mAbs into hPR3^{+/+} mice could lead to an exaggerated immune response. Therefore PR3 complexation with α 1PI was analyzed in the presence of mAbs by SDS PAGE and silver nitrate staining. First, complex formation of PR3 (800 nM) and α 1PI (4 μ M) without mAbs was determined at different timepoints (Figure 3.10 A). Already after 5 seconds PR3- α 1PI complexes could be detected. PR3 was completely covalently attached to α 1PI at this timepoint. To assess the influence of mAbs, PR3 was preincubated with a three-fold molar excess of MCPR3-7 (Figure 3.10 B), CLB-12.8 (Figure 3.10 C) and MCPR3-2 (Figure 3.10 D). In case of CLB-12.8 and MCPR3-2 the first complexes were detected in the gel after 5 seconds and after 15 seconds the reaction was completed. In contrast, MCPR3-7 delayed the complexation. Formation of the first complexes could only be observed after 15 seconds. It took about 3 minutes until the complexation reaction was completed and all PR3 was covalently attached to α 1PI. These findings clearly indicate that binding of MCPR3-7 to PR3 influences and impairs the covalent complexation with α 1PI.

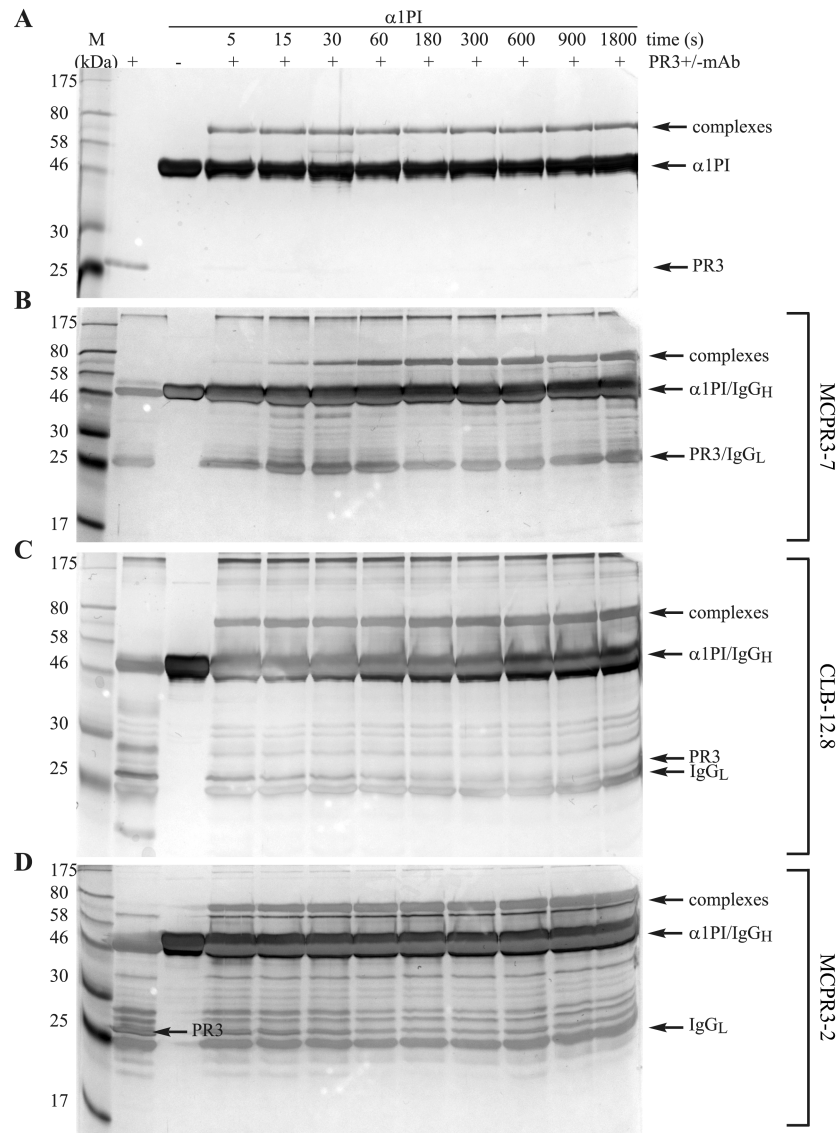


Figure 3.10: MCPR3-7 delays covalent PR3- α 1PI complexation. A, Covalent PR3- α 1PI complexation was observed over time by adding α 1PI at a five-fold molar excess to 800 nM PR3 and incubation at 37 °C. B to D, To detect the effect of mAbs on the covalent complexation 800 nM of PR3 were preincubated with a three-fold molar excess of MCPR3-7 (B), CLB-12.8 (C) or MCPR3-2 (D) for one hour at room temperature. Alpha-1PI was added at a five-fold molar excess to the PR3-mAb complexes and incubated at 37 °C. At different timepoints 10 μ l of the solutions were taken and analyzed by SDS PAGE and silver nitrate staining. Representative examples of three technical repeats are shown (M, molecular weight standard; IgG_H, IgG heavy chain; IgG_L, IgG light chain).

3.3.4 Influence of mAbs on non-covalent α 1PI-PR3 complexation

Covalent complexation of PR3 with α 1PI leads to clearance of PR3 from the neutrophil membrane. To determine if only this type of complexation, or also the canonical interaction, is affected by mAbs, the non-covalent complex formation was examined by thermophoresis measurements. Catalytically inactive PR3, Δ hPR3-S195A, expressed in HEK 293E cells and purified via nickel-chromatography, was used for this approach. After preincubation with

mAbs, NT647-labeled α 1PI was added to a dilution series of Δ hPR3-S195A in presence or absence of mAbs and the binding was measured by thermophoresis (Figure 3.11). The thermophoretic analyses were performed together with Susanne A. I. Seidel (Systems Biophysics and Functional Nanosystems, Ludwig-Maximilians-Universität München, Germany). In the absence of antibodies α 1PI bound to Δ hPR3-S195A with a K_D of $1.9 \pm 1.1 \mu\text{M}$. For the measurements in presence of MCPR3-7 no saturating amounts of MCPR3-7 could be used, due to the low initial antibody concentration. Hence, the Δ hPR3-S195A-antibody solution contained Δ hPR3-S195A-MCPR3-7 complexes and free Δ hPR3-S195A. The binding affinity measured with α 1PI accordingly consisted of the binding of α 1PI to Δ hPR3-S195A-MCPR3-7 complexes and to free Δ hPR3-S195A. Regardless, an inhibiting impact of MCPR3-7 on the canonical interaction of Δ hPR3-S195A and α 1PI could be detected ($K_D = 5.6 \pm 1.0 \mu\text{M}$). As this inhibition could already be observed at relatively low antibody concentrations, a more pronounced decrease can be expected with higher antibody concentrations. In contrast to MCPR3-7, pre-incubation with CLB-12.8 did not alter the affinity of Δ hPR3-S195A and α 1PI. The curve displaying the binding of α 1PI to Δ hPR3-S195A-CLB-12.8 complexes is a nearly perfect overlay to the curve without antibodies. The determined K_D of $1.8 \pm 0.8 \mu\text{M}$ did not differ significantly from the K_D measured without antibodies.

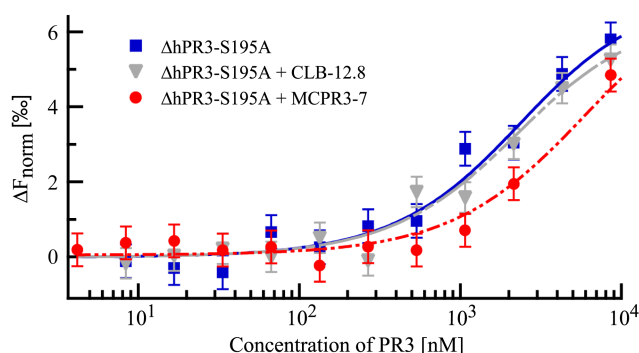


Figure 3.11: Non-covalent PR3- α 1PI complexation is impaired in the presence of MCPR3-7.

Thermophoretic quantification was used to determine the influence of mAbs on non-covalent PR3- α 1PI complex formation. A dilution series of Δ hPR3-S195A was prepared starting at a concentration of $12 \mu\text{M}$. Each sample of the dilution series was mixed 6:1 with PBS with or without mAbs, to yield an antibody concentration of 670 nM . After one hour incubation at room temperature, NT647-labelled α 1PI was added (880 nM). In the absence of antibodies thermophoresis revealed a K_D of $1.9 \pm 1.1 \mu\text{M}$ (blue rectangles). The presence of CLB-12.8 did not change the affinity of α 1PI to PR3 ($K_D = 1.8 \pm 0.8 \mu\text{M}$; grey triangles), whereas the affinity was decreased three-fold by preincubation with MCPR3-7 ($K_D = 5.6 \pm 1.0 \mu\text{M}$; red circles). Thermophoretic measurements were performed together with Susanne A. I. Seidel (Systems Biophysics and Functional Nanosystems, Ludwig-Maximilians-Universität München, Germany). Results of three technical repeats are shown ($n = 3, \pm \text{SD}$).

3.3.5 Characterization of the MCPR3-7 epitope

As MCPR3-7 is the only known mAb, which interferes with PR3 activity and influences the complexation between PR3 and α 1PI, the binding site and the inhibition mechanism of this antibody was further characterized. In an activity assay approach with human and gibbon PR3 variants it could be shown that inhibition by MCPR3-7 is sequence dependent. Gibbon PR3 (gibPR3) is hardly inhibited in the presence of MCPR3-7 in comparison to hPR3 (Figure 3.12 A and B). To localize the MCPR3-7 binding sequence two human/gibbon PR3 chimeras were used. One chimera consisted of the human amino-terminal β -barrel and the gibbon carboxy-terminal β -barrel (h/gibPR3, Figure 3.12 C). The other contained the gibbon amino-terminal and the human carboxy-terminal β -barrel (gib/hPR3, Figure 3.12 D). Only the gib/hPR3 was strongly inhibited by MCPR3-7, whereas the h/gib PR3 still showed activity in presence of MCPR3-7. Thus MCPR3-7 binding could be mapped to the carboxy-terminal β -barrel of PR3.

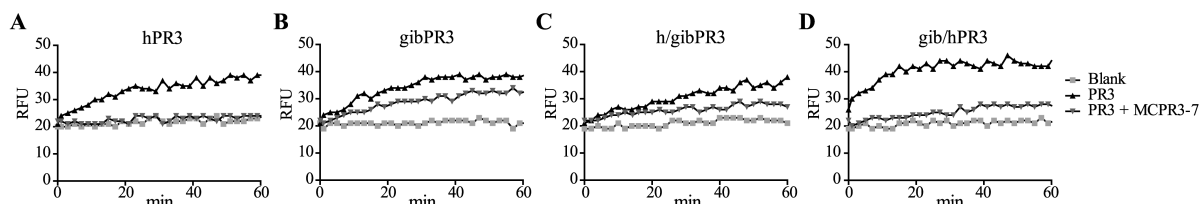


Figure 3.12: Localization of the MCPR3-7 binding epitope on the carboxy-terminal β -barrel of PR3. To determine the MCPR3-7 binding region two gibbon/human PR3 chimeras were tested in an activity assay approach in the presence of MCPR3-7. The h/gibPR3 variant consists of the human N-terminal β -barrel and the gibbon carboxy-terminal β -barrel. In contrast the gib/hPR3 variant contains the gibbon N-terminal and the human carboxy-terminal β -barrel. PR3 activity was measured with the FRET substrate Abz-YYAbu-ANBNH₂ (λ Ex = 320 nm, λ Em = 405 nm). Cleavage of 800 nM FRET substrate by 50 nM hPR3 (A), gibPR3 (B), h/gibPR3 (C) or gib/hPR3 (D) was measured in the absence or presence of a two-fold molar excess of MCPR3-7. The fluorescence signal is displayed in relative fluorescence units (RFU) and one representative example of three technical repeats is shown. Strong inhibition of the hPR3 and the gib/hPR3 variant but not the gibPR3 and the h/gibPR3 variant by MCPR3-7 indicated binding of the antibody to the carboxy-terminal β -barrel.

3.3.6 MCPR3-7 is unable to bind to PR3 in its active conformation

In Figure 3.9 a preferential binding of MCPR3-7 to the proform of PR3 could be detected. To further characterize the binding affinities of MCPR3-7 to proPR3 and mature PR3, thermophoretic measurements were performed. Thermophoretic quantification was performed together with Susanne A. I. Seidel (Systems Biophysics and Functional Nanosystems, Ludwig-Maximilians-Universität München, Germany). Binding of MCPR3-7 to proPR3, PR3 and PR3-CMK (AAPV-chloromethyl ketone) complexes was measured. MCPR3-7 was labeled with NT647 and added to the samples of a dilution series of the different PR3-variants. To generate PR3-CMK complexes the CMK was added to PR3 at a ten-fold molar excess and incubated for one hour at 37 °C. In this complex PR3 is held in its active conformation, whereas mature PR3 in free solution is able to switch from the active conformation into an inactive zymogen-like conformation. Thus PR3 in free solution exists in an allosteric equilibrium of molecules between two extreme conformations, one fully accessible to a substrate (active conformation) and the other with an occluded active site (inactive conformation) (Pozzi et al., 2012). Binding of MCPR3-7 to proPR3 revealed a K_D below 10 nM. In contrast no binding of MCPR3-7 to PR3 in its active conformation, stabilized by binding to CMK, could be detected (Figure 3.13 A). These findings indicate that MCPR3-7 selectively recognizes the zymogen conformation of PR3. Binding to mature PR3 in free solution, however, was detectable (Figure 3.13 B). The binding affinity measured with mature PR3 ($K_D = 0.4 \pm 0.2 \mu\text{M}$), was about 40-fold lower, than with proPR3. Recognition of mature PR3 by MCPR3-7 is probably due to an allosteric switch from the active into the inactive zymogen-like conformation and shifts the equilibrium in the direction of the inactive conformation.

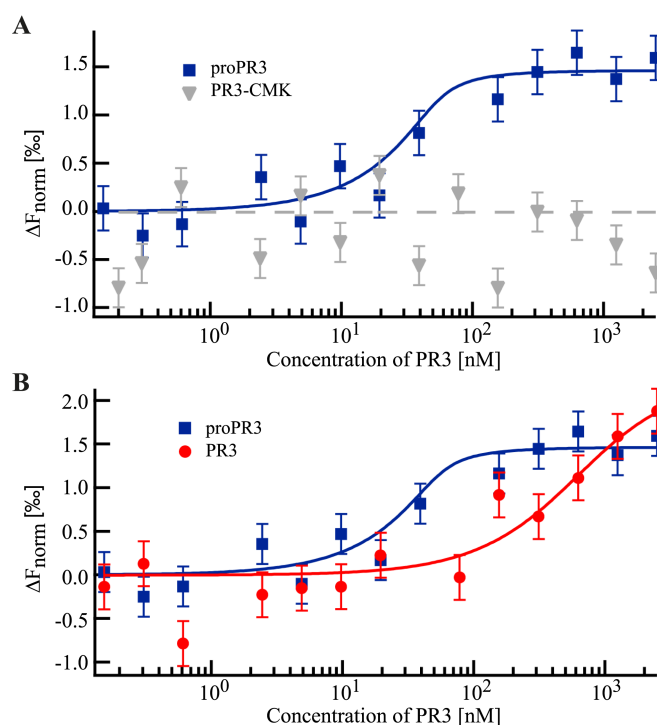


Figure 3.13: MCPR3-7 does not bind to the active PR3 conformation. Affinity of MCPR3-7 to PR3 in different conformations was measured by thermophoresis. Binding of MCPR3-7 to proPR3 was compared to binding of MCPR3-7 to PR3 complexed with AAPV-chloromethyl ketone (CMK) (A) or to PR3 in free solution (B). PR3 in free solution is able to adopt different conformational stages and displays an equilibrium between active and inactive conformations. In contrast PR3 in complex with CMK is held in its active conformation. Complexation was carried out by the addition of a ten-fold molar excess of CMK to PR3 and incubation for one hour. For the affinity measurements a dilution series of the different PR3 variants was prepared, starting at a maximum concentration of $2.5 \mu\text{M}$. NT647-labeled MCPR3-7 was added to the dilution samples at a final concentration of 50 nM . MCPR3-7 revealed a strong binding affinity to proPR3 ($K_D \leq 10 \text{ nM}$, blue rectangles). Active PR3 was bound with a much lower affinity ($K_D = 0.4 \pm 0.2 \mu\text{M}$, red circles), whereas no binding to the mature conformation of the PR3-CMK could be detected (grey triangles). The thermophoretic quantification was measured together with Susanne A. I. Seidel (Systems Biophysics and Functional Nanosystems, Ludwig-Maximilians-Universität München, Germany). Results of three technical repeats are shown ($n = 3, \pm \text{SD}$).

3.3.7 Binding of MCPR3-7 alters the peptide binding pocket

The results of the thermophoretic quantification revealed a better binding of MCPR3-7 to the zymogen conformation of PR3 (see Figure 3.13). As MCPR3-7 furthermore inhibits active PR3, alteration of the active PR3 conformation is probably the mechanism by which MCPR3-7 is able to interfere with PR3 activity. To characterize these conformational changes upon MCPR3-7 binding, activity of PR3 towards different substrates in presence and absence of MCPR3-7 was measured. Therefore substrates with different amino acids at position P1 and with leaving groups of different sizes at P1' were used. Cleavage of the substrate with the best fit non-natural residue at P1, Abz-YYAbu-ANBNH₂ (Figure 3.14 A) was strongly inhibited

by MCPR3-7. Usage of an optimized extended peptide substrate, TAMRA-VADnVVADYQ-Dap(CF) also revealed a strong inhibitory effect by MCPR3-7 (Figure 3.14 B). Furthermore cleavage of the substrate Ahx-PYFA-*p*NA (Figure 3.14 C), which contains a big leaving group in P1', was also impaired by the presence of MCPR3-7. In contrast substrates with a small leaving group in P1' and amino acids of different sizes in P1, Boc-A-ON*p* and Boc-APnV-SBzl (Figure 3.14 D and E), were still cleaved by PR3 in the presence of MCPR3-7. Cleavage of For-AAPAbu-SBzl (Figure 3.14 F), which contains a small leaving group in P1', but a larger amino acid in P1, was partly active after binding of MCPR3-7. An activity of 50% could be determined in the presence of MCPR3-7. These findings indicate that binding of MCPR3-7 mostly affects the S1' pocket of PR3. Smaller leaving groups in P1' are still able to interact with PR3 in the presence of MCPR3-7, whereas cleavage of substrates with big leaving groups in P1' is completely inhibited. Changes in the P1 position of the substrate did hardly alter the effect of MCPR3-7. Thus it is most likely that inhibition of PR3 by MCPR3-7 is due to an allosteric mechanism, which alters the conformation of the S1' pocket of PR3.

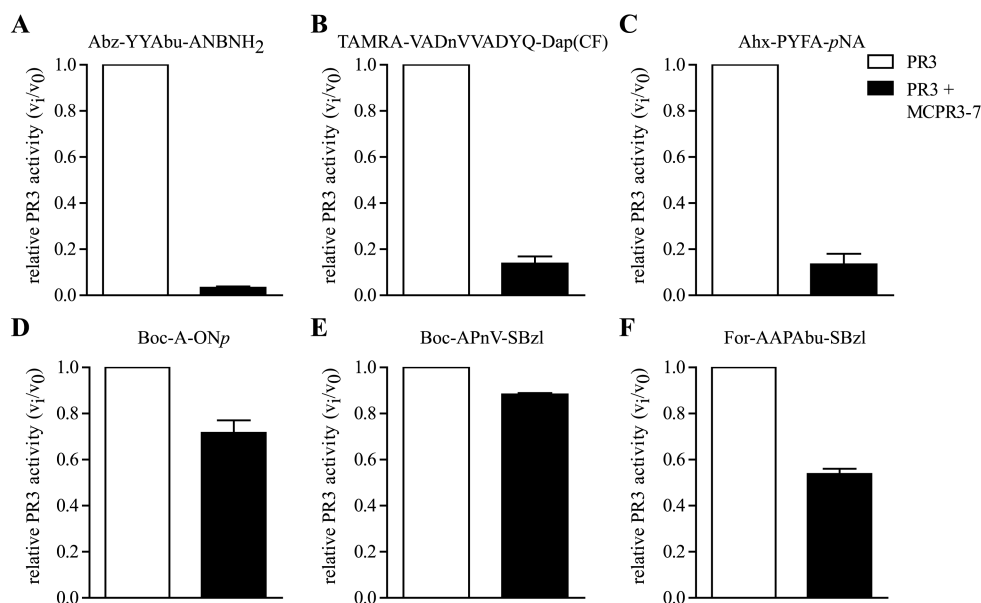


Figure 3.14: Interference of MCPR3-7 with PR3 activity towards different substrates. The effect of MCPR3-7 on cleavage of different PR3 substrates was determined in a FRET-based activity assay, to specify the binding mechanism of MCPR3-7. To a 50 nM PR3 solution (A-E) or a 100 nM PR3 solution (F) a three-fold molar excess of MCPR3-7 was added. Cleavage of 800 nM Abz-YYAbu-ANBNH₂ (A), 5 μ M TAMRA-VADnVVADYQ-Dap(CF) (B), 1 mM Ahx-PYFA-*p*NA (C), 1 mM Boc-A-ON*p* (D), 1 mM Boc-APnV-SBzl (E) and 1 mM For-AAPAbu-SBzl (F) was measured over time. The relative activity was determined by normalizing PR3 activity in absence of MCPR3-7 to 1 ($n = 3, \pm$ SEM).

3.3.8 MCPR3-7 cannot bind to membrane-bound PR3

The inhibitory properties of MCPR3-7, as well as the interference of this antibody with covalent and non-covalent PR3- α 1PI complex formation, as shown above, turn this antibody into a potential candidate for transfer experiments in hPR3^{+/+} mice. To further explore this possibility, detection of membrane-bound PR3 by MCPR3-7 was examined by FACS analysis. These experiments were carried out by Ulrich Specks (Thoracic Disease Research Unit, Mayo Clinic and Foundation, Rochester, MA, USA). Membrane-bound PR3 on freshly isolated hPMNs was detected with MCPR3-2 (Figure 3.15 A, *continuous black line*). A bimodal expression pattern representing PR3-positive and PR3-negative PMNs could be observed. After stimulation with TNF α , the proportion of PR3-positive cells, detected with MCPR3-2 increased (Figure 3.15 B). CD32 staining was used as positive control (*dotted line*). Using MCPR3-7 to detect membrane-bound PR3, only a tiny second population (*arrow*) with marginal MCPR3-7 reactivity could be observed. The vast majority of cells could not be detected as PR3-positive with MCPR3-7. PR3 on the neutrophil surface could neither be detected by MCPR3-7 after TNF α stimulation. The missing recognition of membrane-bound PR3 may be due to conformational reasons. PR3 attached to the membrane forms complexes with NB1 (CD177) and/or lipid bilayers via a hydrophobic patch of the activation domain. Thus, membrane-bound PR3 is present only in a fixed conformation. As MCPR3-7 binds to the activation domain of its proform, membrane-bound PR3 does not appear to fully present the epitope of this antibody. These properties of MCPR3-7 are not favorable for transfer experiments in hPR3^{+/+} mice.

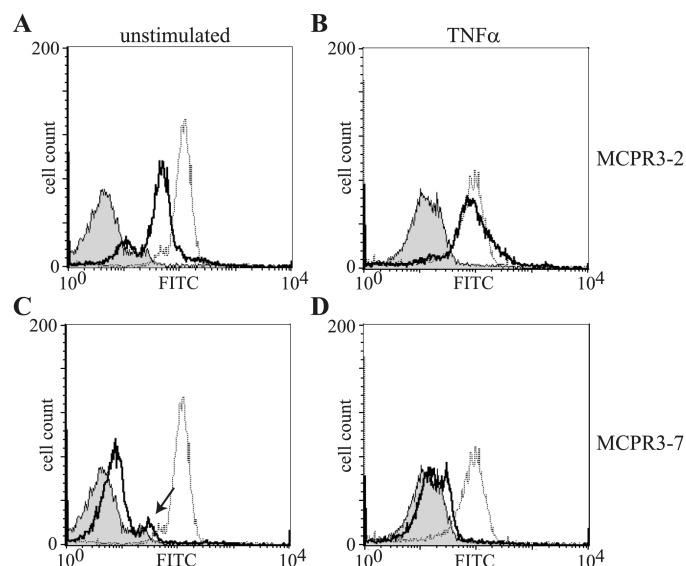


Figure 3.15: MCPR3-7 cannot detect membrane-bound PR3. To test antibody detection of PR3 on the surface, PMNs were isolated from human blood and stimulated with $\text{TNF}\alpha$ (B and D). PR3 (continuous black line) on the surface of unstimulated and $\text{TNF}\alpha$ -primed PMNs was stained with MCPR3-2 (A and B) and MCPR3-7 (C and D) and visualized with a FITC-conjugated goat anti-mouse secondary antibody. As positive control CD32 expression was detected (dotted line). The gray peak represents the isotype control. These experiments were carried out by Ulrich Specks (Thoracic Disease Research Unit, Mayo Clinic and Foundation, Rochester, MA, USA).

3.3.9 Generation of new mAbs against PR3

None of the mAbs available, except MCPR3-7, interfered with PR3 activity or interaction with $\alpha 1\text{PI}$. As shown above, MCPR3-7 cannot be used for transfer experiments in $\text{hPR3}^{+/+}$ mice, due to the lack of recognition of membrane-bound PR3. Thus new monoclonal antibodies against PR3 were produced in cooperation with Elisabeth Kremmer (Helmholtz Zentrum München). Two mice were immunized with $\Delta\text{hPR3-S195A}$ and hybridoma supernatants of 21 different antibodies were gathered. The affinity of these antibodies to PR3 was determined in an ELISA and the hybridoma supernatants with the highest affinity were chosen for further analysis. To test these antibodies for their inhibitory capacity towards PR3, an immune-capture activity assay approach was used. The hybridoma supernatant contains FCS and thereby also bovine $\alpha 1\text{PI}$. Thus in an activity assay in free solution, PR3 would be immediately inhibited by $\alpha 1\text{PI}$ after adding the supernatants and the effect of the antibodies could not be measured. To avoid this problem, the mAbs of the culture medium were captured by anti-mouse polyclonal antibodies, which were immobilized on a black maxisorp 96-well plate. Thereby all FCS proteins, including $\alpha 1\text{PI}$, in the cell culture supernatants were removed during the washing steps, before adding PR3. PR3 was then bound to the antibodies, and after

adding a FRET substrate, the influence of the immobilized antibody on PR3 activity was measured. With this method, three antibodies, with inhibitory capacity towards PR3 could be identified (Figure 3.16). The two antibodies 4B12 and 7D12 strongly inhibited PR3. The third antibody, 5B11, was only able to inhibit PR3 by about 50%. As positive control the mAb CLB-12.8 was captured onto the 96-well plate, as negative control an IgG1 isotype antibody was used.

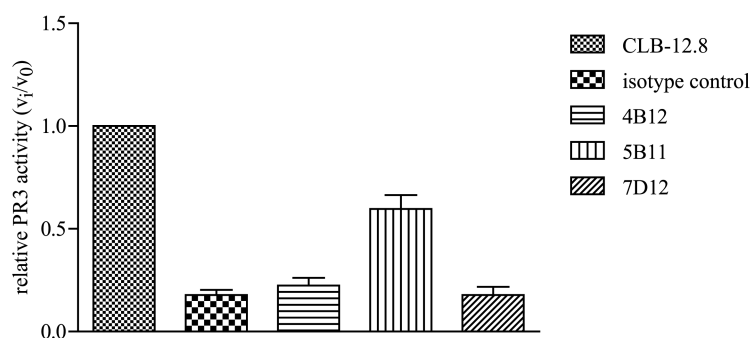


Figure 3.16: Hybridoma supernatants of new mAbs showed inhibitory capacity towards PR3. PR3-specific antibodies from hybridoma supernatants were captured on black 96-well maxisorp plates with anti-mouse immunoglobulin antibodies (1 μ g/well). PR3 was bound to these antibodies (100 ng/well) and PR3 activity was measured with a FRET substrate. 800 nM of Abz-YYAbu-ANBNH₂ were added and fluorescence was measured. The fluorescence signal was normalized to the signal obtained by PR3 captured with CLB-12.8, which was set to 1 ($n = 2$; \pm SEM). In this way inhibitory capacity of PR3-specific antibodies in hybridoma supernatants was determined.

The contents of the hybridoma supernatants, like for example α 1PI, could disturb further characterization and transfer experiments. Thus the antibodies were purified from the hybridoma supernatants by Elisabeth Kremmer (Helmholtz Zentrum München). After purification the inhibitory capacity of the antibodies was again analyzed. An activity assay in free solution was performed (Figure 3.17). The antibodies were added to PR3 at increasing nanomolar concentrations, exceeding the molar concentration of PR3, and the cleavage of a FRET substrate was measured in the presence of these antibodies. Unfortunately, not even a 20-fold molar excess of the antibody was able to inhibit the PR3 in free solution. Purification of the antibodies may have changed their ability to interfere with PR3 activity. What is more likely, immobilized PR3 could be more sensitive to inhibition in this immune-capture activity assay approach in comparison to the activity assay in free solution.

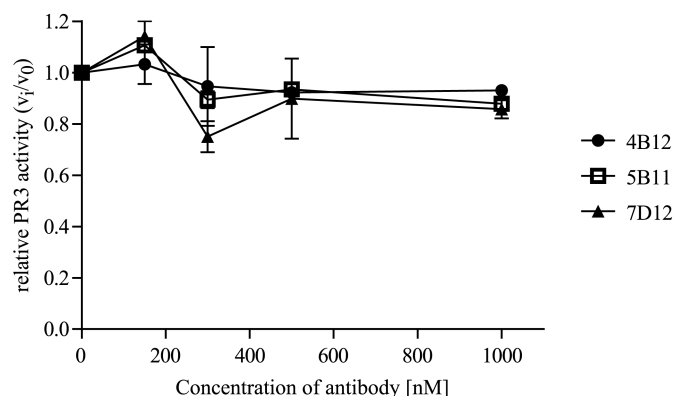


Figure 3.17: New mAbs showed no inhibitory capacity after purification from hybridoma supernatants. PR3-specific antibodies were purified from hybridoma supernatants and their inhibitory capacity towards PR3 was tested in an activity assay in free solution. Antibodies were added to 50 nM PR3 in increasing concentrations (150 – 1000 nM). 5 μ M FRET substrate (TAMRA-VADnVVADYQ-Dap(CF)) were added and fluorescence was detected at $\lambda_{\text{Ex}} = 485$ nm and $\lambda_{\text{Em}} = 520$ nm. The fluorescence signal was normalized to the signal obtained by cleavage of the FRET substrate in the absence of antibodies, which was set to 1 ($n = 2$; \pm SEM).

3.4 Transfer of mAbs into hPR3^{+/+} mice

3.4.1 Infiltration of immune cells in the lungs after antibody injection

As MCPR3-7, the only inhibitory mAb available at the beginning of my doctoral work, was not found suited for transfer experiments as elucidated in chapter 3.3.8, I decided to transfer two mAbs of different IgG subclasses. Hence, besides establishing of a new animal model, I could evaluate the impact of different antibody subclasses on the development of an autoimmune response after antibody transfer into hPR3^{+/+} mice. The newly generated mAbs against PR3 4B12, which belongs to the IgG2a subclass, and 7D12 of the IgG2b subclass were used for the transfers. As these were the antibodies, which were generated in cooperation with Elisabeth Kremmer (Helmholtz Zentrum München), high amounts of antibodies were available. Transfer of the antibodies and the following analysis of the mice were carried out by André Tittel (Institutes of Molecular Medicine and Experimental Immunology, Rheinische Friedrich-Wilhelms Universität, Bonn, Germany). In patients with GPA external factors, for example *Staphylococcus aureus* infections, are known to initiate inflammatory responses and thus can reduce immune tolerance and favor the development of autoimmunity (Scully et al., 2012). For that reason LPS was injected into the transgenic mice intratracheally, in addition to the antibody transfer, to induce mild inflammation in the lungs. LPS was used at a relatively low concentration (3 ng per mouse). Thus after parallel injection

of the isotype control antibodies and LPS, no or very little inflammation was observed after seven days. The mice were sacrificed seven days after injection and the immune cell infiltration in the lungs was analyzed (Figure 3.18). Injection of 7D12 induced a slight increase of PMNs in comparison to its isotype control antibody (Figure 3.18 B right panel). Furthermore the number of macrophages was slightly elevated in the lungs after 7D12 injection (Figure 3.18 B right panel). However no difference in T cells and B cells could be observed after injection of 7D12 (Figure 3.18 C-E right panels). Injection of the mAb 4D12, in contrast, induced a strong infiltration of all types of immune cells in comparison to its isotype control antibody (Figure 3.18 A-E left panels). Not only primary immune cells like PMNs and macrophages were elevated in the lung tissue, but also T cells and B cells. These results indicate a strong, already advanced immune response after 4D12 injection. Based on these results it becomes clear that antibodies against PR3 are able to induce an immune response in the transgenic mice. Furthermore this immune response seems to depend on the antibody isotype, as the reaction to the IgG2a isotype of 4D12 was much more pronounced than to the IgG2b antibody 7D12.

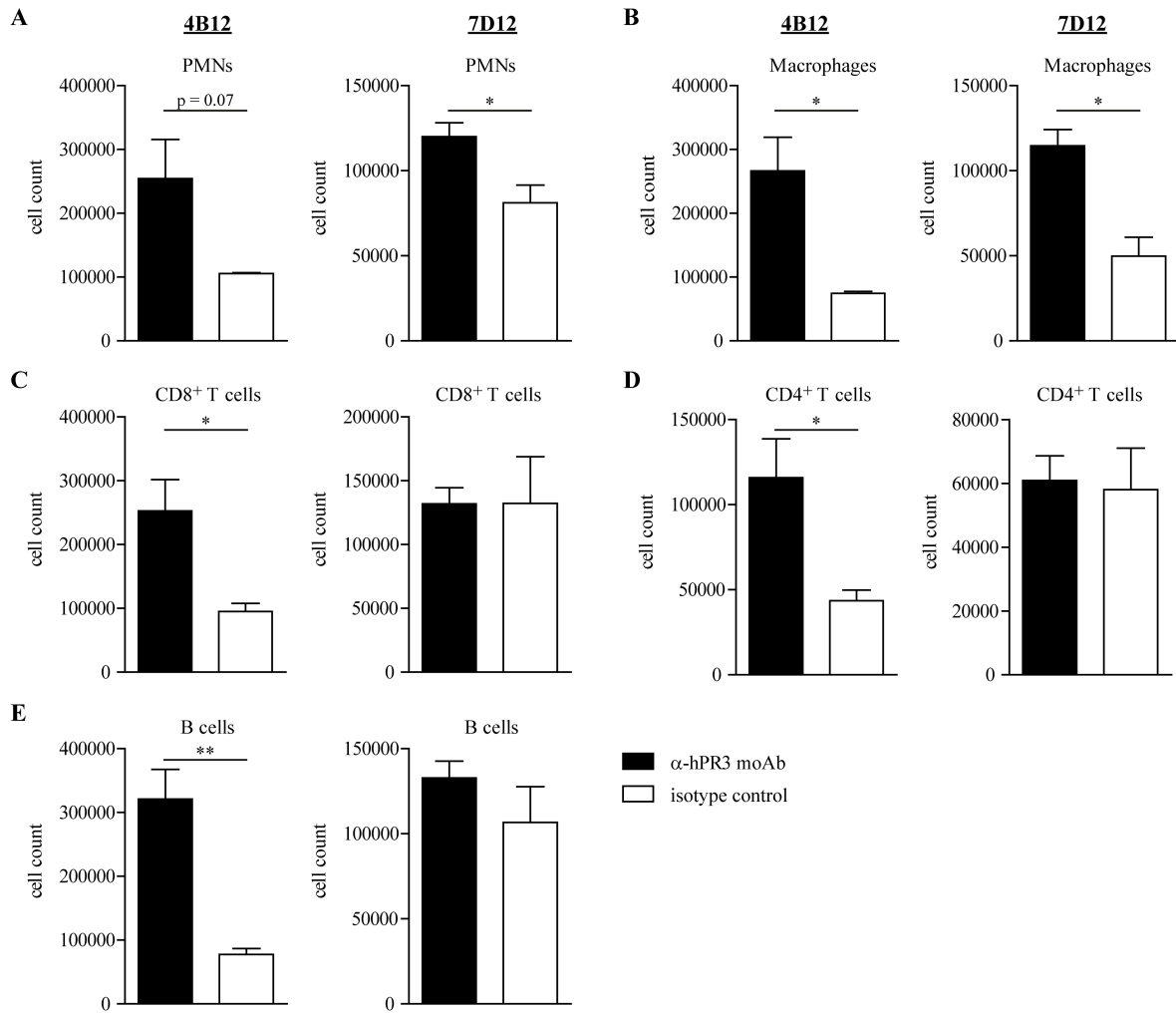


Figure 3.18: Injection of mAbs against hPR3 leads to recruitment of immune cells in the lungs. Two different mAbs against hPR3 (4B12, left panels of A-E and 7D12, right panels of A-E) were injected into the hPR3^{+/+} mice. 300 µg of the mAb were administered intraperitoneal one hour before induction of a mild inflammation by injection of LPS (3 ng per mouse). As control 300 µg of the respective isotype control antibody (IgG2a for 4B12, IgG2b for 7D12) were injected. After seven days the lungs of the mice were dissected and the infiltration of the different types of immune cells (PMNs in A, macrophages in B, CD8⁺ T cells in C, CD4⁺ T cells in D and B cells in E) into the lung tissue was analyzed by FACS staining (n = 3 mice ± SEM). The flow cytometry analysis of the immune cells was carried out by André Tittel (Institutes of Molecular Medicine and Experimental Immunology, Rheinische Friedrich-Wilhelms Universität, Bonn, Germany).

3.4.2 Lung vasculitis and pulmonary lesions after antibody injection

Histopathological analysis was performed to further characterize the immune response to PR3-specific antibodies. During the preparation of histological sections macroscopic differences of the lung vessels could already be detected in the mice injected with 4B12 in comparison to the isotype control injected mice. After injection of 4B12 the vessels showed a plump and swollen shape, indicating vasculitis-like changes in the lungs. For further analysis of the immune cell recruitment after antibody injection, lung slices were prepared and stained by PAS-staining. PAS-staining visualizes glycoproteins and polysaccharides and thus granules of infiltrating immune cells are stained and can be detected. The histopathological analysis of the lungs was carried out by André Tittel and Magdalena Esser (Institutes of Molecular Medicine and Experimental Immunology, Rheinische Friedrich-Wilhelms Universität, Bonn, Germany). Staining of the lung slices revealed a strong immune cell infiltration in the lung tissue after transfer of the mAb 4B12 (Figure 3.19 A and B left panels). Large dense patches could be observed in the lung tissue in these mice, indicating a strong infiltration of neutrophils and a severe inflammation of the lungs. The respective isotype control antibodies did not induce an infiltration of immune cells or an inflammatory response in the lungs (Figure 3.19 A and B right panels). No histological changes of the lung tissue could be observed after transfer of the mAb 7D12 (Figure 3.19 C and D left panels). Here no clear differences to the mice, injected with the isotype control antibody could be detected. These findings indicate that hPR3-specific antibodies indeed are able to induce lung vasculitis and pulmonary lesions in hPR3^{+/+} mice. The pathogenicity of these antibodies, however, seems to be dependent on the subclass of the respective antibody, as only transfer of the IgG2a antibody 4B12 induced development of a GPA-like phenotype.

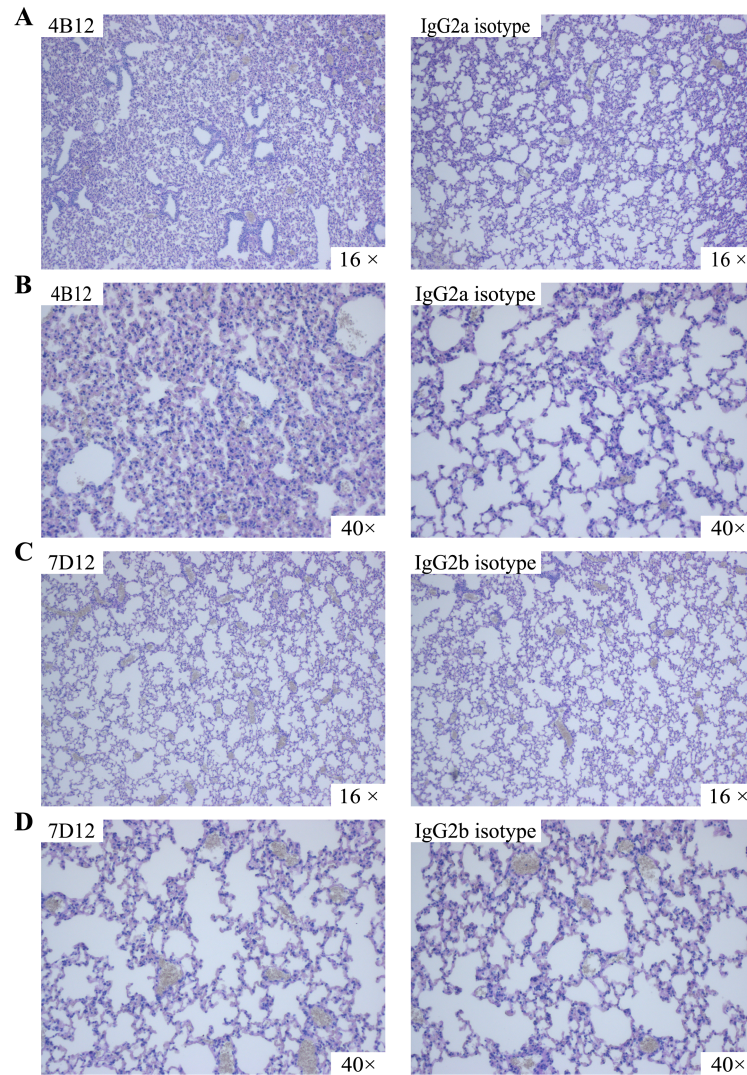


Figure 3.19: Injection of the hPR3-specific antibody 4B12 induced a strong inflammatory response in the lung tissue. Seven days after injection of hPR3-specific antibodies (300 μ g/mouse) and LPS (3 ng/mouse) into hPR3^{+/+} mice, the animals were sacrificed, the lungs of the mice were dissected and the immune cell infiltration was analyzed by PAS-staining. A and B, Injection of the mAb 4B12 (left panels) led to severe inflammation of the lung tissue. In comparison to the isotype control antibody (right panels), large dense patches are visible in the lung tissue, indicating high neutrophil infiltration. C and D, No clear differences in the lung tissue after injection of the mAb 7D12 (left panels) in comparison to the isotype control antibody (right panels) could be observed. Preparation and analysis of the lung slices were carried out by André Tittel and Magdalena Esser (Institutes of Molecular Medicine and Experimental Immunology, Rheinische Friedrich-Wilhelms Universität, Bonn, Germany) (n = 3 mice, one representative example shown for each condition).

3.5 Characterization of different types of ANCA in patients

In the second part of this study the presence of inhibitory ANCA in patients with GPA and their correlation with disease activity was investigated. The initial question as to whether inhibitory ANCA can be identified in GPA samples was answered. Therefore total IgGs from plasmapheresis material of GPA patients, kindly provided by the Klinikum Großhadern, were precipitated. PR3-specific ANCA were affinity purified from the total IgG solution. Therefore biotinylated PR3 was bound to streptavidin columns and the PR3-specific ANCA were isolated. The elution fractions were tested for the presence of PR3-specific ANCA by ELISA. PR3 was immobilized on nickel-plates and the ANCA in the elution fractions were bound. The fractions, which were positively tested for the presence of PR3-specific ANCA, were then analyzed in an activity assay for their inhibitory capacity (Figure 3.20). PR3 activity was measured in the presence of a three-fold molar excess of ANCA. It was possible to detect inhibitory antibodies among the different patient samples. Antibodies, which strongly inhibited PR3 activity, could be observed in two patient samples. These findings clearly indicated that detection of inhibitory ANCA in patient material is possible and characterization of ANCA according to the activity modulating capacity in principle is feasible.

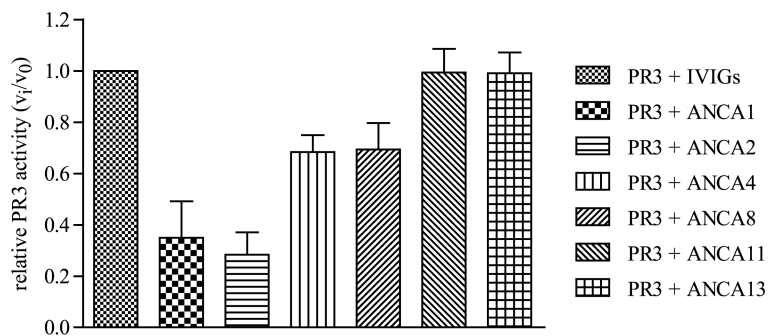


Figure 3.20: Inhibitory ANCA exist in patients with GPA. PR3-specific ANCA, were purified from plasmapheresis material of patients with GPA by affinity chromatography. Biotinylated PR3 was bound to streptavidin columns, the total IgG solution, precipitated from the plasmapheresis material, was loaded onto the columns and PR3-specific ANCA were purified. PR3-specific ANCA were tested for their inhibitory capacity. Therefore ANCA were added to 50 nM PR3 at a three-fold molar excess and PR3 activity towards the FRET substrate TAMRA-VADnVVADYQ-Dap(CF) (5 μ M) was measured ($n = 3$; \pm SEM).

3.6 Detection of activity modulating ANCA in serum from patients with GPA

As the affinity purification of PR3-specific ANCA from plasmapheresis material is very time consuming and a high amount of material is needed, a new method was developed, to characterize ANCA directly in serum or plasma samples from patients with GPA. The high levels of the natural PR3 inhibitor α 1PI in serum and the anticipated low concentration and low affinity of PR3-specific ANCA, however, were challenging circumstances for the development of the new assay. In a standard activity assay PR3 would be immediately inhibited by the α 1PI present in the serum samples. Different approaches, like heat inactivation or depletion of α 1PI, were tested, to remove the α 1PI from the patient samples. But all these attempts did not remove the α 1PI completely. A simple, reliable procedure to purify IgGs from patient samples was needed. By using protein G coupled dynabeads, an IgG solution, which was free of α 1PI, could be obtained. Furthermore the low concentration of PR3-specific ANCA had to be complemented by a very sensitive activity test. For the detection of the inhibitory capacity of these antibodies, they had to be added in quantities to generate at least a two-fold molar excess of PR3-specific IgG over PR3. Hence only a very low amount of PR3 could be used and a very sensitive FRET substrate was needed. For the measurement of the PR3 activity in the presence of ANCA, the used solution contained IgGs at relatively high concentrations. Therefore the intrinsic fluorescence (autofluorescence) of IgGs generated a relatively high background signal. A standard FRET-substrate, with fluorophore-quencher pairs in the short wavelength range was not appropriate, due to the high baseline fluorescence of the IgGs. A FRET substrate with a longer excitation and emission wavelength was required. Hence, a new FRET substrate was designed, containing an optimized peptide sequence for PR3 and TAMRA-fluorescein as a fluorophore-quencher pair. Measurements at the optimal wavelength of this substrate did not generate autofluorescence of the IgGs. Furthermore the optimized substrate was very sensitive, enabling measurements of very low amounts of active PR3. In Figure 3.21 the purification and measurement procedure is summarized. After purification of the total IgGs via protein G coupled dynabeads in a first step, ANCA were added to PR3 in free solution in an estimated four-fold molar excess. Cleavage of the optimized FRET substrate was measured over time. To reduce the sample volume, the measurements were carried out in black 384-microwell plates. Hence, only 4 μ l of patient sample were required for one measurement.

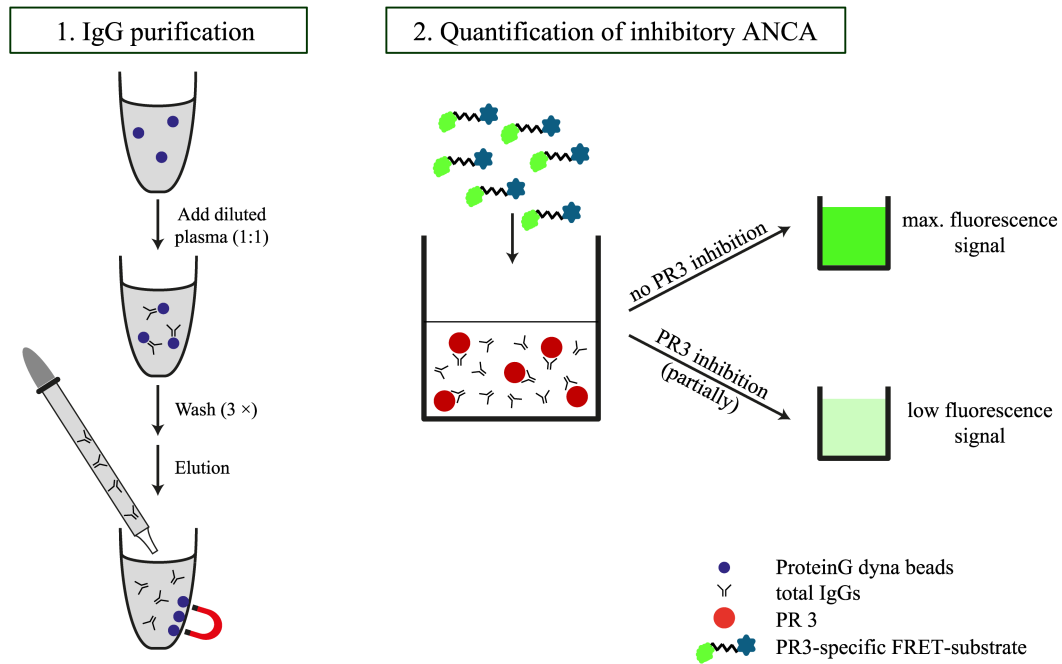


Figure 3.21: New approach to detect activity modulating ANCA in patient samples. Total IgGs from serum or plasma samples of patients with GPA were isolated via protein G dynabeads. To evaluate the amount of PR3-specific inhibitory ANCA, the bound IgGs were taken up in the volume of the original serum sample. Total IgGs at concentrations similar to serum concentrations were added to 10 nM PR3, resulting in an estimated four-fold molar excess of PR3-specific ANCA over PR3. Fluorescence was measured after adding 2.5 μ M of TAMRA-VADnVRDYQ-Dap(CF).

To confirm the practicability of this method, the procedure was tested with three serum samples containing ANCA with known inhibitory properties. The IgGs of the three serum samples R4, R7 and R17 were purified and then tested in the activity assay as described above. The samples R7 and R17 clearly inhibited PR3, whereas R4 did not influence the PR3 activity (Figure 3.22). As a reference for the background, PR3 activity was measured in the presence of therapeutic intravenous immunoglobulins (so-called IVIGs). These IVIG preparations were used at the same concentration as total IgGs. As the inhibitory capacity of R7 and R17 was previously determined in a different way (by Ulrich Specks), the principle feasibility of this method could be ascertained with this experiment. ANCA with activity modulating capacity can be detected with this method.

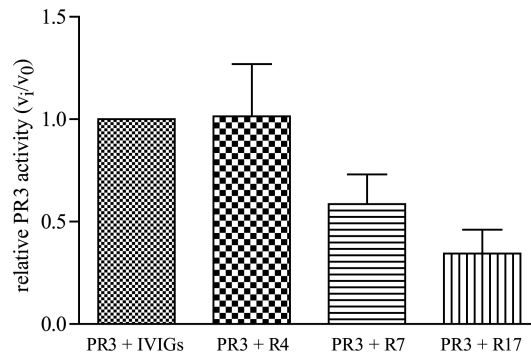


Figure 3.22: Activity modulating ANCA in patient samples. To verify the new method, plasma samples from patients with known ANCA types were tested. Total IgGs were purified from plasma via protein G dynabeads. The inhibitory capacity of PR3-specific ANCA in this solution was measured in an activity assay with 10 nM PR3 and an estimated four-fold molar excess of ANCA. R7 and R17 could be confirmed as PR3-inhibiting ($n = 2$; \pm SEM).

3.7 Correlation of activity modulating ANCA with disease progression in GPA

To study the correlation of activity modulating ANCA with the course of disease in patients with GPA the samples gathered within the scope of the Wegener Granulomatosis Etanercept Trial (The Wegener's Granulomatosis Etanercept Trial (WGET) Research Group, 2005) were used (kindly provided by Ulrich Specks, Mayo Clinic, Rochester, USA). Baseline samples of 180 patients, which were taken at enrollment, were used for the following experiments. In addition 150 follow-up samples of 13 patients with relapses during the assessment time and 106 follow-up samples of eight patients without flares were measured. Activity modulating capacity of all these samples was determined. As negative controls, IgGs isolated from plasma samples of healthy control persons were used. In the patient samples, surprisingly not only ANCA with inhibitory capacity, but also ANCA with activity enhancing capacity towards PR3 could be detected (Figure 3.23). The samples were divided into three groups according to their ANCA type; inhibitory ANCA, neutral ANCA, which did not change PR3 activity, and activity enhancing ANCA. The proportion of these groups in relation to the total sample number was calculated. The vast majority of ANCA in the baseline samples (Figure 3.23 A) as well as in the follow-up samples (Figure 3.23 B) were inhibitory ANCA. Only a relative small proportion of ANCA displayed enhancing or neutral influence towards PR3. In the following the activity modulating capacity of ANCA is displayed as a percentage (%) of PR3 inhibition. As the % PR3 inhibition is calculated by subtracting the measured PR3 activity from 100%, the values representing activity enhancing ANCA are negative.

Furthermore different capture ELISA approaches with all these samples were carried out by Ulrich Specks (Thoracic Disease Research Unit, Mayo Clinic and Foundation, Rochester, MA, USA), to assess the binding properties of the ANCA in the plasma samples.

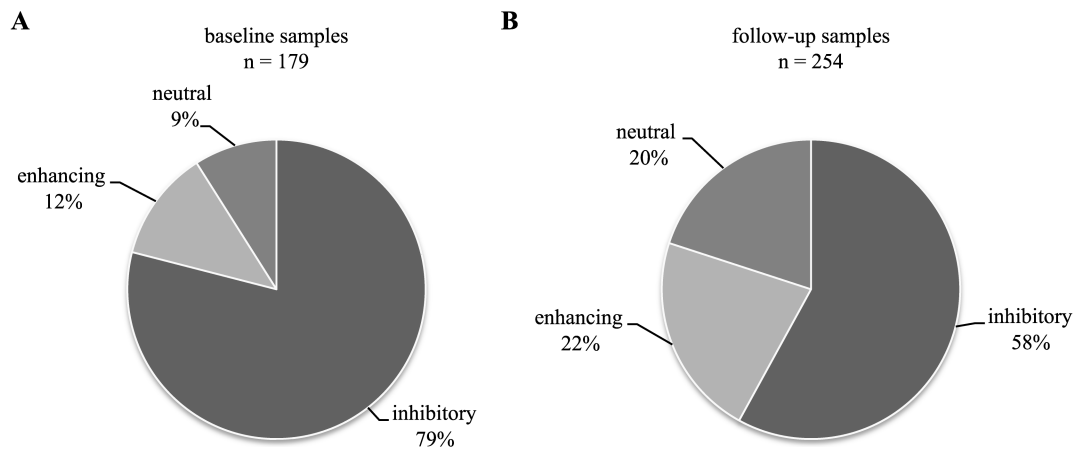


Figure 3.23: The majority of ANCA show inhibitory capacity towards PR3. The activity modulating capacity of PR3-specific ANCA from patients with GPA was determined in an activity assay after isolation of the total IgG fraction with protein G dynabeads. Baseline samples (A), which were taken at enrollment of the patients, and follow-up samples (B), which were taken regularly over the course of disease, were assessed. The samples were divided into groups according to their ANCA type and the proportion in relation to the total sample size was calculated. The vast majority of samples contained ANCA with inhibitory capacity. Only a small proportion of ANCA showed enhancing or neutral activity towards PR3.

3.7.1 Inhibitory ANCA in baseline samples do not correlate with disease severity

As a next step the activity modulating capacity of the baseline samples was examined in relation to disease severity. Disease severity in GPA is measured by the Birmingham Vasculitis Activity Score (BVAS). This score takes the recent disease activity of the previous month in consideration. A BVAS of 0 indicates no active disease, whereas a BVAS above 0 stands for active disease. The BVAS is calculated according to disease severity and severity of organ involvement (Luqmani et al., 1994). Activity modulating capacity of ANCA from all baseline samples was measured and the samples were divided into four groups according to the occurring ANCA type. It was distinguished between ANCA, which inhibited PR3 (PR3 inhibition between 10% and 50%), ANCA, which strongly inhibited PR3 (PR3 inhibition above 50%), ANCA, which did not affect the PR3 activity (PR3 inhibition between -10% and 10%) and activity enhancing ANCA (PR3 inhibition below -10%). The median BVAS of these four groups was calculated and compared (Figure 3.24 A). No significant differences in disease activity between these four groups could be observed. As not all patients were newly diagnosed at the timepoint of enrollment for the study, the patients were additionally

separated into two groups. One group contained the newly diagnosed patients ($n = 80$), and the other group patients, who had recurrent disease at the time of enrollment ($n = 99$). To see if there is a correlation of the occurrence of inhibitory ANCA and disease onset, the median percentage of PR3 inhibition in these two groups was calculated. Comparison of the activity modulating effect revealed no significant difference (Figure 3.24 B). ANCA did not show a stronger inhibitory capacity at the time of diagnosis in comparison to ANCA from patients with recurrent disease. Furthermore the patients were divided into groups according to their disease severity. Patients with local, organ-restricted manifestations (limited disease: $n = 52$) were compared to patients with systemic, multi-organ manifestations (severe disease: $n = 127$). The median PR3 inhibition of these two groups was calculated (Figure 3.24 C). ANCA from patients with severe disease did not display a stronger activity modulating capacity in comparison to patients with limited disease.

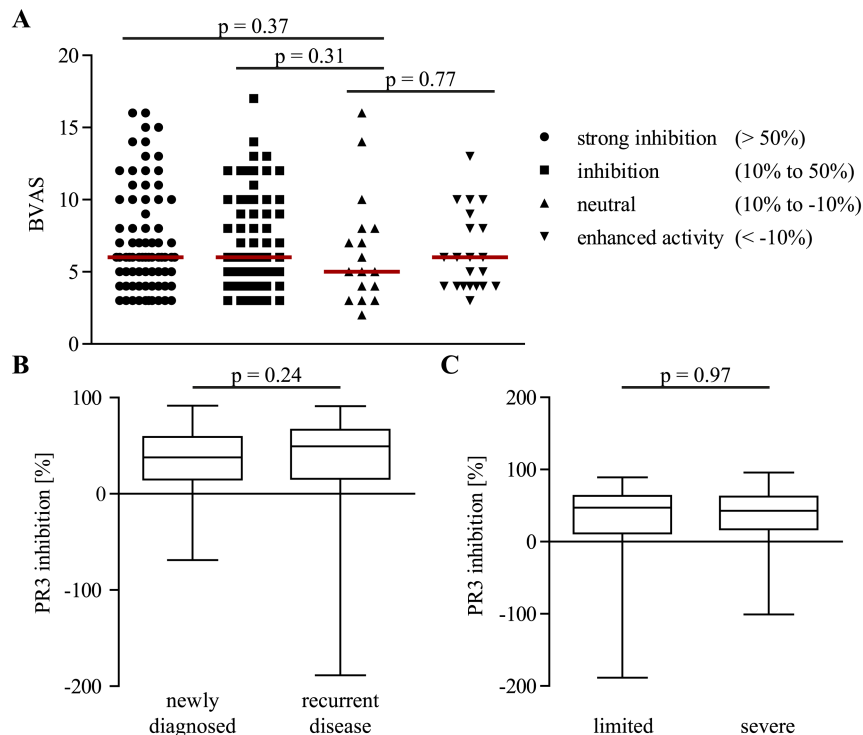


Figure 3.24: ANCA from baseline samples do not correlate with disease severity. To investigate the correlation of activity modulating ANCA with disease severity, baseline samples, which were taken at patient enrollment, were analyzed. A, Patients were divided into four groups, according to the activity modulating type of ANCA. It was distinguished between ANCA, which showed strong (> 50%) or moderate inhibition (10% to 50%), ANCA, that did not change PR3 activity (10% to -10%) and activity enhancing ANCA (< -10%). The median Birmingham Vasculitis Activity Score (BVAS) of these groups was calculated. No significant differences were observed. B, Median PR3 inhibition of ANCA from patients, which were newly diagnosed at enrollment, was compared with median inhibition of ANCA from patients with recurrent disease. No significant differences could be observed. C, Patients with multi-organ manifestations, which were characterized as suffering from severe disease, were compared to patients with local manifestations, with so-called limited disease. The median PR3 inhibition did not differ significantly in those two groups.

3.7.2 Presence of inhibitory ANCA is not related to organ involvement

The BVAS displays only a value for the overall disease activity. To determine the correlation of activity modulating ANCA with single organ involvement, patients were divided into different groups according to the affected organs. The organs strongly affected by GPA are mainly, ear, nose, throat and mucous membrane, the kidneys and the lungs. To compare the ANCA types in regard to organ involvement the patients were separated into two groups for each manifestation, patients with and without involvement of the respective organ. The median PR3 inhibition of ANCA in these groups was calculated and compared. Patients with involvement of mucous membrane and/or ear, nose and throat showed no differences in comparison to patients without these symptoms (Figure 3.25 A). Patients with or without renal manifestations did not disclose differences in PR3 inhibition (Figure 3.25 B). In patients with disease of the lungs a slightly decreased PR3 inhibition could be observed, in comparison to patients without pulmonary involvement (Figure 3.25 C). These differences, however, did not reach statistical significance. To determine the cause for these differences patients were additionally analyzed, considering the occurrence of pulmonary nodules in patients with pulmonary involvement. The group of patients, which displayed pulmonary nodules, was compared to patients without pulmonary nodules. Comparison of these two groups revealed a decrease of PR3 inhibition in patients with pulmonary nodules (Figure 3.25 D). Thus ANCA from patients without pulmonary nodules apparently have ANCA with stronger inhibitory potential.

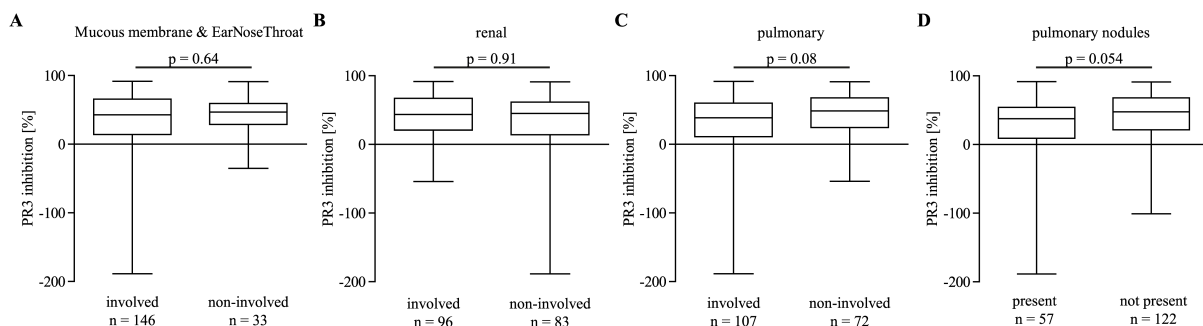


Figure 3.25: Inhibitory ANCA do not correlate with organ involvement. The median PR3 inhibition of ANCA from baseline samples was calculated regarding involvement of certain organs. A, Patients with involvement of mucous membrane and ear, nose and throat were compared to patients without symptoms in these organs. The median PR3 inhibition did not differ in these samples. B, Comparison of patients with or without renal manifestations revealed no differences in PR3 inhibition. C, Median PR3 inhibition was slightly decreased in patients with pulmonary involvement in comparison to patients without pulmonary problems. The differences did not reach statistical significance. D, Median PR3 inhibition of patients with nodule formation in the pulmonary tract was calculated and compared to patients without nodule formation. In patients with pulmonary nodules the median PR3 inhibition was slightly decreased.

3.7.3 Disease activity does not correlate with activity modulating ANCA

Correlation of activity modulating ANCA with disease activity over the course of disease was assessed using the follow-up samples of 12 patients with relapses and eight patients without flares. PR3 inhibition by these ANCA was analyzed considering disease activity at the time, the samples were taken. To answer the question, whether similar changes of PR3 inhibition occur in different patients, ANCA from baseline, remission and relapse samples were compared. No consistent changes in patients with (Figure 3.26 A) and without (Figure 3.26 C) relapses could be observed. Samples taken during timepoints of active disease (baseline and relapse samples) did not show a higher PR3 inhibition in comparison to remission samples (taken three month after enrollment, BVAS = 0). To further characterize the occurrence of inhibitory ANCA the PR3 inhibition over the course of disease was correlated to the BVAS of the respective patient. One example of this correlation of a relapsing patient (Figure 3.26 B) and of a patient without flare (Figure 3.26 D) is shown. In general no correlation of disease activity and presence of inhibitory ANCA could be observed. Inhibitory ANCA did also occur during remission. Over longer remission periods even a rising increase in PR3 inhibition could be observed. This was especially noticeable in patients without flare. In 62.5% of these patients such an increase in PR3 inhibition was detectable. In relapsing patients such an increase of PR3 inhibition could also be observed during remission phases in 58% of the analyzed patients. These findings suggest that there is no direct correlation between disease activity and inhibitory ANCA. However, increasing inhibitory capacity of ANCA during the remission phase in some patients expired in a relapse. Thus increasing inhibition over time in patients in remission could be a sign for future relapses.

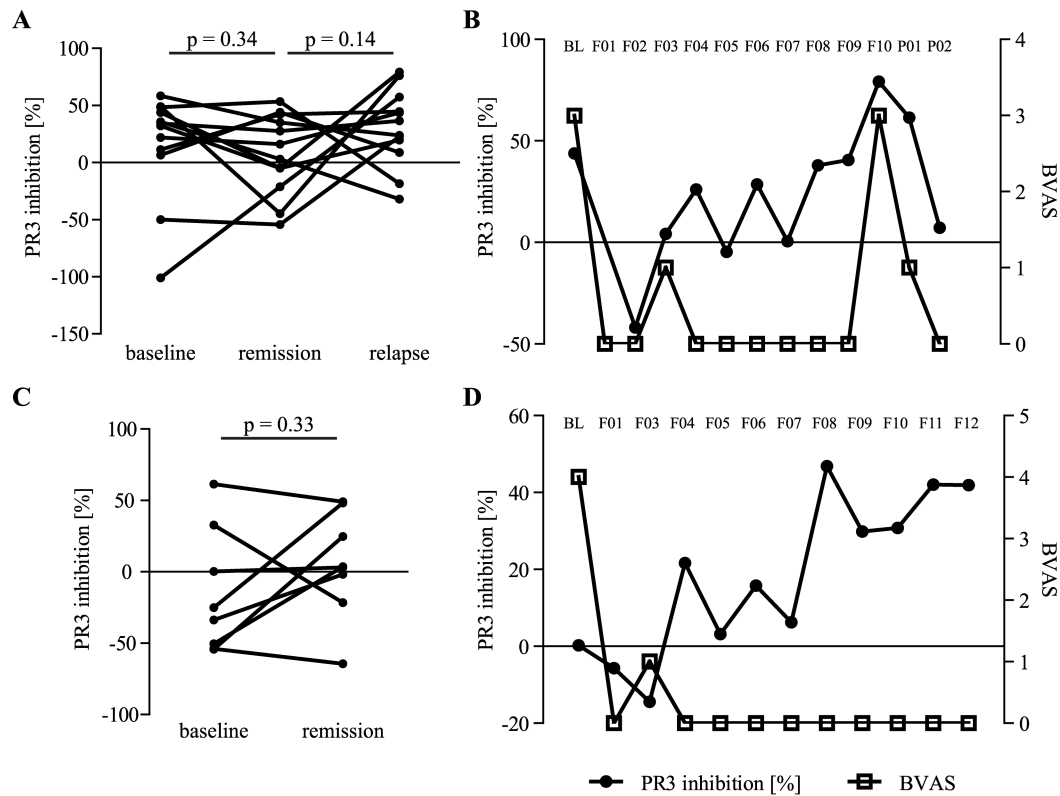


Figure 3.26: Over the course of disease no correlation with activity modulating ANCA could be detected. Follow up samples of patients with relapses (A and B) and of patients without flares (C and D) were analyzed, to investigate correlation of PR3 inhibition with disease activity. A, PR3 inhibition of baseline samples, samples from patients in remission and from relapse samples is displayed. No consistent or significant changes in PR3 inhibition at states of active disease (baseline and relapse) could be detected (n = 12). B, PR3 inhibition of ANCA over the course of disease was correlated to the BVAS of the respective patient. Relapses did not occur in parallel with inhibitory ANCA. However increasing inhibitory potential of ANCA prior to relapses could be detected in 58% of patients (n = 13, one example shown). C, In patients without flares PR3 inhibition of baseline samples (active disease) was compared to remission samples. No consistent differences could be observed (n = 8). D, Correlation of PR3 inhibition in patients without flares with the respective BVAS revealed an increase of PR3 inhibition during remission in 62.5% of patients. In general occurrence of activity modulating ANCA did not correlate with BVAS (n = 8, one example shown).

3.7.4 Epitopes of inhibitory ANCA are located on the active site surface of PR3

The localization of the binding region of inhibitory ANCA was determined with two different capture ELISA approaches. PR3 was captured onto 96-well plates with the antibodies MCPR3-3 or MCPR3-2 and the ANCA binding to PR3 was detected. MCPR3-3 binds to the backside of the PR3 molecule. In a capture ELISA with MCPR3-3 ANCA binding to the front of the molecule (active site region) could be detected. In the MCPR3-2 capture ELISA all available ANCA epitopes are displayed. ANCA from all serum samples are able to bind to PR3 in this capture ELISA approach. The ratio of these two measurements was calculated

(MCPR3-3/2 ratio) and the relative binding epitope was determined. A high ratio suggests binding of the ANCA to the active site region of the molecule. In contrast, a low ratio indicates ANCA binding at the remaining epitopes. To map the binding site of the inhibitory ANCA the activity modulating effect was correlated to the respective MCPR3-3/2 ratio (Figure 3.27). Therefore the follow-up samples of the 13 patients with relapses (Figure 3.27 A) and of the eight patients without flares (Figure 3.27 B) were used. In both patient groups a correlation of PR3 inhibition with the MCPR3-3/2 ratio could be observed. High PR3 inhibition occurred in parallel to high MCPR3-3/2 ratio values. As this high ratio indicates an ANCA binding to the active site region, these results suggest, that inhibitory ANCA mainly bind in the active site region of the molecule.

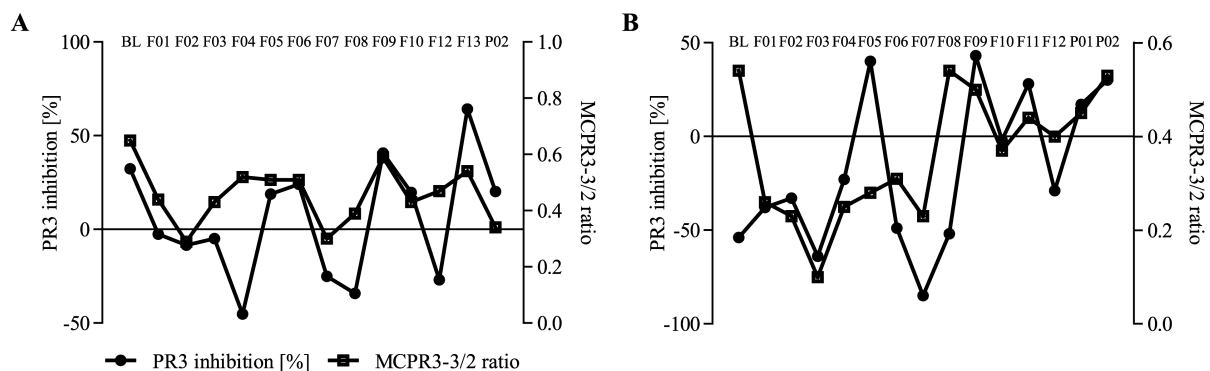


Figure 3.27: Inhibitory ANCA bind to active site surface of PR3. Approximate binding region of all ANCA samples from the WGET study were detected by MCPR3-2 and MCPR3-3 capture ELISA. The ratio of both capture ELISAs was calculated (MCPR3-3/2 ratio). In the MCPR3-2 capture ELISA all available ANCA epitopes are displayed. MCPR3-3 binds to the backside of the molecule and enables ANCA binding to the front (active site region). Thus a high ratio indicates binding of ANCA to the active site region. A low ratio in contrast suggests binding of ANCA to the remaining epitopes. Activity modulating capacity of ANCA from all follow-up samples were determined and correlated to the results of the MCPR3-3/2 ratio. In patients, who had relapses during the course of disease ($n = 13$) (A), as well as in patients without relapses ($n = 8$) (B) the curves for % PR3 inhibition and MCPR3-3/2 ratio showed a strong correlation (one representative sample shown of each group). Plasma samples with high PR3 inhibition in parallel also bound to the active site region of PR3.

Changes in PR3 activity, however, were not only caused by inhibitory ANCA but also by ANCA with enhancing activity. To map the binding region of the activity modulating ANCA in general, the samples were divided into two groups, according to their binding epitope. To this end the MCPR3-3/2 ratio, obtained in the two capture ELISA formats, was used. Samples with a high ratio were taken together in a group, displaying ANCA, which bind to the active site region of the molecule. The other samples, with a low ratio, represent ANCA with preferential binding to the remaining epitopes. The occurrence of activity modulating ANCA in these two groups were calculated (Figure 3.28). A higher proportion of activity modulating ANCA (85%) was observed in the group containing the ANCA, which bound to the active

site region. ANCA with preferential binding to the other epitopes contained only 75% activity modulating ANCA. These findings suggest a more frequent binding of activity modulating ANCA to the active site region.

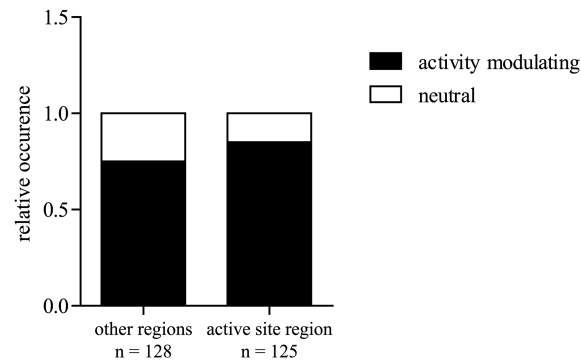


Figure 3.28: Activity modulating ANCA occur more frequently in samples with ANCA binding to the active site surface. The follow-up samples of 21 patients were divided into two subgroups according to their binding epitope. ANCA binding to the active site region (high MCPR3-3/2 ratio) were separated from ANCA which bound to the remaining regions (low MCPR3-3/2 ratio). The proportion of activity modulating ANCA in those groups were calculated and compared. ANCA with activity modulating capacity occurred more frequently in samples which displayed binding to the active site region. 85% of ANCA in this group changed the activity of PR3 in comparison to 75% in the samples containing ANCA, which bound to the remaining epitopes.

3.7.5 Inhibitory ANCA bind not directly into the active site cleft

In Figure 3.27 it could be shown, that the epitope of the inhibitory ANCA is located at the active site region. However the direct binding site as well as the mechanism of inhibition has yet to be addressed. To examine, if the inhibitory ANCA bind directly to the active site cleft, the active site cleft of PR3 was blocked by elafin. PR3-elafin complexes were formed by adding elafin at a ten-fold molar excess to PR3 and incubation for one hour. The complexes as well as PR3 alone were immobilized on nickel-plates and ANCA binding to both PR3-variants was compared by ELISA. For the analysis the 150 follow-up samples of the patients with relapses were used. OD measurements revealed a strong binding of ANCA to both, free PR3 and PR3-elafin complexes. No differences between the two variants could be observed, indicating that binding of elafin to the active site cleft did not obscure the epitope of inhibitory ANCA (Figure 3.29). In contrast, ANCA binding to PR3 and PR3-elafin is strongly correlated to each other. Despite the mapping of the epitope in the active site region, PR3 inhibition by ANCA is not carried out by a direct blocking of the active site cleft. Thus inhibition of PR3 by an indirect allosteric mechanism is most likely.

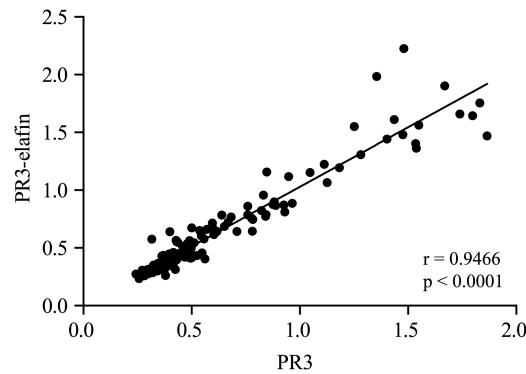


Figure 3.29: The epitopes of inhibitory ANCA are still accessible in the presence of elafin. Binding of ANCA to PR3 and to PR3-elafin complexes was detected in an ELISA. Elafin was added to PR3 in a ten-fold molar excess and incubated for one hour at 37 °C. PR3 and PR3-elafin complexes were immobilized on nickel plates via the 6 × His-tag of PR3 and the binding of ANCA from plasma samples (dilution 1:50) was observed. The 150 follow up samples of the relapsing patients have been investigated. ANCA binding to PR3 was strongly correlated to ANCA binding to PR3-elafin complexes ($r = 0.9466$, $p < 0.0001$).

3.7.6 Inhibition mechanism of some ANCA resembles MCPR3-7 inhibition

To further clarify the inhibition mechanism of ANCA, the extent of epitope sharing with MCPR3-7 was analyzed. MCPR3-7 is able to inhibit PR3 by an allosteric mechanism as described above (see chapter 3.3.6 and 3.3.7). The question as to whether inhibitory ANCA inhibit PR3 by a similar mechanism was answered by employing a MCPR3-7 capture ELISA. In this capture ELISA overlapping of ANCA with the MCPR3-7 epitope could be determined. A high signal in the MCPR3-7 capture ELISA indicated a different binding epitope, whereas a low signal indicated ANCA binding at the same epitope as MCPR3-7. The capture ELISA measurements were carried out using the follow-up samples of the 13 patients with relapses (Figure 3.30 A and B) and the eight patients without flares (Figure 3.30 C and D). The results were then correlated to the PR3 inhibition values of these ANCA. In some graphs the curves for PR3 inhibition and the MCPR3-7 capture ELISA correlated strongly to each other (Figure 3.30 A and C). This means that ANCA, which inhibited PR3 activity, at the same time were able to bind to the MCPR3-7 capture ELISA. Thus these ANCA do not bind to the same epitope as MCPR3-7. In contrast some patients also showed a negative correlation of the two curves (Figure 3.30 B and D). Here samples with inhibitory ANCA could not bind in the MCPR3-7 capture ELISA, indicating a similar inhibition mechanism as MCPR3-7. These findings suggest a heterogeneous inhibition mechanism of ANCA, which may sometimes be mediated by ANCA subpopulations with MCPR3-7-like properties.

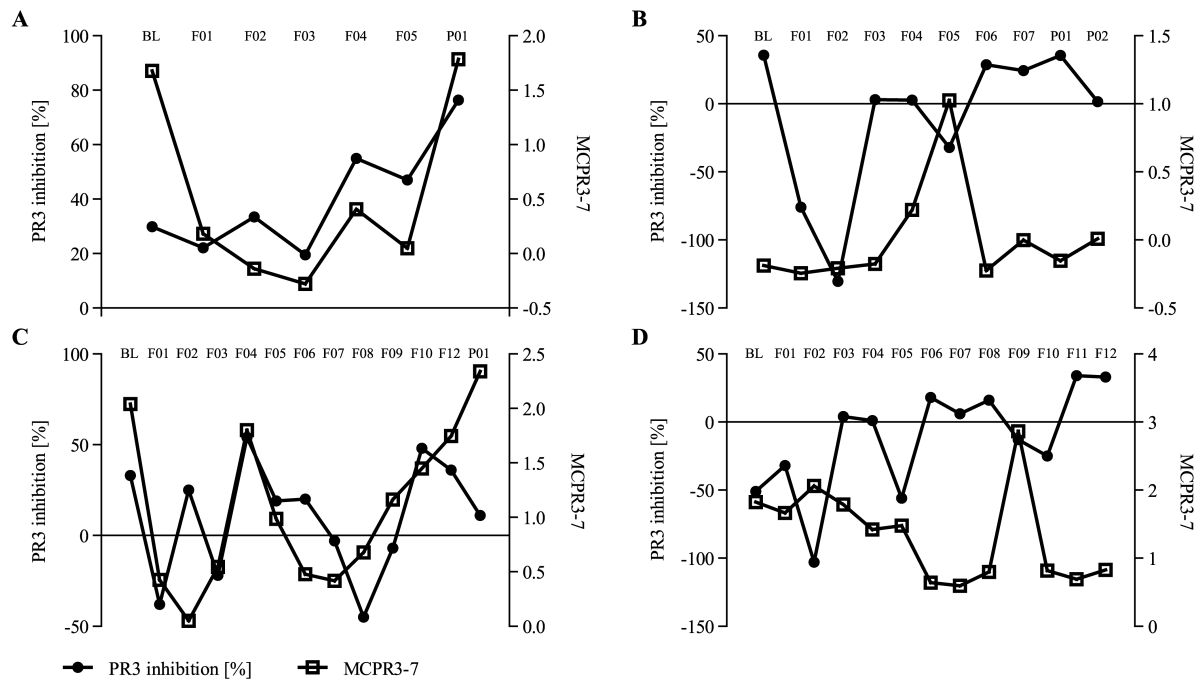


Figure 3.30: Some inhibitory ANCA bind to the MCPR3-7 epitope. To determine an overlap of the epitope from inhibitory ANCA with the MCPR3-7 epitope a MCPR3-7 capture ELISA was performed. A low signal in this ELISA strongly indicates a binding epitope similar to MCPR3-7. Thus a low signal in the MCPR3-7 capture ELISA, which occurs in parallel with high PR3 inhibition, suggests a similar binding mechanism of inhibitory ANCA and MCPR3-7. An overlap of the curves for PR3 inhibition and the MCPR3-7 capture ELISA, in contrast, implies no epitope sharing of inhibitory ANCA and MCPR3-7. PR3 inhibition of relapsing patients (A and B; n = 13; one sample shown for each condition) and of patients without flares (C and D; n = 8; one sample shown for each condition) were correlated with the signals obtained in the MCPR3-7 capture ELISA. In some patients correlation of both curves was observed (A and C), whereas the curves in other patients were negatively correlated (B and D). These findings indicate that only some ANCA inhibit PR3 by a similar mechanism as MCPR3-7.

The overlap with the MCPR3-7 epitope of activity modulating ANCA in general was analyzed in Figure 3.31. The samples were subdivided into two groups, according to the results of the MCPR3-7 capture ELISA. One group contained the ANCA, which displayed a low signal in this ELISA, thus representing ANCA, which shared the MCPR3-7 epitope. The other group contained ANCA, which bound to different epitopes than MCPR3-7 and showed a high signal in the MCPR3-7 capture ELISA. The occurrence of activity modulating ANCA in both groups was calculated. No differences between these two groups could be observed. ANCA that bound to the same epitope as MCPR3-7 displayed a proportion of 79% activity modulating ANCA. Comparably, 81% of ANCA, which bound to the other epitopes, were activity modulating ANCA. A correlation of activity modulating ANCA with the binding to the MCPR3-7 epitope could not be observed.

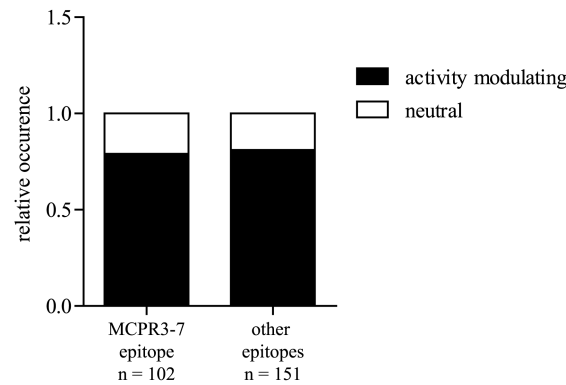


Figure 3.31: Activity modulating ANCA do not bind more frequently to the MCPR3-7 epitope.

The samples were divided into two groups according to their ability to bind to the MCPR3-7 epitope. One group consisted of ANCA, which shared the MCPR3-7 epitope, and the other group contained ANCA, which bound to the remaining epitopes. The proportion of activity modulating ANCA was calculated for both groups. Comparison of both groups revealed no differences in the amount of activity modulating ANCA, indicating a low occurrence rate of MCPR3-7 like ANCA in GPA patients.

However, as shown in Figure 3.30 some ANCA apparently bind to the same epitope as MCPR3-7. To answer the question if these ANCA also inhibit by the same mechanism as MCPR3-7 an activity assay in the presence of an excess of proPR3 was carried out. MCPR3-7 is able to bind to mature PR3 and inhibit its activity. As already described mature PR3 can adopt different conformations and is not held rigidly in its active conformation. Binding of MCPR3-7 induces changes in the PR3 conformation, resulting in an inactive zymogen-like conformation. However, MCPR3-7 preferably binds to proPR3. By adding proPR3 to a mix of PR3 and MCPR3-7 it is able to prevent the inhibition of the mature PR3 (Figure 3.32 A). To see if this is also possible in the case of ANCA, three patient samples were chosen (# 117, # 125, # 143), which bound to proPR3 at least to the same extent as to mature PR3. An activity assay in the presence of a ten-fold molar excess of proPR3 was performed with these samples. In two of the three samples (# 117, # 143) the inhibitory capacity towards PR3 was decreased in the presence of proPR3 (Figure 3.32 B). These findings suggest that some specificities of inhibitory ANCA appear to overlap with that of MCPR3-7. However, the majority of ANCA regulate the catalytic activity of PR3 by another, as yet unknown allosteric mechanism.

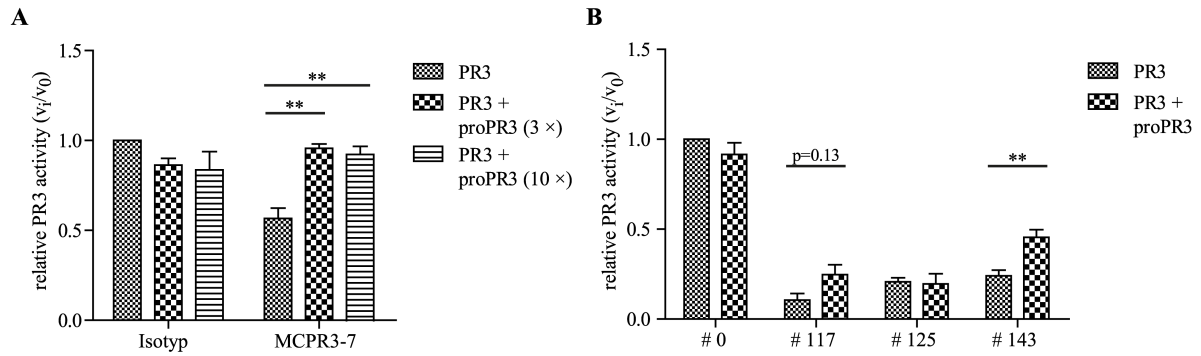


Figure 3.32: Inhibition mechanism of some ANCA reflects inhibition by MCPR3-7. A, To reduce the inhibitory effect of MCPR3-7 on PR3, a three-fold and a ten-fold molar excess of proPR3 was added to the reaction. PR3 (10 nM) was mixed with proPR3 and a four-fold molar excess of MCPR3-7 was added. After incubation at 37 °C for one hour, PR3 activity was measured with TAMRA-VADnVRDYQ-Dap(CF) (2.5 μM) (n = 3; ± SEM). B, Three plasma samples (# 117, # 125, # 143), which showed strong binding to the proform and to the mature form of PR3 were examined, regarding the effect of a ten-fold molar excess of proPR3 on their inhibitory capacity. ANCA from protein G purified IgGs were added at a four-fold molar excess to PR3 (10 nM) with proPR3 (100 nM), incubated for one hour at 37 °C and activity was measured with TAMRA-VADnVRDYQ-Dap(CF) (2.5 μM). As control protein G purified IgGs from a healthy control person were used (# 0). The relative PR3 activity was determined by normalizing PR3 activity in presence of the control antibodies to 1 (n = 3; ± SEM). Presence of proPR3 resulted in weaker PR3 inhibition in only two samples (# 117, # 143). These observations suggest that most inhibitory ANCA do not bind and inhibit PR3 in the same way as MCPR3-7.

4. Discussion

4.1 Expression and functionality of PR3 in the humanized mouse

The human promotor region of the PR3 gene contains a TATA-box, a CAAT-box and GC-rich elements (Jenne, 1994). In contrast, the murine PR3 promotor region includes, besides a TATA-box, a c-myb and a PU.1 binding region (Sturrock et al., 1998). To ensure the expression of hPR3 in the transgenic mice under natural conditions, the murine sequence of the promotor region, exon 1 and large parts of intron1 were maintained in the humanized gene locus. Indeed, no differences could be observed in the transcription of the mPR3 and the hPR3 gene in transgenic mice, which were heterozygous for the humanized gene locus (Figure 3.2 A). Despite the similar mRNA levels of mPR3 and hPR3 in heterozygous mice, the protein expression of hPR3 in the knock-in mice was reduced in comparison to mPR3 in wildtype mice (Figure 3.2 B). The propeptide of PR3, which is located at the beginning of exon 2 and consists of only two amino acids, is not conserved between the human and the murine PR3. The propeptide in hPR3 is Ala-Glu, the propeptide in hNE and mNE is Ser-Glu. In the mPR3 the propeptide is Ser-Lys. Here the amino acid at the P1 position is changed to a basic amino acid and the propeptide is now positively charged (Sturrock et al., 1998). Due to these differences, it is unclear, if the human propeptide is effectively cleaved by the murine dipeptidyl aminopeptidase I (DPPI). The human DPPI is able to cleave Glu-Lys (Kummer et al., 1996). About mouse DPPI, however, it is only known, that it is able to activate neutral murine serine proteases in general (Pham et al., 1997). Furthermore DPPI deficiency leads to decreased PR3 expression levels in patients with Papillon-Lefèvre syndrome (Pham et al., 2004). Thus it is possible that a reduced capability of murine DPPI to cleave the propeptide of hPR3 causes the lower expression of mature hPR3, in particular as no differences on transcription levels could be observed.

Surface expression of PR3 is an important factor in the development of GPA. Antibodies against PR3 interact with the protein on the neutrophil surface and induce activation of the neutrophils, resulting in inflammation of the vessel walls and the surrounding tissue. Thus detection of hPR3 on the surface of the mouse neutrophils was crucial for the generation of an animal model for GPA. After activation of neutrophils with PMA hPR3 was slightly expressed on the surface of knock-in PMNs (Figure 3.5). In contrast to mPR3, which cannot be found on the surface of naïve neutrophils (Pfister et al., 2004), hPR3 is able to bind to the NB1 receptor on the neutrophil surface via its hydrophobic patch (Korkmaz et al., 2008). Besides protein expression, correct folding and catalytic activity of hPR3 in the transgenic neutrophils is an important prerequisite for a useful new animal model. A new method, with a lipidated FRET-reporter, which is specific for a protease and is targeted to the plasma membrane, was the perfect tool, to assess the catalytic activity of PR3 on the membrane surface of neutrophils. Local activity of MMP-12 and NE on the cell surface was already analyzed with such a lipidated FRET-reporter (Cobos-Correa et al., 2009; Gehrig et al., 2012). Similarly the activity of membrane-bound PR3 could be assessed with a PR3-specific lipidated FRET-reporter (Figure 3.6 and 3.7). As this method is highly sensitive, active PR3 was also detected on TNF α -primed neutrophils of knock-in mice (Figure 3.7 B and E). Despite the detectable surface expression of PR3 in PMA treated PMNs, PR3 activity on the surface of these cells was reduced in comparison to TNF α -primed neutrophils (Figure 3.6 E and 3.7 E). Stimulation of neutrophils with PMA leads to a strong degranulation of azurophilic and specific granules (Yurewicz and Zimmerman, 1977). Mason et al. demonstrated that α 1PI, the natural inhibitor of PR3, is not only expressed by hepatocytes, but can also be synthesized in neutrophils (Mason et al., 1991). In the neutrophils α 1PI is localized in the azurophil granules and is thus released after PMA activation. Hence it is likely that despite an increased expression of PR3 on the neutrophil surface after PMA stimulation, PR3 activity is partly inhibited by α 1PI and thus only a reduced activity signal of PR3 could be observed.

4.2 MCPR3-7, a unique antibody with PR3-inhibiting potential

4.2.1 MCPR3-7 in comparison to other antibodies

Based on the literature, antibodies with inhibitory capacity towards the proteolytic activity of PR3, have a high pathogenic potential (Daouk et al., 1995; Dolman et al., 1993; van der Geld et al., 2002) and thus seemed most promising for the transfer into the transgenic mice. The inhibitory potential and binding properties of a set of mAbs were characterized to this end. One of these antibodies, MCPR3-7, was found to display inhibitory capacity towards PR3 (Figure 3.8). The other antibodies did not affect the activity of PR3. In case of CLB-12.8 this was rather surprising. Due to its binding epitope, which is located in close proximity to the active site cleft (Silva et al., 2010), inhibitory capacity of this antibody was expected. In addition to the lack of inhibitory capacity of CLB-12.8, it also did not interfere with the covalent or canonical complexation of PR3 to α 1PI (Figure 3.10 C and 3.11). The binding of CLB-12.8 to the covalent PR3- α 1PI complex, however, was impaired (Figure 3.9 B). This loss of binding ability of CLB-12.8 towards the covalent PR3- α 1PI complexes can be explained by the conformational transition of the active site cleft of PR3 after covalent interaction with α 1PI. This conformational change could already be observed with elastase and α 1PI (Huntington et al., 2000) and in the complex between trypsin and an Arg-mutant of α 1-antitrypsin (Dementiev et al., 2006). In the covalent complex the P1 residue of the RCL is no longer buried in the S1 pocket of the enzyme. Furthermore the autolysis loop 142 – 129, the 186 – 190 loop and the four N-terminal residues are disordered resulting in an inactive conformation of the protease. These changes probably affect the CLB-12.8 epitope and prevent the interaction with the antibody. In case of MCPR3-7, however, which has higher binding affinity to the proform of PR3, covalent complexation induces the foundation of the MCPR3-7 epitope (Figure 3.9 A). Conversely, binding of MCPR3-7 to the fixed active conformation of PR3 was not possible. As MCPR3-7 nevertheless inhibits PR3 activity, it apparently is only able to interact with PR3 in an intermediate conformation of the mature molecule. For that reason MCPR3-7 is able to inhibit PR3 activity and interaction of PR3 with α 1PI (Figure 3.10 B and 3.11). The inhibition mechanism of MCPR3-7 is discussed in detail in the following chapter. Among the tested antibodies, MCPR3-7 was the only one with

inhibitory capacity towards PR3 activity and its complexation with α 1PI, turning it into an interesting candidate for transfer experiments in hPR3^{+/+} mice.

4.2.2 MCPR3-7 and its mechanism of inhibition

The proform and the mature form of PR3 adopt two different conformations of high structural similarity. The only differences detected in those two forms are in the activation domain (Fehlhammer et al., 1977). The differential binding of MCPR3-7 to the two conformations, which was observed in the course of this thesis, suggests a binding epitope near the activation domain. Binding of MCPR3-7 to the stabilized active conformation was not possible. AAPV-CMK, a mechanism-based small inhibitor, forms a stable covalent complex with PR3 and stabilizes the active conformation of the molecule. No binding of MCPR3-7 to these PR3-inhibitor complexes could be observed in the thermophoretic quantification (Figure 3.13) as well as in ELISA experiments (Figure 3.9 A). Consistent with these findings, MCPR3-7 was not able to bind to the canonical PR3- α 1PI-complexes or the PR3-elafin complexes, which both display PR3 in its active conformation. MCPR3-7 appears to be a conformation specific antibody, which discriminates between the active and the inactive conformation of PR3. Mapping of the MCPR3-7 epitope to the active site region was confirmed in an activity assay with human/gibbon chimeras (Figure 3.12). On the carboxy-terminal half, which contains the activation domain, the gibbon PR3 has non-conservative residue substitutions (Lys187Gly; Trp218Arg; Ala146Thr) (Kuhl et al., 2010). PR3 variants containing this gibbon carboxy-terminal β -barrel were not inhibited by MCPR3-7, indicating binding of the mAb to the carboxy-terminal half of the molecule. These results were consistent with the findings of Silva et al. (Silva et al., 2010). Here the MCPR3-7 epitope in mPR3 could be reconstituted with human residues, and the binding near to the active site region could be confirmed.

Despite an inability of MCPR3-7 to bind to the fixed active conformation of PR3, it is able to bind to free mature PR3 and to inhibit its activity. Mature PR3 is not held rigidly in its active conformation. Even after propeptide cleavage it can adopt a zymogen like conformation (Pozzi et al., 2012), enabling MCPR3-7 to interact with the mature form. This interaction of MCPR3-7 with the mature PR3, however, was weak and about 40-fold lower than the binding to proPR3 (Figure 3.9 A and 3.13). Nevertheless MCPR3-7 strongly inhibited the activity of mature PR3 (Figure 3.8). Binding of the antibody probably can force PR3 into an inactive conformation, which results in the loss of the S1 binding site and the oxyanion hole. The inhibitory effect of MCPR3-7 was first detected with the optimized peptide substrate Abz-

YYAbu-ANBNH₂. The amino acid residues of this substrate occupy the S1 – S3 pockets. In addition, the S4 and the S1' pocket are engaged by the fluorophore-quencher pair. Thus the inhibitory effect could not be traced back to a distinct peptide binding pocket on the basis of this substrate. Substrates with other leaving groups in the P1' position, like for example 5-amino-2-nitrobenzoic acid (ANB-OH), para-nitroaniline (*p*NA), the benzyl mercaptan from SBzl or the para nitrophenol (Boc-L-A-ONp) are known to interact less efficiently with the S1' subsite of PR3, than ANB-NH₂ substrates (Wysocka et al., 2008). PR3 was indeed able to cleave two such substrates in the presence of MCPR3-7 (Figure 3.14 D and E), indicating that MCPR3-7 primarily alters the shape and access of the S1' pocket. After MCPR3-7 binding only smaller and less polar leaving groups were accepted in the S1' pocket. To exclude an influence of MCPR3-7 on the S1 pocket of PR3, substrates with smaller (Ala) and larger (nVal) P1 residues were tested. No changes of PR3 activity after variation of P1 residues was observed. As elucidated in Figure 4.1, these findings confirm, that besides the preference of MCPR3-7 for the proform of PR3 (Z), interaction with mature PR3 (E) is possible, due to the ability of mature PR3 to adopt different conformations. Binding of MCPR3-7 to mature PR3 shifts the equilibrium of the different mature conformations towards the inactive conformation (E*), by altering the S1' pocket. Hence, the presence of MCPR3-7 reduces the activity and alters the interaction of PR3 with substrates. Due to the altered accessibility of the active site cleft the interaction of α 1PI with PR3 in presence of MCPR3-7 is furthermore reduced and the complexation delayed (Figure 3.10 and 3.11).

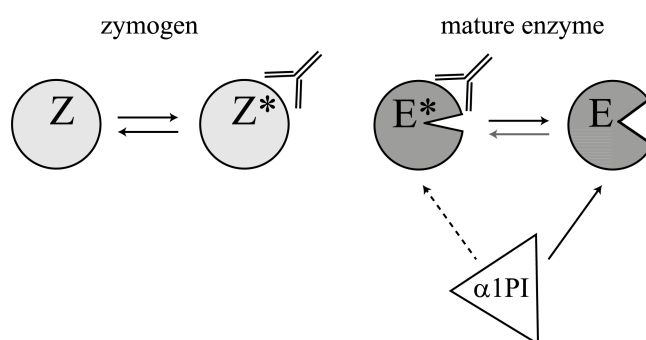


Figure 4.1: Interaction of MCPR3-7 with proPR3 and mature PR3. MCPR3-7 binds preferentially to the proform (Z) of PR3. Binding of MCPR3-7 to proPR3 results in slight conformational changes of the zymogen (Z*). Mature PR3 occurs in two different conformations, an active (E) and an inactive (E*) conformation, which are in equilibrium in free solution. Binding of MCPR3-7 shifts this equilibrium towards the inactive conformation (E*). Interaction with the antibody stabilized the inactive conformation of PR3 and changed the activity and substrate interaction with PR3. Furthermore MCPR3-7 has an inhibitory effect on the complexation of PR3 with α 1PI (dotted line).

Antibodies, which can interfere with the activity of proteases, can be divided into two different groups according to their mode of action (Ganesan et al., 2010). One group contains antibodies, like MCPR3-7, which inhibit the protease activity by induction of an allosteric switch in the protease. These antibodies do not compete directly with the substrate for the active binding pocket. In contrast, they bind a region at the periphery of the substrate binding cleft and cause a conformational switch of surface loops, which determine the size and the shape of the binding pockets. Such antibodies are able to reduce, alter or completely suppress the catalytic activity of proteases. The second group of antibodies inhibits the protease activity by direct binding to the active site cleft. The surface loops of these antibodies insert directly into the substrate binding pockets. Thereby the access of the substrate to the active site is blocked. This form of antibodies is rarely found in mammals and hardly induced by immunizations. These previous observations are consistent with our findings, indicating that MCPR3-7 inhibited PR3 by an allosteric effect. The autolysis loop, as well as the 187-190 loop, are loops, which shape the S1, S1' and S2' pockets (Fujinaga et al., 1996). Thus these loops are good targets for allosteric regulation of enzyme activities. Binding of MCPR3-7 is probably facilitated by partial rearrangement of these loops in the mature enzyme and this interaction then results in changes in substrate recognition and interactions of PR3 with the RCL of α 1PI.

4.2.3 Limitations of MCPR3-7

Despite the interesting properties of MCPR3-7, utilization of this mAb for transfer experiments proves to be difficult. Detection of membrane-bound PR3 with MCPR3-7 was not possible (Figure 3.15). The epitope of MCPR3-7 was mapped to a region, which lies near the hydrophobic patch of PR3 (Silva et al., 2010). Korkmaz et al. identified this hydrophobic patch as the region of PR3, which interacts with the NB1 receptor (CD177) on human neutrophil membranes. Binding of PR3 to the neutrophil membrane most likely obscures the epitope of MCPR3-7 (Korkmaz et al., 2008) and prohibits the detection of membrane-bound PR3 by MCPR3-7. Thus neutrophil activation by MCPR3-7, which was crucial for disease induction in mice, is not possible. Activation of neutrophils via MCPR3-7-PR3 immune complexes would be another possibility to provoke an inflammatory response. The low affinity of MCPR3-7 for mature PR3 (Figure 3.9 and 3.13), however, makes the formation of such immune complexes unlikely. Hence, transfer of MCPR3-7 into the hPR3 knock-in mice would probably not lead to the induction of systemic vasculitis.

4.3 The GPA mouse model

4.3.1 Induction of inflammation by transfer of hPR3 antibodies

Interaction of PR3-ANCA with neutrophils induces respiratory burst, degranulation of the neutrophils and release of cytokines (Falk et al., 1990; Grimminger et al., 1996; Kettritz et al., 1997). Despite several attempts to assess the pathogenicity of ANCA in a mouse model, direct evidence for ANCA pathogenicity is still missing. Differences in the expression of human and murine PR3 as well as differences in interactions of Fc γ Rs and IgGs in mice and humans complicated the development of a suitable mouse model for GPA. The first indication that antibodies against PR3 are able to trigger inflammatory responses was published by Pfister et al. in 2004. Antibodies against murine PR3 were generated in PR3/NE double knock-out mice and transferred into wildtype mice. A pro-inflammatory activity of these antibodies in combination with a primary inflammatory stimuli (LPS or TNF α) was observed (Pfister et al., 2004). These mice did not develop disease related symptoms, probably due to the weak direct interaction of antibodies with mPR3 on murine neutrophils. In another study human neutrophils, expressing hPR3 on their surface, were used to enable direct interaction of hPR3-specific antibodies with neutrophils (Hattar et al., 2010). Here TNF α -primed human neutrophils and monoclonal antibodies against hPR3 were injected into isolated rat lungs. The direct interaction of the mAb with hPR3 on the surface of neutrophils led to severe vascular leakage and edema formation. However, no morphological changes could be observed in these lungs. As only an isolated organ system was examined in this study a statement about the pathogenicity of ANCA in GPA could not be made. To study the effect of PR3 antibodies on the whole organism two different transgenic mouse models, expressing hPR3, were already created. In one of these mouse models, however, hPR3 was expressed under the control of a podocin promotor and thus expression was redirected and restricted to the kidneys (Relle et al., 2013). Injection of mAbs against hPR3 did not lead to morphological changes of the kidneys in this model. The expression of hPR3 in the kidneys, however, was only analyzed at RNA level. Lack of pathogenic changes in the kidneys could also be due to a lack of hPR3 expression. Involvement of the kidneys is a hallmark of the generalized form of GPA. In early localized stages of the disease, manifestations in the kidneys are rarely observed in patients. Analysis of the mice already five days after injection of the antibodies might thus have been too early.

To overcome differences in human and murine FcγRs and IgGs and due to the lack of cross-reactive epitopes between human and mouse PR3, a human hematopoietic system was reconstituted in severely immune-compromised mice by injection of human hematopoietic stem cells in irradiated, bone marrow-depleted mice (Little et al., 2012). In this model the lungs of the mice indeed showed vasculitic changes and hemorrhage after injection of human IgG from patients with GPA. Furthermore mild glomerulonephritis with leukocyte infiltration was observed in these mice. These findings led the authors to postulate a clear pathogenic role of total IgG from GPA-patients *in vivo*. Nevertheless they admitted that the ability of human leukocytes to adhere to the murine endothelium and to transmigrate through mouse blood vessels was questionable. Furthermore the majority of recruited leukocytes were murine. Only a few human leukocytes infiltrated the tissue. The humanization of the murine immune system thus was not complete in this model. Hence it is possible that the present murine immune cells disturb the tolerance induction of the human immune cells and lead to a graft versus host reaction. Therefore it is likely that the observed immune response is not only caused by interaction of antibodies with hPR3 on human neutrophils, but also by an immune defense reaction to the human bone marrow graft.

Due to the many discrepancies in the existing animal models for GPA and due to the lack of evidence for the pathogenicity of ANCA a new mouse model was generated within the work of this thesis, to analyze the role of ANCA. In the transgenic mouse generated in this study the hPR3 is expressed in and on the mouse neutrophils, enabling expression of PR3 under natural conditions and direct interaction of hPR3-specific antibodies. Apart from the expression of the hPR3 the murine immune system was kept unchanged resulting in normal expression of the murine FcγRs and normal effector functions of the immune cells. Hence usage of murine mAbs enabled interaction of FcγR and IgG under natural conditions. In addition to the antibodies LPS was injected into the transgenic mice, to induce a mild inflammation. LPS is an initial trigger to prime neutrophils for degranulation and also induces endothelial activation (Li et al., 2010). Furthermore it was already shown by Pfister et al. that the proinflammatory effect of the antibodies is increased in combination with a primary inflammatory stimulus like LPS (Pfister et al., 2004). Injection of the antibody induced a recruitment of immune cells to the lungs in the transgenic mice (Figure 3.18) and an inflammatory response. This immune cell infiltration was confirmed by histopathological analysis of the lungs, which revealed a strong inflammation in the lung vessels and the lung tissue. Hence, it could be shown that hPR3 antibodies indeed have the capacity to induce

vasculitis and inflammations in the lungs. However, the effect of the antibody transfer on the kidneys has not yet been examined. To gather a complete comprehension of the pathogenicity of PR3-specific antibodies this aspect of the model still needs to be investigated in further detail.

4.3.2 The immune response is triggered by properties of immunoglobulins

The immune response to antibodies is triggered by the interaction of the immunoglobulins with the FcγRs on the immune cells. This interaction on one hand is characterized by the heterogenicity of the FcγRs, regarding expression pattern, specificity and effector functions. On the other hand binding of FcγRs to the immunoglobulins is influenced by the different affinities of the IgG subclasses for the receptors. Posttranslational modifications like for example glycosylation of antibodies and receptors can further modulate the interaction. Abnormalities in one of these factors can favor the development of different diseases. Polymorphisms in FcγRs that are known to reduce the immune complex clearance for example are a risk factor for Systemic Lupus Erythematosus and GPA (Dijstelbloem et al., 1999, 2000). The use of mice, which are transgenic for the human FcγR further enabled the analysis of the pathological mechanisms and role of the human FcγR. With these mice a contribution of the human FcγRs to antibody-mediated disease could be shown (Gillis et al., 2014). Mice as well as humans have three activating FcγRs and one inhibitory receptor (Nimmerjahn and Ravetch, 2012). Despite this general similarity of the receptors in mice and men, they exhibit differences in the expression pattern and their binding abilities (Bruhns, 2012). Thus interaction with the different IgG subclasses can lead to activation of different effector functions. These differences have to be considered for the generation of mouse models. In the new transgenic mouse model of this thesis these discrepancies have been avoided. Only the gene for murine PR3 was replaced in the mice by the human variant. The transferred antibodies were murine antibodies, ensuring the correct interaction of the murine FcγRs and the immunoglobulins. Usage of human antibodies would nevertheless be possible, due the ability of murine FcγRs to bind to human IgG (Bruhns, 2012). However, it is not clear if the binding affinities of murine FcγRs to human IgG subclasses differ from the affinities to murine IgG subclasses and if therefore other effector functions would be activated. Mice and humans have four different IgG subclasses (mice: IgG1, IgG2a, IgG2b and IgG3; humans: IgG1, IgG2, IgG3 and IgG4). The most potent subclasses in activating effector responses in mice are IgG2a and IgG2b. Therefore these antibody types are most frequently observed in

autoimmune diseases (Nimmerjahn and Ravetch, 2005). The different subclasses vary in their activation potential towards FcγRs (Kocher et al., 1998; Mulder et al., 1995). Thus the functional responses are dependent on the respective subclass. Each IgG subclass has a unique activation profile of effector functions and efficacy (Roux et al., 1997). For ANCA it could already be shown, that the different subclasses indeed can have a differential influence on disease progression. The subclasses differ especially with regard to the activation of neutrophils and the induction of inflammatory responses. IgG3 are the most potent mediators of neutrophil activation followed by IgG1, which is still more potent than IgG4 (Pankhurst et al., 2011). Based on these differences, I decided to inject antibodies of different subclasses into the transgenic knock-in mice. IgG2a and IgG2b are able to bind to all activating FcγRs in mice. Among the different subclasses IgG2a binds with the highest affinity to the activating FcγRs (Bruhns, 2012). Therefore it is not surprising that the PR3-specific antibody 4B12, which is an IgG2a antibody, had the strongest effect on immune cell recruitment and induction of inflammation (Figure 3.18). In contrast, injection of 7D12 led only to a slight recruitment of neutrophils and macrophages. The resulting inflammation was less pronounced in comparison to 4B12. 7D12 is an IgG2b antibody. The slightly lower affinity of IgG2b for the activating FcγRs probably is the reason for the differences in the immune response to these two antibodies. These findings clearly indicate a pathogenic role of the PR3-specific antibodies in the development of inflammation and a GPA-like phenotype. According to these results pathogenicity of PR3 antibodies seems to depend on the respective subclasses.

Besides structural differences in immunoglobulins and FcγRs, posttranslational modifications can also influence the interaction between receptors and IgGs and thus modulate the immune response. IgGs have a conserved N-glycosylation site at Asn297 (Ferrara et al., 2011). The attached glycans can change the affinity of the immunoglobulin for the receptors and therefore regulate the immune response. Deglycosylation of IgG for example reduces the binding to FcγR or complement and thus impairs the activation of the effector functions. Lack of fucosylation, by contrast, enhances the interaction with FcγRs. The binding affinity to the receptor increases and the effector functions are activated (Krapp et al., 2003). Also an influence of glycosylation on autoimmune diseases could already be shown. A reduced galactosylation is further known to be associated with ANCA associated vasculitides (Holland et al., 2002). Thus it is conceivable, that the development of an immune response in the present mouse model can also be influenced by the carbohydrate structure and composition of the injected antibodies.

4.4 Contribution of ANCA to GPA development and disease progression

4.4.1 Influence of activity modulating ANCA on disease progression

Enzymes, which are presented on the membrane, are possible targets, as they are directly accessible for autoantibodies. Hence, enzymes in neutrophil granules, like for example PR3, NE and MPO, which are released upon activation of neutrophils and can be bound to the neutrophil surface, are often target antigens in autoimmune diseases. Due to the fact that autoantibodies are often directed against proteolytic enzymes it is possible, that their pathogenic effect is based on an interference of the antibodies with biological functions of the enzymes. Interference of the autoantibodies with the proteolytic activity of the respective enzyme, however, is still questionable. Studies to answer these questions were already initiated a long time ago. Inhibition of the three major ANCA-autoantigens, PR3, NE and MPO, by autoantibodies was not observed in one of the first studies (Chang and Savige, 1993). It is possible, however, that the assay used for these observations was not sensitive enough to detect the low subpopulation of autoantibodies, which interact with the catalytic surface region. In another study, conducted by van de Wiel et al., the inhibitory potential of PR3-ANCA from eight patients was analyzed. A 45-fold molar excess of total IgG was able to reduce the PR3 activity towards Suc-AAPV-pNA and FITC-labeled elastin (van de Wiel et al., 1992). The strong inhibitory effect of small amounts of ANCA and the high fraction of PR3-specific antibodies (16%), however, was puzzling.

Besides interference of autoantibodies with enzymatic functions, also correlation of this interference with disease progression and severity was in question. Daouk et al. analyzed the effect of purified total IgG on PR3 activity towards Boc-A-ONp dependent on disease activity. With a 20-fold molar excess of total IgG over PR3, inhibitory ANCA were detected in eight out of ten patients with active disease and one out of seven patients in remission. The apparent constant determined for the inhibitory effects was pretty high (56.5 μ M), suggesting that IgG populations with low PR3 affinity accounted for these effects (Daouk et al., 1995). Conversely, van der Geld et al. analyzed samples of 26 patients with active disease and 17 patients in remission and identified inhibitory ANCA in all these samples. For these measurements a lower total IgG concentration was used (100 μ g/ml). This latter group furthermore observed on average higher ANCA titers during relapse phases. The fraction of

the non-inhibitory ANCA, however, increased during active disease, whereas the pool of inhibitory ANCA did not (van der Geld et al., 2002). According to this study inhibitory ANCA did not appear to cause or initiate active disease and were not regarded as a predictor for relapses.

The previous studies, discussed in the last paragraphs, do not give a clear answer to the question as to whether inhibitory ANCA correlate with disease activity. The reason for the controversial discussions in the literature may be due to differences in the methodologies. Based on the uncertainties and technical inadequacies detected in these studies, a new method was developed in this thesis to solve this controversy. To determine the allosteric effects of autoantibodies on PR3 activity, the properties of the used substrate plays an important role. Its interaction with PR3 is dependent on the type and concentration of the substrate. Small substrates, like for example Boc-A-ON_p, react only with a small region of the active site cleft (S1 and S1' pocket). To assess conformational changes along the entire active site cleft extended peptide substrates are necessary, which align with up to eight prime and non-prime subsites. Usage of FRET-based reporters increases further the sensitivity to distortions along the binding cleft and work at lower concentrations. Due to the high concentrations of total IgG required to test the functional properties of ANCA, autofluorescence of IgG in the low excitation wavelength range causes a high background and limits sensitivity. To overcome the autofluorescence problem, a TAMRA-fluorescein pair was chosen for the newly developed assay in combination with a highly sensitive peptide sequence.

In previous studies the inhibitory capacity of ANCA was directly compared to changes in ANCA titers over the course of disease. ANCA titer measurements, which are carried out by ELISA, however, identify a different set of antibodies than activity measurements in free solution. The direct immobilization of the antigen in ELISA experiments can lead to loss or alteration of epitopes, changes in enzymatic or biological activity or generation of new epitopes in the antigen. Immobilized antigens are not displayed in the same manner as in solution. Hence, indirect ELISA approaches are sometimes preferred. The performed washing steps further reduce the level of bound ANCA with lower affinities. Thus only high affinity antibodies can be detected. In an activity assay, in contrast, the measurements are performed in free solution. For that reason binding of low affinity antibodies is not reduced by washing steps and a different set of antibodies can be detected. Measurement of PR3 inhibition could only be achieved with concentrated IgG solutions. The low affinity ANCA are recognized in these assays, whereas high serum dilutions in ELISA experiments disfavor the binding of

these ANCA. Already van der Geld et al. noticed the low concentrations and affinity of inhibitory ANCA. Consistent with these findings and the methodological discrepancies, a dilution of the IgG samples led to a loss of signal in the activity assay, whereas an ELISA signal could be observed at even higher dilutions. Therefore it is not too surprisingly that no correlation between ANCA titers and inhibitory capacity was reported (Dolman et al., 1993).

To detect these low affinity and low concentrated inhibitory ANCA, a high molar excess of purified IgG had to be added to a small amount of PR3. In the newly developed assay the IgG concentrations after purification were only slightly lower as found in human serum. Already at these slightly lower concentrations of ANCA an influence on PR3 activity could be determined. Analysis of baseline samples from 180 patients and follow-up samples of 21 patients revealed that the majority of ANCA was able to inhibit the activity of PR3 (Figure 3.23). Additionally a group of ANCA was identified, which was able to enhance the activity of PR3. As all ANCA were able to bind to PR3-elafin complexes, activity modulating ANCA do not appear to directly interact with the active site cleft of PR3 and probably interfere with PR3 activity by an allosteric mechanism. Mature PR3 in free solution is able to adopt different conformations (Pozzi et al., 2012) as already explained in chapter 4.2.2. For that reason, it is likely that PR3 activity enhancing ANCA stabilize the active conformation of PR3 and thus shift the conformational continuum of PR3 towards its active conformation.

As the amount of ANCA in human serum is even slightly higher than in our activity test, it can be assumed that ANCA interfere with functions of PR3 in vascular compartments or at sites of neutrophil extravasation. Hence, inhibitory ANCA must be considered as a potential determinant for disease severity, organ manifestations or disease progression. However no correlation between disease activity and PR3 activity modulating ANCA was detectable in the present study. Separation of baseline samples into groups according to their type of activity modulating ANCA did not reveal differences in the median BVAS (Figure 3.24 A). The occurrence of inhibitory ANCA was furthermore not correlated with disease outbreaks (Figure 3.24 B) or intensity of disease (Figure 3.24 C). Organ involvement is, as already described, a marker for disease severity. Especially involvement of lungs and kidneys occurs mostly in patients with severe or generalized GPA. Comparison of the median PR3 inhibition in patient groups, subdivided according to the involvement of certain organs, however, did not reveal any significant differences (Figure 3.25). In patients with lung involvement PR3 inhibition was slightly reduced. This reduction of PR3 inhibition was even more pronounced in patients with lung nodules. Over extended periods of observation times inhibitory ANCA

did not solely occur in phases of active disease, but could also be detected during remission (Figure 3.26). No consistent changes in inhibitory capacity were seen at any time over the course of the disease (Figure 3.26 A and C).

One reason for the discrepancy between the present study and the study conducted by Daouk et al. might be the low number of samples, especially for remission phases in the latter. Usage of the substrate Boc-A-ONp furthermore evaluated only interactions of ANCA with the S1 site. Thus more subtle allosteric effects were not recognized and could be the reason for the lack of inhibitory ANCA in the remission samples. As already explained, in the new activity assay the concentration of total IgGs was not kept at a fixed PR3-IgG ratio. In contrast to Daouk et al. and van der Geld et al., who used the IgG at a fixed concentration, the concentration of total IgG here was close to the IgG concentrations of the respective samples and reflected the fluctuations of IgG in the patients. Hence, the detection of inhibitory ANCA was more sensitive and inhibitory ANCA could also be detected during remission. Van der Geld et al. also noticed inhibitory ANCA during remission. They observed that these inhibitory ANCA did not rise at the same extend as non-inhibitory ANCA during active disease phases. Similarly, in the present study an increase in the inhibitory potential of ANCA could be observed during stable remission phases (Figure 3.26 B and D). In patients, who did not display a flare during the time of assessment, 62.5% of patients displayed such an increasing inhibitory potential of ANCA over time. In relapsing patients this effect could be detected in 58% of patients. As this increase in inhibitory potential could be seen in both patient groups no statement can be made about the occurrence of a following relapse.

In summary no correlation between inhibitory ANCA and active disease could be observed in the present study. Inhibitory ANCA occurred also during remission phases and thus cannot be seen as harbingers of relapses. A review of previous patient studies furthermore showed, that total ANCA titers during remission, can only restrictedly be used for the prediction of relapses (Tomasson et al., 2012). In line with these findings no characteristic fluctuations of functional ANCA types with predictive value could be observed in this study. Thus it is most likely that no close relationship between activity modulating ANCA and overall disease process exists.

4.4.2 Interference of activity modulating ANCA with α 1PI inhibition of PR3

It is well known that in patients with GPA different subsets of PR3-specific ANCA occur, which recognize different epitopes (Sommarin et al., 1995). In this thesis the focus lay on ANCA, which were able to modify the catalytic activity of PR3. Inhibitory ANCA as well as activity enhancing ANCA were found to bind predominantly to the active site surface of the PR3 molecule (Figure 3.27 and 3.28). Due to the location of their binding site, activity modulating ANCA interfere with PR3 activity and may thus influence disease development in several different ways. Interaction of ANCA with PR3 could for example directly hinder access to substrates. However, it could already be shown for one patient sample, that inhibition of PR3 rather takes place by an allosteric, non-competitive interaction (Daouk et al., 1995). Blocking of the active site cleft of PR3 with elafin did also not influence the ability of ANCA to bind to PR3 (Figure 3.29), confirming an interference of activity modulating ANCA with PR3 by an allosteric mechanism.

Binding of activity modulating ANCA could further impair the inhibition of PR3 by α 1PI. Indirect alterations of the active site cleft by ANCA can hinder interaction with α 1PI and thus antigen clearance or removal of PR3 from the neutrophil surface. As a consequence neutrophil activation via membrane-bound PR3 and via ANCA binding to PR3 and Fc γ Rs would be increased, leading to excessive inflammations and development or worsening of GPA. Several studies already reported an interference of ANCA with PR3- α 1PI interaction (Daouk et al., 1995; Dolman et al., 1993; van der Geld et al., 2002; van de Wiel et al., 1992). In the experiments conducted by Dolman et al. patient sera were diluted 1:40 and small amounts of PR3 were added to measure the inference of ANCA with PR3- α 1PI complexation. In a RIA the extent of complex formation in presence of ANCA was evaluated after 30 minutes (Dolman et al., 1993). In this assay the PR3- α 1PI complexes were captured with the mAb CLB-12.8. Characterization of the mAbs in this thesis, however, revealed that CLB-12.8 has only poor affinity for covalent α 1PI-PR3 complexes (Figure 3.9, see also Kuhl et al., 2010). Thus it is likely that with this method only the minor fraction of reversible, non-covalent complexes (Duranton and Bieth, 2003) was precipitated. Therefore the extend of complex formation in ANCA sera after addition of external PR3 remains unclear. In a similar study by Gross et al. a lack of interference of PR3-ANCA with α 1PI complexation was

reported. The results of this study, however, were only mentioned in a review of the literature (Gross et al., 1993).

In general it has to be considered that the *in vitro* experiments to assess the interference of ANCA with PR3- α 1PI complexation were conducted with specifically designed ratios and concentrations of inhibitor, antibodies and PR3. In presence of these low concentrations of inhibitor the inhibitory ANCA may be able to change the kinetics of the PR3 interaction. The concentration of α 1PI in plasma and in epithelial lining fluid, however, is very high and inactivates PR3 within milliseconds (Duranton and Bieth, 2003), making a significant interference of ANCA with α 1PI-inhibition unlikely. Such low concentrations of α 1PI, which would favor the interference of inhibitory ANCA with PR3- α 1PI complexation, are rarely seen in patients with GPA. Most GPA-patients have normal levels of α 1PI. An exception are carriers of the Z-allele. Individuals, who are homozygous for the Z-allele, are known to have a slightly higher risk for GPA. With regard to the overall GPA-risk, however, homozygosity for the Z-allele only plays a minor role in the Caucasian population. In recent studies it could be shown that deficiency of α 1PI in general induces excessive activation and degranulation of neutrophils via TNF α . This excessive degranulation additionally was detected to favor the development of autoantibodies against granule proteins like for example lactoferrin (Bergin et al., 2014). It is already known that α 1PI deficiency worsens the clinical presentation and outcome of GPA patients (Segelmark et al., 1995). Biosynthesis of the mutated Z-variant by liver cells and primary airway epithelial cells lead to aggregation of α 1PI. This aggregation can trigger stress responses via pro-inflammatory signaling and may lower the threshold for the adaptive immune response. However PR3- or MPO-positive ANCA are only rarely found in homozygous healthy carriers of the Z-allele, indicating that other factors, not the clearance of PR3 by α 1PI, are important for PR3-directed immune response (Audrain et al., 2001). Thus Audrain et al. postulated that α 1PI deficiency rather acts as an amplifying factor in GPA.

4.4.3 Activity modulating ANCA inhibit PR3 by different allosteric mechanisms

For the better understanding of the pathogenic potential of ANCA, the specific molecular interactions between ANCA and PR3 need to be understood. A potential interference of antibodies with PR3 activity could be shown with the mAb MCPR3-7. In addition to the preferential binding of this mAb to the proform of PR3 it is able to induce a conformational

transition of mature PR3. This conformational alteration of PR3 affected furthermore the interaction with α 1PI. Due to these unique properties of MCPR3-7, I decided to search for ANCA subtypes, which displayed MCPR3-7 like properties, to characterize the interaction of ANCA and PR3 further. Therefore the excess of epitope sharing between ANCA and MCPR3-7 was analyzed. In some patients an overlap with the MCPR3-7 epitope occurred in parallel with strong inhibitory capacity (Figure 3.30 B and D). In other patients, however, the inhibitory ANCA showed strong binding to the remaining epitopes in the MCPR3-7 capture ELISA (Figure 3.30 A and C). Furthermore comparison of the proportion of activity modulating ANCA in general in relation to the MCPR3-7 epitope did not reveal any differences (Figure 3.31). These results argue for at least two different mechanisms of interference with PR3 activity. MCPR3-7 is further known to have a higher affinity to proPR3. ProPR3 was able to neutralize the inhibitory effect of MCPR3-7 towards PR3 (Figure 3.32 A). Hence, the inhibitory capacity of ANCA with MCPR3-7 like properties should also be influenced by proPR3. ProPR3 could only partly reverse the inhibitory effect of ANCA, which showed a high affinity for the proform. Only in two from the three analyzed samples the inhibitory fraction was neutralized by proPR3 (Figure 3.32 B). These findings indicate that only a small proportion of ANCA inhibit PR3 by a similar mechanism as MCPR3-7. The vast majority of ANCA, however, probably regulate the activity of PR3 by an allosteric alteration of its mature conformation.

4.5 Conclusions

The aim of this thesis was to explore whether antibodies against hPR3 play a pathogenic role in the development of GPA and by which mechanisms these antibodies could contribute to the disease progression. Based on the literature, antibodies, which are able to inhibit the proteolytic activity of PR3, were thought to influence the development of relapses. Analysis of a large GPA patient cohort, however, revealed that activity modulating antibodies, despite their high occurrence rate among the patients, do not correlate with active disease and do not influence the disease progression. Due to shared interaction sites of activity modulating antibodies and α 1PI on the PR3 molecule, it is likely that these antibodies impair the inhibition by α 1PI and thus also the clearance of PR3. As these antibodies were not found to correlate with active disease in this study, the interference with α 1PI inhibition, however, can only be seen as amplifying factor and not as a causative trigger of relapses. Due to the missing

evidence of the higher pathogenicity of inhibitory antibodies PR3-specific antibodies with different IgG subclasses were used for the generation of a GPA mouse model. The PR3-specific antibodies were indeed able to induce an inflammatory response in the mice, proofing their pathogenic potential. After recruitment of immune cells, activation and degranulation of neutrophils led to a local type of lung vasculitis and pulmonary lesions. The development of a GPA-like phenotype in this model, however, seemed to be dependent on the IgG subclass, as IgG2a antibodies were able to elicit a stronger inflammatory response than IgG2b antibodies. In future further optimization of this model and injection of different types of antibodies opens the possibility to investigate the pathogenicity of different hPR3-specific antibody subsets, with regard to their subclass identity, in ANCA associated vasculitis in more detail.

5. Bibliography

- Adkison, A.M., Raptis, S.Z., Kelley, D.G., and Pham, C.T.N. (2002). Dipeptidyl peptidase I activates neutrophil-derived serine proteases and regulates the development of acute experimental arthritis. *J. Clin. Invest.* 109, 363–371.
- Almouhawis, H.A., Leao, J.C., Fedele, S., and Porter, S.R. (2013). Wegener's granulomatosis: a review of clinical features and an update in diagnosis and treatment. *J. Oral. Pathol. Med.* 42, 507–516.
- Audrain, M.A., Sesboüé, R., Baranger, T.A., Elliott, J., Testa, A., Martin, J.P., Lockwood, C.M., and Esnault, V.L. (2001). Analysis of anti-neutrophil cytoplasmic antibodies (ANCA): frequency and specificity in a sample of 191 homozygous (PiZZ) alpha1-antitrypsin-deficient subjects. *Nephrol. Dial. Transplant.* 16, 39–44.
- Baggiolini, M., Bretz, U., Dewald, B., and Feigenson, M.E. (1978). The polymorphonuclear leukocyte. *Agents and Actions.* 8, 3–10.
- Bergin, D.A., Reeves, E.P., Hurley, K., Wolfe, R., Jameel, R., Fitzgerald, S., and McElvaney, N.G. (2014). The circulating proteinase inhibitor α -1 antitrypsin regulates neutrophil degranulation and autoimmunity. *Sci. Transl. Med.* 6, 217ra1.
- Blow, D.M., Birktoft, J.J., and Hartley, B.S. (1969). Role of a buried acid group in the mechanism of action of chymotrypsin. *Nature.* 221, 337–340.
- Bories, D., Raynal, M.C., Solomon, D.H., Darzynkiewicz, Z., and Cayre, Y.E. (1989). Down-regulation of a serine protease, myeloblastin, causes growth arrest and differentiation of promyelocytic leukemia cells. *Cell.* 59, 959–968.
- Brinkmann, V., Reichard, U., Goosmann, C., Fauler, B., Uhlemann, Y., Weiss, D.S., Weinrauch, Y., and Zychlinsky, A. (2004). Neutrophil extracellular traps kill bacteria. *Science.* 303, 1532–1535.
- Brooks, C.J., King, W.J., Radford, D.J., Adu, D., McGrath, M., and Savage, C.O. (1996). IL-1 beta production by human polymorphonuclear leucocytes stimulated by anti-neutrophil cytoplasmic autoantibodies: relevance to systemic vasculitis. *Clin. Exp. Immunol.* 106, 273–279.
- Bruhns, P. (2012). Properties of mouse and human IgG receptors and their contribution to disease models. *Blood.* 119, 5640–5649.

- Campanelli, D., Melchior, M., Fu, Y., Nakata, M., Shuman, H., Nathan, C., and Gabay, J.E. (1990). Cloning of cDNA for proteinase 3: a serine protease, antibiotic, and autoantigen from human neutrophils. *J. Exp. Med.* 172, 1709–1715.
- Caughey, G.H., Schaumberg, T.H., Zerweck, E.H., Butterfield, J.H., Hanson, R.D., Silverman, G.A., and Ley, T.J. (1993). The human mast cell chymase gene (CMA1): mapping to the cathepsin G/granzyme gene cluster and lineage-restricted expression. *Genomics*. 15, 614–620.
- Chang, L., and Savige, J. (1993). Studies to demonstrate inhibition of functional activity of neutrophil lysosomal enzymes with ANCA. *Adv. Exp. Med. Biol.* 336, 97–100.
- Charles, L.A., Caldas, M.L., Falk, R.J., Terrell, R.S., and Jennette, J.C. (1991). Antibodies against granule proteins activate neutrophils in vitro. *J. Leukoc. Biol.* 50, 539–546.
- Cobos-Correa, A., Trojanek, J.B., Diemer, S., Mall, M.A., and Schultz, C. (2009). Membrane-bound FRET probe visualizes MMP12 activity in pulmonary inflammation. *Nat. Chem. Biol.* 5, 628–630.
- Coeshott, C., Ohnemus, C., Pilyavskaya, A., Ross, S., Wieczorek, M., Kroona, H., Leimer, A.H., and Cheronis, J. (1999). Converting enzyme-independent release of tumor necrosis factor alpha and IL-1beta from a stimulated human monocytic cell line in the presence of activated neutrophils or purified proteinase 3. *Proc. Natl. Acad. Sci. U. S. A.* 96, 6261–6266.
- Csernok, E., Ernst, M., Schmitt, W., Bainton, D.F., and Gross, W.L. (1994). Activated neutrophils express proteinase 3 on their plasma membrane in vitro and in vivo. *Clin. Exp. Immunol.* 95, 244–250.
- Daouk, G.H., Palsson, R., and Arnaout, M.A. (1995). Inhibition of proteinase 3 by ANCA and its correlation with disease activity in Wegener's granulomatosis. *Kidney Int.* 47, 1528–1536.
- Davies, D.J., Moran, J.E., Niall, J.F., and Ryan, G.B. (1982). Segmental necrotising glomerulonephritis with antineutrophil antibody: possible arbovirus aetiology? *Br. Med. J.* 285, 606.
- Delèvaux, I., Khellaf, M., André, M., Michel, J., Piette, J.C., and Aumaître, O. (2005). Spontaneous pneumothorax in Wegener granulomatosis. *Chest*. 128, 3074–3075.
- Dementiev, A., Dobó, J., and Gettins, P.G.W. (2006). Active site distortion is sufficient for proteinase inhibition by serpins: structure of the covalent complex of alpha1-proteinase inhibitor with porcine pancreatic elastase. *J. Biol. Chem.* 281, 3452–3457.
- Dijstelbloem, H.M., Scheepers, R.H., Oost, W.W., Stegeman, C.A., van der Pol, W.L., Sluiter, W.J., Kallenberg, C.G., van de Winkel, J.G., and Tervaert, J.W. (1999). Fcgamma receptor polymorphisms in Wegener's granulomatosis: risk factors for disease relapse. *Arthritis & Rheum.* 42, 1823–1827.
- Dijstelbloem, H.M., Bijl, M., Fijnheer, R., Scheepers, R.H., Oost, W.W., Jansen, M.D., Sluiter, W.J., Limburg, P.C., Derksen, R.H., van de Winkel, J.G., et al. (2000). Fcgamma

receptor polymorphisms in systemic lupus erythematosus: association with disease and in vivo clearance of immune complexes. *Arthritis & Rheum.* *43*, 2793–2800.

Dolman, K.M., Stegeman, C.A., van de Wiel, B.A., Hack, C.E., von dem Borne, A.E.G.K., Kallenberg, C.G.M., and Goldschmeding, R. (1993). Relevance of classic anti-neutrophil cytoplasmic autoantibody (C-ANCA)-mediated inhibition of proteinase 3- α 1-antitrypsin complexation to disease activity in Wegener's granulomatosis. *Clin. Exp. Immunol.* *93*, 405–410.

Duranton, J., and Bieth, J.G. (2003). Inhibition of proteinase 3 by [alpha]1-antitrypsin in vitro predicts very fast inhibition in vivo. *Am. J. Respir. Cell. Mol. Biol.* *29*, 57–61.

Durocher, Y., Perret, S., and Kamen, A. (2002). High-level and high-throughput recombinant protein production by transient transfection of suspension-growing human 293-EBNA1 cells. *Nucleic. Acids. Res.* *30*, E9.

Esnault, V.L., Testa, A., Audrain, M., Rogé, C., Hamidou, M., Barrier, J.H., Sesboüé, R., Martin, J.P., and Lesavre, P. (1993). Alpha 1-antitrypsin genetic polymorphism in ANCA-positive systemic vasculitis. *Kidney Int.* *43*, 1329–1332.

Ewert, B.H., Jennette, J.C., and Falk, R.J. (1992). Anti-myeloperoxidase antibodies stimulate neutrophils to damage human endothelial cells. *Kidney Int.* *41*, 375–383.

Falk, R.J., and Jennette, J.C. (1988). Anti-neutrophil cytoplasmic autoantibodies with specificity for myeloperoxidase in patients with systemic vasculitis and idiopathic necrotizing and crescentic glomerulonephritis. *N. Engl. J. Med.* *318*, 1651–1657.

Falk, R.J., Terrell, R.S., Charles, L.A., and Jennette, J.C. (1990). Anti-neutrophil cytoplasmic autoantibodies induce neutrophils to degranulate and produce oxygen radicals in vitro. *Proc. Natl. Acad. Sci. U. S. A.* *87*, 4115–4119.

Fehlhammer, H., Bode, W., and Huber, R. (1977). Crystal structure of bovine trypsinogen at 1.8 Å resolution. II. Crystallographic refinement, refined crystal structure and comparison with bovine trypsin. *J. Mol. Biol.* *111*, 415–438.

Ferrara, C., Grau, S., Jäger, C., Sondermann, P., Brünker, P., Waldhauer, I., Hennig, M., Ruf, A., Rufer, A.C., Stihle, M., et al. (2011). Unique carbohydrate-carbohydrate interactions are required for high affinity binding between Fc γ RIII and antibodies lacking core fucose. *Proc. Natl. Acad. Sci. U. S. A.* *108*, 12669–12674.

Finkelstein, J.D., Merkel, P.A., Schroeder, D., Hoffman, G.S., Spiera, R., St Clair, E.W., Davis, J.C., McCune, W.J., Lears, A.K., Ytterberg, S.R., et al. (2007). Antiproteinase 3 antineutrophil cytoplasmic antibodies and disease activity in Wegener granulomatosis. *Ann. Intern. Med.* *147*, 611–619.

Freer, T., Kraut, J., Robertur, J.D., Wright, H.T., and Xuong, N.H. (1970). Chymotrypsinogen: 2,5-A Crystal Structure, Comparison with α -Chymotrypsin, and Implications for Zymogen Activation. *Biochemistry.* *9*, 1997–2009.

- Fujinaga, M., Chernaia, M.M., Halenbeck, R., Koths, K., and James, M.N. (1996). The crystal structure of PR3, a neutrophil serine proteinase antigen of Wegener's granulomatosis antibodies. *J. Mol. Biol.* *261*, 267–278.
- Ganesan, R., Eigenbrot, C., and Kirchhofer, D. (2010). Structural and mechanistic insight into how antibodies inhibit serine proteases. *Biochem. J.* *430*, 179–189.
- Gehrig, S., Mall, M.A., and Schultz, C. (2012). Spatially resolved monitoring of neutrophil elastase activity with ratiometric fluorescent reporters. *Angew. Chem. Int. Ed. Engl.* *51*, 6258–6261.
- Van der Geld, Y.M., Tool, a. T.J., Videler, J., Haas, M. De, Tervaert, J.W.C., Stegeman, C. a., Limburg, P.C., Kallenberg, C.G.M., and Roos, D. (2002). Interference of PR3-ANCA with the enzymatic activity of PR3: differences in patients during active disease or remission of Wegener's granulomatosis. *Clin. Exp. Immunol.* *129*, 562–570.
- Van der Geld, Y.M., Hellmark, T., Selga, D., Heeringa, P., Huitema, M.G., Limburg, P.C., and Kallenberg, C.G.M. (2007). Rats and mice immunised with chimeric human/mouse proteinase 3 produce autoantibodies to mouse Pr3 and rat granulocytes. *Ann. Rheum. Dis.* *66*, 1679–1682.
- Gillis, C., Gouel-Chéron, A., Jönsson, F., and Bruhns, P. (2014). Contribution of Human FcγRs to Disease with Evidence from Human Polymorphisms and Transgenic Animal Studies. *Front. Immunol.* *5*, 254.
- Goldmann, W.H., Niles, J.L., and Arnaout, M.A. (1999). Interaction of purified human proteinase 3 (PR3) with reconstituted lipid bilayers. *Eur. J. Biochem.* *261*, 155–162.
- Gooptu, B., and Lomas, D.A. (2009). Conformational pathology of the serpins: themes, variations, and therapeutic strategies. *Annu. Rev. Biochem.* *78*, 147–176.
- Griffith, M.E., Lovegrove, J.U., Gaskin, G., Whitehouse, D.B., and Pusey, C.D. (1996). C-antineutrophil cytoplasmic antibody positivity in vasculitis patients is associated with the Z allele of alpha-1-antitrypsin, and P-antineutrophil cytoplasmic antibody positivity with the S allele. *Nephrol. Dial. Transplant.* *11*, 438–443.
- Grimminger, F., Hattar, K., Papavassilis, C., Temmesfeld, B., Csernok, E., Gross, W.L., Seeger, W., and Sibelius, U. (1996). Neutrophil activation by anti-proteinase 3 antibodies in Wegener's granulomatosis: role of exogenous arachidonic acid and leukotriene B4 generation. *J. Exp. Med.* *184*, 1567–1572.
- Gross, W.L., Csernok, E., and Flesch, B.K. (1993). "Classic" anti-neutrophil cytoplasmic autoantibodies (cANCA), "Wegener's autoantigen" and their immunopathogenic role in Wegener's granulomatosis. *J. Autoimmun.* *6*, 171–184.
- Halbwachs-Mecarelli, L., Bessou, G., Lesavre, P., Lopez, S., and Witko-Sarsat, V. (1995). Bimodal distribution of proteinase 3 (PR3) surface expression reflects a constitutive heterogeneity in the polymorphonuclear neutrophil pool. *FEBS Lett.* *374*, 29–33.

- Hattar, K., Oppermann, S., Ankele, C., Weissmann, N., Schermuly, R.T., Bohle, R.M., Moritz, R., Krögel, B., Seeger, W., Grimminger, F., et al. (2010). c-ANCA-induced neutrophil-mediated lung injury: a model of acute Wegener's granulomatosis. *Eur. Respir. J.* *36*, 187–195.
- Hewins, P., Tervaert, J.W., Savage, C.O., and Kallenberg, C.G. (2000). Is Wegener's granulomatosis an autoimmune disease? *Curr. Opin. Rheumatol.* *12*, 3–10.
- Hoffman, G.S., and Specks, U. (1998). Antineutrophil cytoplasmic antibodies. *Arthritis & Rheum.* *41*, 1521–1537.
- Holland, M., Takada, K., Okumoto, T., Takahashi, N., Kato, K., Adu, D., Ben-Smith, a, Harper, L., Savage, C.O.S., and Jefferis, R. (2002). Hypogalactosylation of serum IgG in patients with ANCA-associated systemic vasculitis. *Clin. Exp. Immunol.* *129*, 183–190.
- Huntington, J.A., Read, R.J., and Carrell, R.W. (2000). Structure of a serpin-protease complex shows inhibition by deformation. *Nature.* *407*, 923–926.
- Jenne, D.E. (1994). Structure of the Azurocidin, Proteinase 3, and Neutrophil Elastase Genes. *Am. J. Respir. Crit. Care. Med.* *150*, S147–S154.
- Jenne, D.E., Tschopp, J., Lüdemann, J., Utecht, B., and Gross, W.L. (1990). Wegener's autoantigen decoded. *Nature.* *346*, 520.
- Jenne, D.E., Fröhlich, L., Hummel, A.M., and Specks, U. (1997). Cloning and functional expression of the murine homologue of proteinase 3: implications for the design of murine models of vasculitis. *FEBS Lett.* *408*, 187–190.
- Kallenberg, C.G.M. (2011). Pathogenesis of ANCA-associated vasculitis, an update. *Clin. Rev. Allergy Immunol.* *41*, 224–231.
- Kallenberg, C.G.M., Heeringa, P., and Stegeman, C.A. (2006). Mechanisms of Disease: pathogenesis and treatment of ANCA-associated vasculitides. *Nat. Clin. Pr. Rheumatol.* *2*, 661–670.
- Kao, R.C., Wehner, N.G., Skubitz, K.M., Gray, B.H., and Hoidal, J.R. (1988). Proteinase 3. A distinct human polymorphonuclear leukocyte proteinase that produces emphysema in hamsters. *J. Clin. Invest.* *82*, 1963–1973.
- Kessenbrock, K., Fröhlich, L., Sixt, M., Lämmermann, T., Pfister, H., Bateman, A., Belaouaj, A., Ring, J., Ollert, M., Fässler, R., et al. (2008). Proteinase 3 and neutrophil elastase enhance inflammation in mice by inactivating antiinflammatory progranulin. *J. Clin. Invest.* *118*, 2438–2447.
- Kettritz, R., Jennette, J.C., and Falk, R.J. (1997). Crosslinking of ANCA-antigens stimulates superoxide release by human neutrophils. *J. Am. Soc. Nephrol.* *8*, 386–394.
- Kobayashi, S.D., Voyich, J.M., Burlak, C., and DeLeo, F.R. (2005). Neutrophils in the innate immune response. *Arch. Immunol. Ther. Exp.* *53*, 505–517.

- Kocher, M., Edberg, J.C., Fleit, H.B., and Kimberly, R.P. (1998). Antineutrophil cytoplasmic antibodies preferentially engage Fc gammaRIIIb on human neutrophils. *J. Immunol.* *161*, 6909–6914.
- Korkmaz, B., Kuhl, A., Bayat, B., Santoso, S., and Jenne, D.E. (2008). A hydrophobic patch on proteinase 3, the target of autoantibodies in Wegener granulomatosis, mediates membrane binding via NB1 receptors. *J. Biol. Chem.* *283*, 35976–35982.
- Korkmaz, B., Horwitz, M.S., Jenne, D.E., and Gauthier, F. (2010). Neutrophil elastase, proteinase 3, and cathepsin G as therapeutic targets in human diseases. *Pharmacol. Rev.* *62*, 726–759.
- Krapp, S., Mimura, Y., Jefferis, R., Huber, R., and Sondermann, P. (2003). Structural analysis of human IgG-Fc glycoforms reveals a correlation between glycosylation and structural integrity. *J. Mol. Biol.* *325*, 979–989.
- Kuhl, A., Korkmaz, B., Utecht, B., Kniepert, A., Schönermarck, U., Specks, U., and Jenne, D.E. (2010). Mapping of conformational epitopes on human proteinase 3, the autoantigen of Wegener's granulomatosis. *J. Immunol.* *185*, 387–399.
- Kummer, J.A., Kamp, A.M., Citarella, F., Horrevoets, A.J., and Hack, C.E. (1996). Expression of human recombinant granzyme A zymogen and its activation by the cysteine proteinase cathepsin C. *J. Biol. Chem.* *271*, 9281–9286.
- Langford, C.A., and Hoffman, G.S. (1999). Wegener's granulomatosis. *Thorax.* *54*, 629–637.
- Ley, K., Laudanna, C., Cybulsky, M.I., and Nourshargh, S. (2007). Getting to the site of inflammation: the leukocyte adhesion cascade updated. *Nat. Rev. Immunol.* *7*, 678–689.
- Li, B., Cohen, A., Hudson, T.E., Motlagh, D., Amrani, D.L., and Duffield, J.S. (2010). Mobilized human hematopoietic stem/progenitor cells promote kidney repair after ischemia/reperfusion injury. *Circulation.* *121*, 2211–2220.
- Little, M.A., Al-Ani, B., Ren, S., Al-Nuaimi, H., Leite, M., Alpers, C.E., Savage, C.O., and Duffield, J.S. (2012). Anti-proteinase 3 anti-neutrophil cytoplasm autoantibodies recapitulate systemic vasculitis in mice with a humanized immune system. *PloS One.* *7*, e28626.
- Luisetti, M., and Seersholm, N. (2004). Alpha1-antitrypsin deficiency. 1: epidemiology of alpha1-antitrypsin deficiency. *Thorax.* *59*, 164–169.
- Luqmani, R.A., Bacon, P.A., Moots, R.J., Janssen, B.A., Pall, A., Emery, P., Savage, C., and Adu, D. (1994). Birmingham Vasculitis Activity Score (BVAS) in systemic necrotizing vasculitis. *Q. J. Med.* *87*, 671–678.
- Lyons, P.A., Rayner, T.F., Trivedi, S., Holle, J.U., Watts, R.A., Jayne, D.R.W., Baslund, B., Brenchley, P., Bruchfeld, A., Chaudhry, A.N., et al. (2012). Genetically distinct subsets within ANCA-associated vasculitis. *N. Engl. J. Med.* *367*, 214–223.

- Mahr, A.D. (2009). Epidemiological features of Wegener's granulomatosis and microscopic polyangiitis: two diseases or one "anti-neutrophil cytoplasm antibodies-associated vasculitis" entity? *APMIS. Suppl. 117*, 41–47.
- Mason, D.Y., Cramer, E.M., Massé, J.M., Crystal, R., Bassot, J.M., and Breton-Gorius, J. (1991). Alpha 1-antitrypsin is present within the primary granules of human polymorphonuclear leukocytes. *Am. J. Pathol. 139*, 623–628.
- McKenzie, S.E., and Schreiber, A.D. (1998). Fc gamma receptors in phagocytes. *Curr. Opin. Hematol. 5*, 16–21.
- Mulder, A.H.L., Stegeman, C.A., and Kallenberg, C.G.M. (1995). Activation of granulocytes by anti-neutrophil cytoplasmic antibodies (ANCA) in Wegener's granulomatosis: a predominant role for the IgG3 subclass of ANCA. *Clin. Exp. Immunol. 101*, 227–232.
- Nimmerjahn, F., and Ravetch, J. V. (2005). Divergent immunoglobulin g subclass activity through selective Fc receptor binding. *Science. 310*, 1510–1512.
- Nimmerjahn, F., and Ravetch, J. V. (2012). Translating basic mechanisms of IgG effector activity into next generation cancer therapies. *Cancer. Immun. 12*, 13.
- Olivencia-Simmons, I. (2007). Wegener's granulomatosis: symptoms, diagnosis, and treatment. *J. Am. Acad. Nurse. Pr. 19*, 315–320.
- Padrines, M., Wolf, M., Walz, A., and Baggiolini, M. (1994). Interleukin-8 processing by neutrophil elastase, cathepsin G and proteinase-3. *FEBS Lett. 352*, 231–235.
- Pankhurst, T., Nash, G., Williams, J., Colman, R., Hussain, A., and Savage, C. (2011). Immunoglobulin subclass determines ability of immunoglobulin (Ig)G to capture and activate neutrophils presented as normal human IgG or disease-associated anti-neutrophil cytoplasm antibody (ANCA)-IgG. *Clin. Exp. Immunol. 164*, 218–226.
- Perera, N.C., Schilling, O., Kittel, H., Back, W., Kremmer, E., and Jenne, D.E. (2012). NSP4, an elastase-related protease in human neutrophils with arginine specificity. *Proc. Natl. Acad. Sci. U. S. A. 109*, 6229–6234.
- Perera, N.C., Wiesmüller, K.H., Larsen, M.T., Schacher, B., Eickholz, P., Borregaard, N., and Jenne, D.E. (2013). NSP4 is stored in azurophil granules and released by activated neutrophils as active endoprotease with restricted specificity. *J. Immunol. 191*, 2700–2707.
- Pfister, H., Ollert, M., Fröhlich, L.F., Quintanilla-Martinez, L., Colby, T. V., Specks, U., and Jenne, D.E. (2004). Antineutrophil cytoplasmic autoantibodies against the murine homolog of proteinase 3 (Wegener autoantigen) are pathogenic in vivo. *Blood. 104*, 1411–1418.
- Pham, C.T., Armstrong, R.J., Zimonjic, D.B., Popescu, N.C., Payan, D.G., and Ley, T.J. (1997). Molecular cloning, chromosomal localization, and expression of murine dipeptidyl peptidase I. *J. Biol. Chem. 272*, 10695–10703.

- Pham, C.T.N., Ivanovich, J.L., Raptis, S.Z., Zehnbauser, B., and Ley, T.J. (2004). Papillon-Lefèvre syndrome: correlating the molecular, cellular, and clinical consequences of cathepsin C/dipeptidyl peptidase I deficiency in humans. *J. Immunol.* *173*, 7277–7281.
- Porges, A.J., Redecha, P.B., Kimberly, W.T., Csernok, E., Gross, W.L., and Kimberly, R.P. (1994). Anti-neutrophil cytoplasmic antibodies engage and activate human neutrophils via Fc gamma RIIa. *J. Immunol.* *153*, 1271–1280.
- Pozzi, N., Vogt, A.D., Gohara, D.W., and Di Cera, E. (2012). Conformational selection in trypsin-like proteases. *Curr. Opin. Struct. Biol.* *22*, 421–431.
- Rao, N. V., Wehnere, N.G., Marshall, B.C., Grayt, W.R., Gray, B.H., and Hoidal, J.R. (1991). Characterization of Proteinase-3 (PR-3), a Neutrophil Serine Proteinase. *J. Biol. Chem.* *266*, 9540–9548.
- Reeves, E.P., Lu, H., Jacobs, H.L., Messina, C.G.M., Bolsover, S., Gabella, G., Potma, E.O., Warley, A., Roes, J., and Segal, A.W. (2002). Killing activity of neutrophils is mediated through activation of proteases by K⁺ flux. *Nature.* *416*, 291–297.
- Reinhold-Keller, E., Herlyn, K., Wagner-Bastmeyer, R., and Gross, W.L. (2005). Stable incidence of primary systemic vasculitides over five years: results from the German vasculitis register. *Arthritis & Rheum.* *53*, 93–99.
- Relle, M., Cash, H., Schommers, N., Reifenberg, K., Galle, P.R., and Schwarting, A. (2013). PR3 antibodies do not induce renal pathology in a novel PR3-humanized mouse model for Wegener's granulomatosis. *Rheumatol. Int.* *33*, 613–622.
- Reumaux, D., Vossebeld, P.J., Roos, D., and Verhoeven, A.J. (1995). Effect of tumor necrosis factor-induced integrin activation on Fc gamma receptor II-mediated signal transduction: relevance for activation of neutrophils by anti-proteinase 3 or anti-myeloperoxidase antibodies. *Blood.* *86*, 3189–3195.
- Robache-Gallea, S., Morand, V., Bruneau, J.M., Schoot, B., Tagat, E., Réalo, E., Chouaib, S., and Roman-Roman, S. (1995). In vitro processing of human tumor necrosis factor-alpha. *J. Biol. Chem.* *270*, 23688–23692.
- Rooney, C.P., Taggart, C., Coakley, R., McElvaney, N.G., and Neill, S.J.O. (2001). Anti – Proteinase 3 Antibody Activation of Neutrophils Can Be Inhibited by α 1-Antitrypsin. *Am. J. Respir. Cell Mol. Biol.* *24*, 747 – 754.
- Roux, K.H., Strelets, L., and Michaelsen, T.E. (1997). Flexibility of human IgG subclasses. *J. Immunol.* *159*, 3372–3382.
- Savige, J.A., Chang, L., Cook, L., Burdon, J., Daskalakis, M., and Doery, J. (1995). Alpha 1-antitrypsin deficiency and anti-proteinase 3 antibodies in anti-neutrophil cytoplasmic antibody (ANCA)-associated systemic vasculitis. *Clin. Exp. Immunol.* *100*, 194–197.
- Schechter, I., and Berger, A. (1967). On the size of the active site in proteases. I. Papain. *Biochem. Biophys. Res. Commun.* *27*, 157–162.

- Scully, C., Langdon, J., and Evans, J. (2012). Marathon of eponyms: 23 Wegener granulomatosis. *Oral. Dis.* 18, 214–216.
- Segelmark, M., Elzouki, A.N., Wieslander, J., and Eriksson, S. (1995). The PiZ gene of α_1 -antitrypsin as a determinant of outcome in PR3-ANCA-positive vasculitis. *Kidney Int.* 48, 844–850.
- Seidel, S.A.I., Dijkman, P.M., Lea, W.A., van den Bogaart, G., Jerabek-Willemsen, M., Lazic, A., Joseph, J.S., Srinivasan, P., Baaske, P., Simeonov, A., et al. (2013). Microscale thermophoresis quantifies biomolecular interactions under previously challenging conditions. *Methods.* 59, 301–315.
- Silva, F., Hummel, A.M., Jenne, D.E., and Specks, U. (2010). Discrimination and variable impact of ANCA binding to different surface epitopes on proteinase 3, the Wegener's autoantigen. *J. Autoimmun.* 35, 299–308.
- Sommarin, Y., Rasmussen, N., and Wieslander, J. (1995). Characterization of monoclonal antibodies to proteinase-3 and application in the study of epitopes for classical anti-neutrophil cytoplasm antibodies. *Exp. Nephrol.* 3, 249–256.
- Stegeman, C.A., Tervaert, J.W., Sluiter, W.J., Manson, W.L., de Jong, P.E., and Kallenberg, C.G. (1994). Association of chronic nasal carriage of *Staphylococcus aureus* and higher relapse rates in Wegener granulomatosis. *Ann. Intern. Med.* 120, 12–17.
- Stone, J.H., and The Wegener's Granulomatosis Etanercept Trial Research Group (2003). Limited versus severe Wegener's granulomatosis: baseline data on patients in the Wegener's granulomatosis etanercept trial. *Arthritis & Rheum.* 48, 2299–2309.
- Sturrock, A., Franklin, K.F., Wu, S., and Hoidal, J.R. (1998). Characterization and localization of the genes for mouse proteinase-3 (Prtn3) and neutrophil elastase (Ela2). *Cytogenet. Cell. Genet.* 83, 104–108.
- The Wegener's Granulomatosis Etanercept Trial (WGET) Research Group (2005). Etanercept plus Standard Therapy for Wegener's Granulomatosis. *N. Engl. J. Med.* 352, 351–361.
- Tomasson, G., Grayson, P.C., Mahr, A.D., Lavalley, M., and Merkel, P. a (2012). Value of ANCA measurements during remission to predict a relapse of ANCA-associated vasculitis--a meta-analysis. *Rheumatol. (Oxford).* 51, 100–109.
- Van de Wiel, B.A., Dolman, K.M., van der Meer-Gerritsen, C.H., Hack, C.E., von dem Borne, A.E., and Goldschmeding, R. (1992). Interference of Wegener's granulomatosis autoantibodies with neutrophil Proteinase 3 activity. *Clin. Exp. Immunol.* 90, 409–414.
- Van der Woude, F.J., Rasmussen, N., Lobatto, S., Wiik, A., Permin, H., van Es, L.A., van der Giessen, M., van der Hem, G.K., and The, T.H. (1985). Autoantibodies against neutrophils and monocytes: tool for diagnosis and marker of disease activity in Wegener's granulomatosis. *Lancet.* 1, 425–429.
- Wung, P.K., and Stone, J.H. (2006). Therapeutics of Wegener's granulomatosis. *Nat. Clin. Pr. Rheumatol.* 2, 192–200.

Wysocka, M., Lesner, A., Guzow, K., Mackiewicz, L., Legowska, A., Wicz, W., and Rolka, K. (2008). Design of selective substrates of proteinase 3 using combinatorial chemistry methods. *Anal. Biochem.* 378, 208–215.

Yurewicz, E.C., and Zimmerman, M. (1977). Cytochalasin B-dependent release of azurophil granule enzymes from human polymorphonuclear leukocytes. *Inflammation*. 2, 259–264.

Zarbock, A., and Ley, K. (2008). Mechanisms and consequences of neutrophil interaction with the endothelium. *Am. J. Pathol.* 172, 1–7.

Zimmer, M., Medcalf, R.L., Fink, T.M., Mattmann, C., Lichter, P., and Jenne, D.E. (1992). Three human elastase-like genes coordinately expressed in the myelomonocyte lineage are organized as a single genetic locus on 19pter. *Proc. Natl. Acad. Sci. U. S. A.* 89, 8215–8219.

6. Abbreviations

α 1PI	Alpha-1-proteinase inhibitor
AAV	ANCA-associated vasculitis
Abu	Aminobutyric acid
ANCA	Anti-neutrophil cytoplasmic antibody
APS	Ammonium persulfate
BCA	Bicinchonic acid
Boc	Tert-butoxycarbonyl
BSA	Bovine serum albumin
CDR	Complementarity determining region
CG	Cathepsin G
CMK	Chloromethyl ketone
CSS	Churg-Strauss Syndrome
DMSO	Dimethyl sulfoxide
dNTP	Deoxyribonucleotide triphosphate
DPPI	Dipeptidyl aminopeptidase I
EDTA	Ethylenediaminetetraacetic acid
Fc γ R	Fc γ receptor
FCS	Fetal calf serum
FITC	Fluorescein isothiocyanate
FRET	Fluorescence/Förster resonance energy transfer
gibPR3	Gibbon PR3
GPA	Granulomatosis with Polyangiitis
GWAS	Genome wide association study
HBSS	Hank's Balanced Salt solution
HEK	Human embryonic kidney cell line
hNE	Human NE
hPMNs	Human PMNs
hPR3	Human PR3
hPR3 ^{+/+}	Human PR3 knock-in
HRP	Horseradish peroxidase
IgG	Immunoglobulin G
IL	Interleukin
IVIG	Intravenous Immunoglobulin
λ Ab	Absorption wavelength

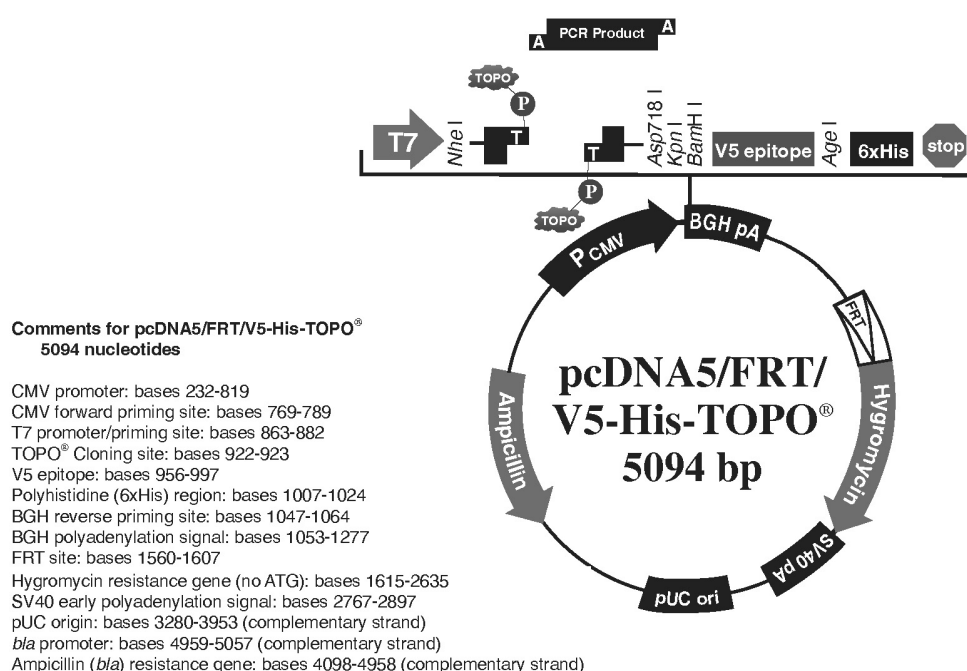
Abbreviations

λ_{Em}	Emission wavelength
λ_{Ex}	Extinction wavelength
LPS	Lipopolysaccharide
mAb	Monoclonal antibody
MMP	Matrix metalloproteinase
mNE	Mouse NE
MPA	Microscopic polyangiitis
mPMNs	Murine PMNs
MPO	Myeloperoxidase
mPR3	Mouse PR3
NE	Neutrophil elastase
NET	Neutrophil extracellular trap
NSP	Neutrophil serine protease
NSP4	Neutrophil serine protease 4
PAGE	Polyacrylamide gel electrophoresis
PBS	Phosphate buffered saline
PCR	Polymerase chain reaction
PEI	Polyethylenimine
PFA	Paraformaldehyde
PMA	Phorbol-12-myristate-13-acetate
PMNs	Polymorphonuclear cells
PR3	Proteinase 3
proPR3	Proform of PR3
PVDF	Polyvinylidene difluoride
RFU	Relative fluorescence unit
ROS	Reactive oxygen species
RPMI	Roswell Park Memorial Institute medium
RT-PCR	Reverse transcription polymerase chain reaction
SBzl	Thiobenzyl ester
SD	Standard deviation
SDS	Sodium dodecyl sulfate
SEM	Standard error of the mean
SigIg κ	Signal peptide derived from Ig κ
TNF α	Tumor necrosis factor α

7. Appendix

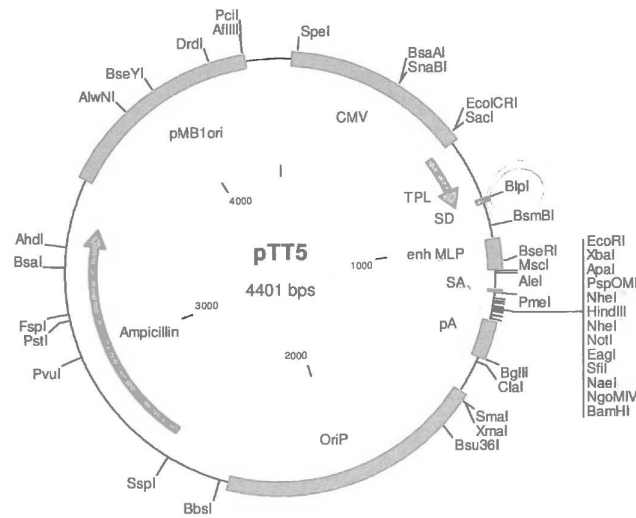
7.1 Vector maps

7.1.1 pcDNA5/FRT/V5-His-TOPO[®]



Vector 7.1: Vector map of the pcDNA5/FRT/V5-His-TOPO vector. The pcDNA5 vector contains a promoter of the cytomegalovirus (CMV), two different polyadenylation signals (BGH and SV40), an *E. coli* origin of replication (pUC ori) and two resistance genes (Ampicillin and Hygromycin) for selection in *E. coli*. All relevant recognition sites of restriction enzymes, the V5 epitope and the 6 × His tag are depicted. The vector was purchased from life technologies.

7.1.2 pTT5



Vector 7.2: Vector map of the pTT5 vector. The important components of the pTT5 vector are an *E. coli* origin of replication (pMB1ori) and an EBV specific origin of replication (OriP), a promoter of the cytomegalovirus (CMV), an adenovirus tripartite leader (TPL), a major late promoter (MLP), a rabbit beta-globin polyadenylation signal (pA) and an ampicillin resistance gene for selection in *E. coli*. All important recognition sites of restriction enzymes are depicted. The vector was procured from the NRC Biotechnology Research Institute.

7.2 Sequences

7.2.1 SigIgk-proPR3-H₆

The amino acid sequence is shown in single letter code. The sequence begins with the SigIgk signal peptide, the N-terminal S-tag is displayed in bold and underlined. The enterokinase cleavage site was underlined. The sequence of the mature PR3 is displayed in bold. The C-terminal 6 × His-tag is marked in italics and the stop codon is represented by a star (*).

1	ATGGAGACAGACACACTCCTGCTATGGGTACTGCTGCTCTGGGTACCAGGTTCCACTGGT	60
1	M E T D T L L L W V L L L W V P G S T G	20
61	GACGTGAAAGAAACCGCTGCTGCTAAATTCTGAACGCCAGCACATGGACAGCGGAAGCGGT	120
21	D V <u>K E T A A A K F E R Q H M D S</u> G S G	40
121	GGACACGTGGATGACGACGACAAAATCGTGGGCGGTACAGAGGCGCAGCCACACTCCCCGG	180
41	G H V <u>D D D D K</u> I V G G H E A Q P H S R	60
181	CCCTACATGGCCTCCCTGCAGATGCGGGGAACCCGGGCAGCCACTTCTGCGGAGGCACC	240
61	P Y M A S L Q M R G N P G S H F C G G T	80
241	TTGATCCACCCCAGCTTCGTGCTGACGGCCGCGCACTGCCTGCGGGACATACCCCAGCGC	300
81	L I H P S F V L T A A H C L R D I P Q R	100
301	CTGGTGAACGTGGTGTCTCGGAGCCCACAACGTGCGGACGCAGGAGCCCACCCAGCAGCAC	360
101	L V N V V L G A H N V R T Q E P T Q Q H	120
361	TTCTCGGTGGCTCAGGTGTTTCTGAACAACCTACGACGCGGAGAACAACCTGAACGACATT	420
121	F S V A Q V F L N N Y D A E N K L N D I	140
421	CTCCTCATCCAGCTGAGCAGCCCAGCCAACCTCAGTGCCTCCGTGCGCCACAGTCCAGCTG	480
141	L L I Q L S S P A N L S A S V A T V Q L	160
481	CCACAGCAGGACCAGCCAGTGCCCCACGGCACCCAGTGCCTGGCCATGGGCTGGGGCCGC	540
161	P Q Q D Q P V P H G T Q C L A M G W G R	180
541	GTGGGTGCCCACGACCCCCCAGCCAGGTCCTGCAGGAGCTCAATGTCACCGTGGTCAACC	600
181	V G A H D P P A Q V L Q E L N V T V V T	200
601	TTCTTCTGCCGGCCACATAACATTTGCACTTTTCGTCCCTCGCCGCAAGGCCGGCATCTGC	660
201	F F C R P H N I C T F V P R R K A G I C	220
661	TTCGGAGACTCAGGTGGCCCCCTGATCTGTGATGGCATCATCCAAGGAATAGACTCCTTC	720
221	F G D S G G P L I C D G I I Q G I D S F	240
721	GTGATCTGGGGATGTGCCACCCGCCTTTTCCCTGACTTCTTCACGCGGGTAGCCTTCTAC	780
241	V I W G C A T R L F P D F F T R V A L Y	260
781	GTGGACTGGATCCGTTCTACCCTGAAAACCGGTCATCATCACCATCACCATTGA	834
261	V D W I R S T L K T G H H H H H H *	278

7.2.2 Δ hPR3-S195A

The amino acid sequence is shown in single letter code. The sequence begins with the signal peptide. This mutant lacks the codons for the amino-terminal propeptide, starting directly with the sequence of the mature PR3, which is displayed in bold. The S195A mutation is marked bold and underlined. The C-terminal 6 \times His-tag is marked in italics and the stop codon is represented by a star (*).

1	ATGGCTCACC	GGCCCCCAGCCCTGCCCTGGCGTCCGTGCTGCTGGCCTTGCTGCTGAGC	60
1	M A H R P P S P A L A S V L L A L L L S		20
61	GGTGCTGCCC	GAGCTATCGTGGGCGGTACAGAGGCGCAGCCACACTCCCGGCCCTACATG	120
21	G A A R A I V G G H E A Q P H S R P Y M		40
121	GCCTCCCTGC	AGATGCGGGGGAACCCGGGCAGCCACTTCTGCGGAGGCACCTTGATCCAC	180
41	A S L Q M R G N P G S H F C G G T L I H		60
181	CCCAGCTTCG	TGCTGACGGCCGCGCACTGCCTGCGGGACATAACCCAGCGCCTGGTGAAC	240
61	P S F V L T A A H C L R D I P Q R L V N		80
241	GTGGTGCTCG	GAGCCCACAACGTGCGGACGCAGGAGCCCACCCAGCAGCACTTCTCGGTG	300
81	V V L G A H N V R T Q E P T Q Q H F S V		100
301	GCTCAGGTGT	TTTCTGAACAACACTACGACGCGGAGAACAACAACTGAACGACGTTCTCCTCATC	360
101	A Q V F L N N Y D A E N K L N D V L L I		120
361	CAGCTGAGCAG	CCCAGCCAACCTCAGTGCCTCCGTGCGCCACAGTCCAGCTGCCACAGCAG	420
121	Q L S S P A N L S A S V A T V Q L P Q Q		140
421	GACCAGCCAG	TGCCCCACGGCACCCAGTGCCTGGCCATGGGCTGGGGCCGCGTGGGTGCC	480
141	D Q P V P H G T Q C L A M G W G R V G A		160
481	CACGACCCCC	CAGCCAGGTCTGCAGGAGCTCAATGTACCGTGGTACCTTCTTCTGC	540
161	H D P P A Q V L Q E L N V T V V T F F C		180
541	CGGCCACATA	AACATTTGCACTTTTCGTCCCTCGCCGCAAGGCCGGCATCTGCTTCGGAGAC	600
181	R P H N I C T F V P R R K A G I C F G D		200
601	GCCGGTGGCC	CCCCCTGATCTGTGATGGCATCATCCAAGGAATAGACTCCTTCGTGATCTGG	660
201	<u>A</u> G G P L I C D G I I Q G I D S F V I W		220
661	GGATGTGCCA	CCCGCCTTTTCCCTGACTTCTTCACGCGGGTAGCCCTCTACGTGGACTGG	720
221	G C A T R L F P D F F T R V A L Y V D W		240
721	ATCCGTTCCAC	GCTGCGCCGTGTGGAGGCCAAGGGCCGCCCCGGGCCCTTCGAACAAAAA	780
241	I R S T L R R V E A K G R P G P F E Q K		260
781	CTCATCTCAGA	AAGAGGATCTGAATATGCATAACCGGTCATCATCACCATCACCATTGA	837
261	L I S E E D L N M H T G H H H H H H *		279

8. Curriculum vitae

Lisa Christina Hinkofer

PERSONAL INFORMATION

Address:	Siemensstr. 1b 84405 Dorfen Germany
Date of birth:	10. December 1986
Place of birth:	Altötting

EDUCATION

05/2011 – today	Doctoral candidate (Dr. rer. nat.) Ludwig-Maximilians-Universität München, faculty of Biology, Max-Planck-Institute of Neurobiology, Martinsried and Comprehensive Pneumology Center, Helmholtz Zentrum München
10/2013 – 07/2014	Graduate Student Research School for Lung Biology and Disease and HELENA Helmholtz Graduate School Environmental Health
10/2006 – 03/2011	Diploma in Biology Ludwig-Maximilians-Universität München Diploma thesis: „Die Funktion der alternativen 3´ untranslatierten Regionen im Bezug auf die Expression des HLA-EG-Allels“
09/1997 – 07/2006	Abitur Ruperti-Gymnasium, Mühldorf

9. Publications and meetings

9.1 Publications

- **Hinkofer LC**, Seidel SAI, Korkmaz B, Silva F, Hummel AM, Braun D, Jenne DE, Specks U. A Monoclonal Antibody (MCPR3-7) Interfering with the Activity of Proteinase 3 by an Allosteric Mechanism. *The Journal of biological chemistry*, 2013 Sept; 288:26635-48; Epub 2013 July
- **Hinkofer LC**, Hummel AM, Stone JH, Hoffman GS, Merkel PA, Spiera ERF, St.Clair W, McCune JW, Davis JC, Specks U and Jenne DE. Allosteric modulation of proteinase 3 activity by anti-neutrophil cytoplasmic antibodies in granulomatosis with polyangiitis. *Journal of Autoimmunity*, 2015, *in press*

9.2 Conference Abstracts

- **Hinkofer LC**, Jenne D. An Animal model for Granulomatosis with Polyangiitis. *ERS international congress*, 2014; P3918

9.3 Presentations at international conferences

9.3.1 Oral presentations

- Antibodies interfering with the catalytic activity of Proteinase 3: implications for ANCA-associated vasculitis. *30th International Winter School on Proteinases and Their Inhibitors*. Italy, 2013
- Pathogenic relevance of antibodies interfering with the activity of proteinase 3: Implications for ANCA-associated vasculitis. *German-French Lung Retreat*. France 2013
- Mechanism of activity modulating antibodies in vasculitis. *31st International Winter School on Proteinases and Their Inhibitors*. Italy, 2014

9.3.2 Poster presentations

- Vasculitis of the Lungs – Pathogenicity of Autoantibodies Interfering with the Activity of Proteinase 3. *Munich Lung conference*. Germany 2013
- Are PR3-inhibitory antibodies correlated with inflammatory exacerbation? *DZL Annual meeting*. Germany 2014
- An animal model for Granulomatosis with Polyangiitis. *ERS International Congress 2014*. Germany 2014

Eidesstattliche Erklärung

Ich versichere hiermit an Eides statt, dass die vorgelegte Dissertation von mir selbständig und ohne unerlaubte Hilfe angefertigt ist.

München, den

(Unterschrift)

Erklärung

Hiermit erkläre ich, *

- ☐ dass die Dissertation nicht ganz oder in wesentlichen Teilen einer anderen Prüfungskommission vorgelegt worden ist.
- ☐ dass ich mich anderweitig einer Doktorprüfung ohne Erfolg **nicht** unterzogen habe.
- ☐ dass ich mich mit Erfolg der Doktorprüfung im Hauptfach und in den Nebenfächern bei der Fakultät für der
(Hochschule/Universität) unterzogen habe.
- ☐ dass ich ohne Erfolg versucht habe, eine Dissertation einzureichen oder mich der Doktorprüfung zu unterziehen.

München, den.....

(Unterschrift)

*) Nichtzutreffendes streichen